

Chapter 4 Structural Performance and Damage Criteria

4-1. General

a. The purpose of this chapter is to use linear time-history analysis to formulate a systematic and rational methodology for qualitative estimate of the level of damage. In linear time-history analysis, deformations, stresses, and section forces are computed in accordance with elastic stiffness characteristics of various members and components. Using acceleration time-histories as the seismic input, the linear time-history analysis computes both the magnitudes and time-varying characteristics of the seismic response. A systematic interpretation and evaluation of these results in terms of the demand-capacity ratios, cumulative inelastic duration, spatial extent of overstressed regions, and consideration of possible modes of failure form the basis for approximation and appraisal of probable level of damage. The damage in this manual refers to cracking of the concrete, opening of construction joints, and yielding of the reinforcing steel. If the estimated level of damage falls below the acceptance curve for a particular type of structure, the damage is considered to be low and the linear time-history analysis will suffice. Otherwise the damage is considered to be severe, in which case a nonlinear time-history analysis would be required to estimate damage more accurately. The methodologies and procedures for estimation of the probable level of damage in this chapter were adopted from Ghanaat (2002).

b. If the results of linear time-history analysis indicate only limited performance inadequacy, the use of a nonlinear procedure may demonstrate acceptable performance. This is because the nonlinear procedures provide more accurate estimates of demands than do linear procedures. Linear procedures are most applicable to structures that actually have sufficient strength to remain nearly elastic when subjected to the MDE demands and to structures with regular geometries and distributions of stiffness and mass. To the extent that concrete hydraulic structures analyzed by this method do not have such strength or regularities, the indications of inelastic ductility demands predicted by the elastic methods may be inaccurate. In recognition of the relative inaccuracy of the linear techniques in predicting nonlinear response, the acceptance criteria have intentionally been set conservatively to provide a reasonable level of confidence in the method. Although the methodology formulated in this chapter is considered to be conservative, estimation of damage by the linear time-history analysis should still be used with considerable caution and careful interpretation and evaluation of the results. Examples of a gravity dam, two arch dams, a pile-founded navigation lock, and a free-standing intake tower are provided to illustrate the methodology and discuss probable nonlinear response and failure mechanisms for each structure.

4-2. Basis for the Proposed Performance and Damage Criteria

a. Traditional Criteria. Seismic performance of concrete hydraulic structures is being assessed on the basis of simple stress (or section-force) checks obtained from the linear elastic analysis combined with engineering judgment. The acceptance criterion for compressive stresses is that they should be less than the compressive strength of the concrete by a factor of 1.5 for new designs (USACE, 1994) and 1.1 for existing dams (FERC, 1999). Generally tensile stresses should not exceed tensile strength of the concrete. However, in practice up to five stress excursions above the tensile strength of the concrete have been considered acceptable based on engineering judgment and other considerations. This criterion neither puts limit on the magnitudes of stresses exceeding the tensile strength of the concrete nor offers any provisions regarding the spatial extent of such stresses. Rather it is left to the analyst to judge how high the magnitudes of critical tensile stresses could reach and how large an area they could occupy.

b. Proposed Criteria. To overcome the above shortcomings, this manual proposes a systematic approach for assessment of the seismic performance and probable level of damage using linear-elastic time history analyses. The performance evaluation and assessment of level of damage is formulated based on magnitudes of demand-capacity ratios, cumulative duration of stress excursions beyond the tensile strength of the concrete, spatial extent of overstressed regions, and load combination cases defined below. The acceptable level of damage on the basis of linear-elastic analysis is presented by a performance curve, as shown in Figure 4-1 (c), bounded by a demand-capacity ratio of 2 and an inelastic cumulative duration that varies with the type of structure.

(1) Demand-Capacity Ratios

(a) The demand-capacity ratio (DCR) for plain concrete is defined as the ratio of computed tensile stress to tensile strength of the concrete. For gravity dams, DCR is computed using principal stress demands. In the case of arch dams, where high stresses are usually oriented in the arch and cantilever directions, DCR is evaluated using arch or cantilever stress demands. The tensile strength or capacity of the plain concrete used in computation of DCR is obtained from the uni-axial splitting tension tests or from the static tensile strength

$$f_t = 1.7 f_c'^{2/3}$$

proposed by Raphael (1984), in which f_c' is the compressive strength of the concrete. The maximum permitted DCR for linear analysis of dams is 2. This corresponds to a stress demand twice the tensile strength of the concrete. As illustrated in the stress-strain curve in Figure 4-1(d), the stress demand associated with a DCR of 2 corresponds to the so called "apparent" dynamic tensile strength of the concrete (i.e. $3.4 f_c'^{2/3}$, Raphael 1984), used for evaluation of the results of linear dynamic analysis.

(b) DCR for the reinforced concrete hydraulic structures such as locks and intake towers is defined as the ratio of the section force demand to section force capacity. The maximum DCR is taken equal to 2 for bending moments and 1 for shears.

(2) Cumulative Inelastic Duration. The main problem with the traditional stress criterion is that the number of stress cycles alone is not always a good indicative of the level of damage. For example, the stress history in Figure 4-2 with 2 energetic stress cycles poses much higher damage potential than the stress history in Figure 4-3 with more than five stress cycles exceeding the tensile strength of the concrete. Both magnitudes and duration of stress cycles in Figure 4-2 are greater than those of the Figure 4-3, two factors that the traditional stress criterion ignores. For this reason the proposed damage criterion employs the cumulative inelastic duration in conjunction with DCR to account for these factors in assessment of the probable level of damage. The cumulative inelastic duration refers to the total duration of stress excursions above the tensile strength of the concrete, which as a measure of energy is a better indicator of the damage than the number of stress cycles.

(a) The cumulative inelastic duration of stress excursions, as defined in Figure 4-1(a) and 4-1(b), refers to the total duration of stress excursions above the tensile strength of the concrete (a DCR of 1 or greater). Figure 4-1(a) shows a sinusoidal stress history with five stress cycles and Figure 4-1(b) with one cycle exceeding a DCR of 1. In both cases the peak values are twice the tensile strength (i.e. DCR = 2). For each sinusoidal cycle duration of the stress excursion above the tensile strength is equal to $T/3$, where T is the period of the sinusoid. Thus for the Figure 4-1(a) the total inelastic duration for all five stress excursions (shaded area) amounts to $5T/3$. Considering that the periods of signals in Figures 4-1(a) and 4-1(b) are respectively 0.24 and 1.2 sec, the cumulative inelastic duration of stress excursions above f_t for both signals is 0.4 sec. Similarly, the cumulative inelastic duration of stress magnitudes exceeding $1.5f_t$ is 0.2 sec and of those exceeding $2f_t$ is zero.

(b) The limit values set for the cumulative inelastic duration vary with the type of hydraulic structures. The cumulative-inelastic-duration is estimated based on the dynamic characteristics, load resisting mechanism, and

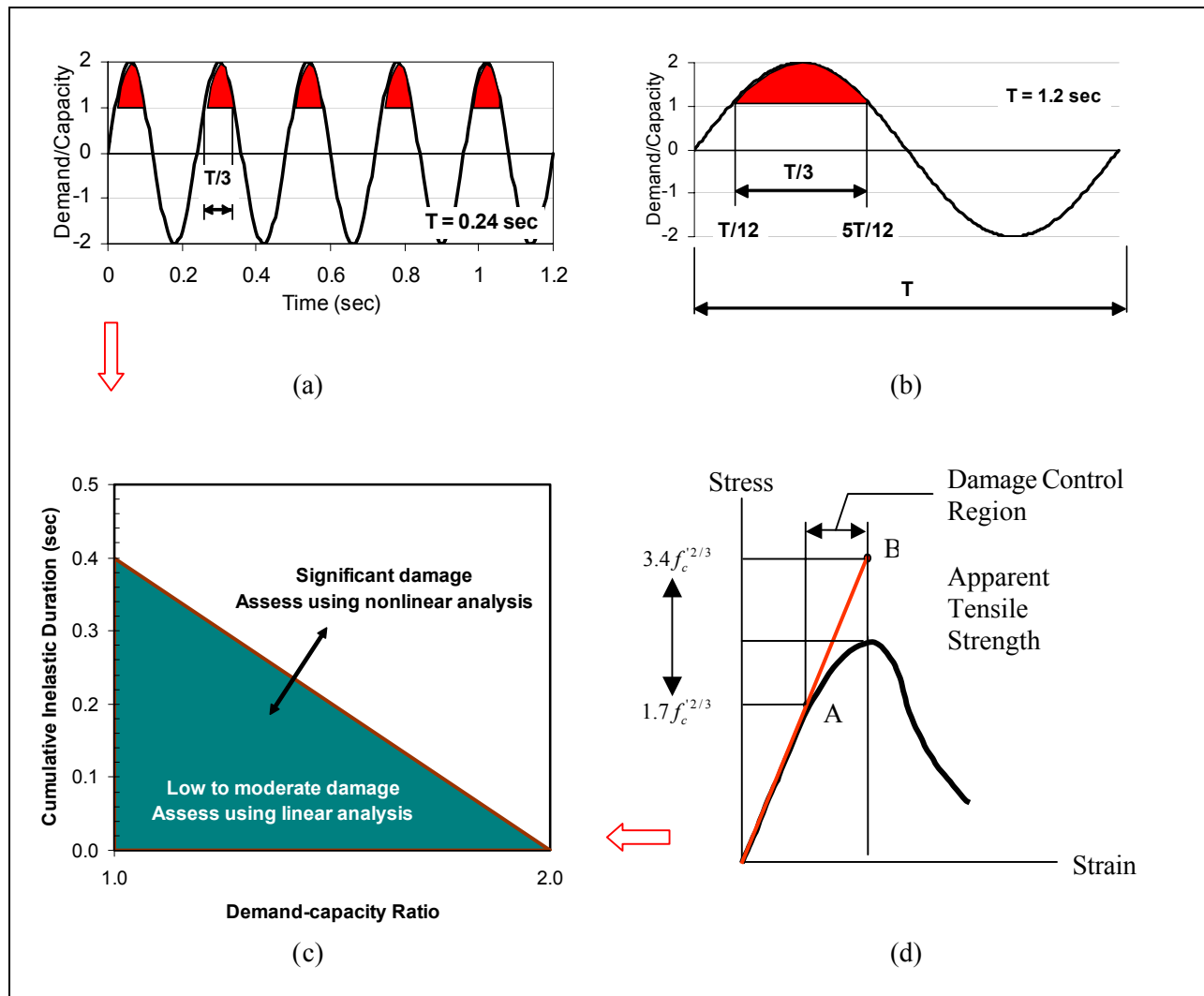


Figure 4-1. Basis for upper limit demand-capacity ratio and cumulative inelastic duration

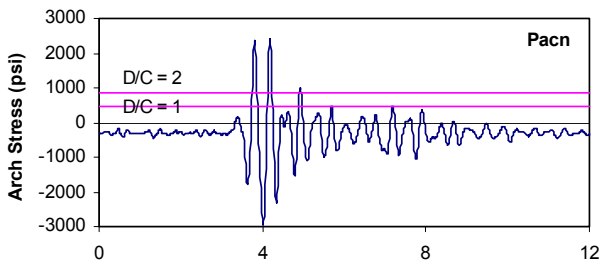


Figure 4-2. Fewer than five cycles exceed the capacity

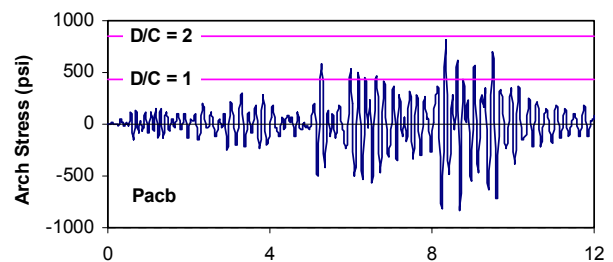


Figure 4-3. More than five cycles exceed the capacity

redundancy of the structure. For example arch dams that resist loads through both the arch and cantilever actions can sustain higher level of nonlinear deformation (or longer cumulative-inelastic-duration) than gravity dams that rely on cantilever mechanism alone to resist loads. Similarly, a reinforced concrete free-standing inlet/outlet tower exhibiting dominant flexural mode of behavior can tolerate even higher amount of nonlinear behavior. Another important factor in determining the cumulative inelastic duration is the frequency content of the earthquake input to ensure that the effects of most intense input pulses have been considered. Figure 4-4 shows that on the average the most intense earthquake pulses have frequencies roughly in the range of 0.8-to-4.4 Hz or periods in the range of 1.2-to-0.24 seconds. Making use of this, a single stress pulse with a period of 1.2 sec and the peak amplitude of $2f_i$ (Figure 4-1(b)) forms the basis for cumulative-inelastic-duration on the long-period end and five stress pulses with a period of 0.24 (Figure 4-1 (a)) on the short-period end of the intense shaking range. The cumulative inelastic durations for these signals are respectively $T/3$ and $5T/3$ or 0.4 seconds. This means a structure with a predominant period of 1.2 sec. can have only one stress cycle exceeding the tensile strength, while another with a period of 0.24 sec. can have up to five cycles. However, in either case the total cumulative inelastic duration remains at 0.4 seconds. In addition to these considerations, the selected cumulative-inelastic-duration for each type of structure was validated through numerous linear and nonlinear time history analyses and response evaluations, as discussed in 4-3 to 4-6 below.

(3) Extent of damage or nonlinear behavior. In addition to the foregoing performance curve (Figure 4-1(c)) the proposed damage criteria require the damage be confined to small regions, so that the evaluation on the basis of linear analysis is still valid. The spatial extent of damage or nonlinear response for each type of hydraulic structure is presented in the following paragraphs specific to that structure.

(4) Load Combination Cases. The performance and damage criteria discussed above require the use of three or more sets of earthquake acceleration time histories. For each set of two- (2D analysis) or three-component (3D analysis) ground motions the effects of static loads and earthquake ground motions components are combined by multiplying each earthquake component by +1 or -1 to account for the most unfavorable direction of earthquake attack.

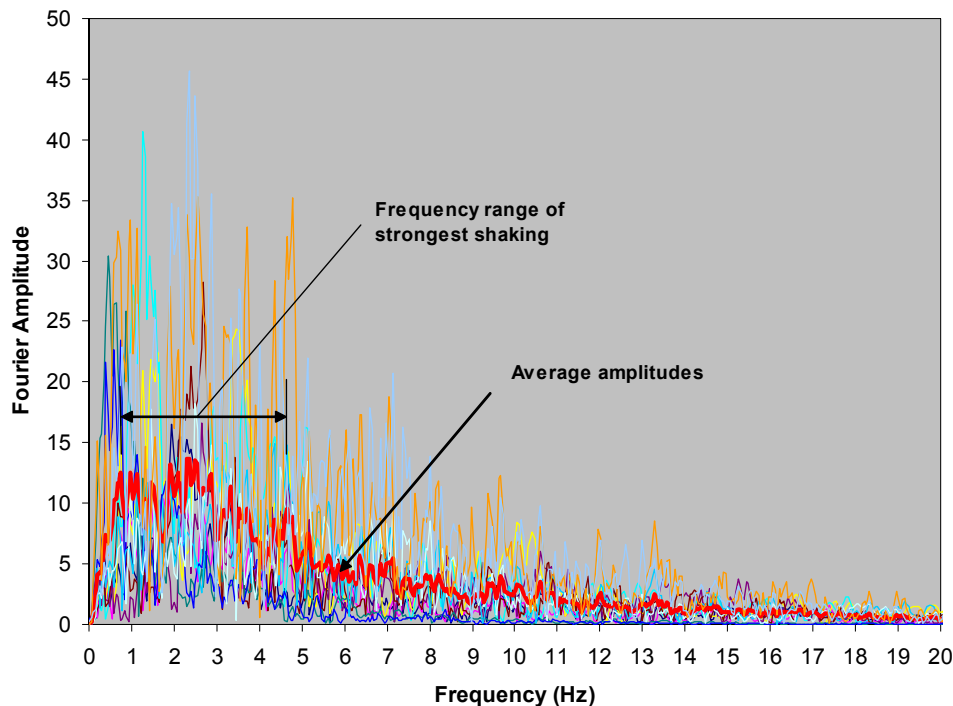


Figure 4-4. Fourier amplitudes of 12 earthquake recordings and their average

EM 1110-2-6051
22 Dec 03

used to determine frequency range of strongest shaking

4-3. Gravity Dams

Concrete gravity dams are modeled and analyzed in accordance with the linear dynamic analysis procedures outlined in Chapters 1 and 2. The results of such analyses include peak values and time-histories of displacements and stresses. Combined static and seismic stresses obtained for three or more sets of earthquake ground motions and load combination cases described in this paragraph form the basic parameters needed for evaluation of the dam. Other parameters include an understanding of nonlinear response of the dam in the form of probable cracking profiles and possible modes of failure and evaluation of demand-capacity ratios and cumulative duration of stress excursions beyond the tensile strength of the concrete. Types of probable damage, modes of failure, and influence of earthquake ground motion on the level of damage are described using the results from a nonlinear analysis of a typical gravity dam, followed by performance criteria and presentation and evaluation of results for the linear time-history analysis.

a. Nonlinear response and modes of failure. Figure 4-5 provides some examples of probable cracking profiles and possible modes of failure for a typical gravity dam analyzed using nonlinear fracture mechanics and various types of earthquake input motions (Leger and Leclerc 1996). Leger and Leclerc's results show that the cracking always initiates at the base of the dam, starting from the upstream face and propagating in the downstream direction. The cracks at the top of the dam generally initiate from the downstream face during an upstream swing of the dam and are either horizontal or sloping downward. A crack profile sloping downward from the downstream toward the upstream is considered more stable against a sliding failure than a crack with a reverse slope. This is because in the former case the water pressure is opposing the sliding whereas in the latter it is acting as a driving force. Any failure mode would likely involve sliding stability along the cracked surfaces with the water pressure as a driving force, acting both on the upstream face of the dam and in the crack. Should through cracks form near the crest of the dam, the consequences of failure may not be as critical as lower cracks, mainly because the failure of the upper portion of the dam might release only a small portion of the impounded water provided that the remaining section can resist overtopping.

b. Influence of earthquake ground motion. The results in Figure 4-5 clearly demonstrate that formation, location, extent, and orientation of tensile cracking are sensitive to characteristics of the earthquake ground motion. Three types of earthquake ground motions were considered: scaled recorded, spectrum-compatible recorded, and spectrum-compatible synthetic records. The top three graphs in this figure show dam responses to the horizontal components of scaled recorded signals from the 1989 Loma Prieta, 1988 Saguenay, and 1985 Nahanni earthquakes. The critical peak ground acceleration (CPGA) in this figure refers to a peak ground acceleration (PGA) value required to induce dynamic instability in the system. The Loma Prieta record containing significant energy near the fundamental period of the dam was scaled down from a recorded PGA of 0.44 g to a CPGA = 0.2 g, Saguenay was scaled up from 0.131 g to 0.65 g, and Nahanni from 0.545 g to 0.57 g. The middle three graphs are the crack profiles and required CPGA for the same natural records but with modified Fourier amplitude spectra compatible with a target response spectrum. The modified Loma Prieta record provided results comparable with the modified Saguenay and Nahanni records, as variation of the system energy was reduced as a result of spectrum compatibility. The modified records generally produced cracks at the same elevation as those estimated for the scaled natural records. The spectrum-compatible synthetic ground motion records produced somewhat similar cracks among themselves (lower graphs in Figure 4-5) but different from those obtained from the scaled and modified natural records. The cracks for the synthetic records formed and propagated at higher elevations than those for other records. Such sensitivity to characteristics of earthquake ground motion proves that damage should be estimated using a series of natural records scaled consistent with the design response spectra in the range of important structural periods.

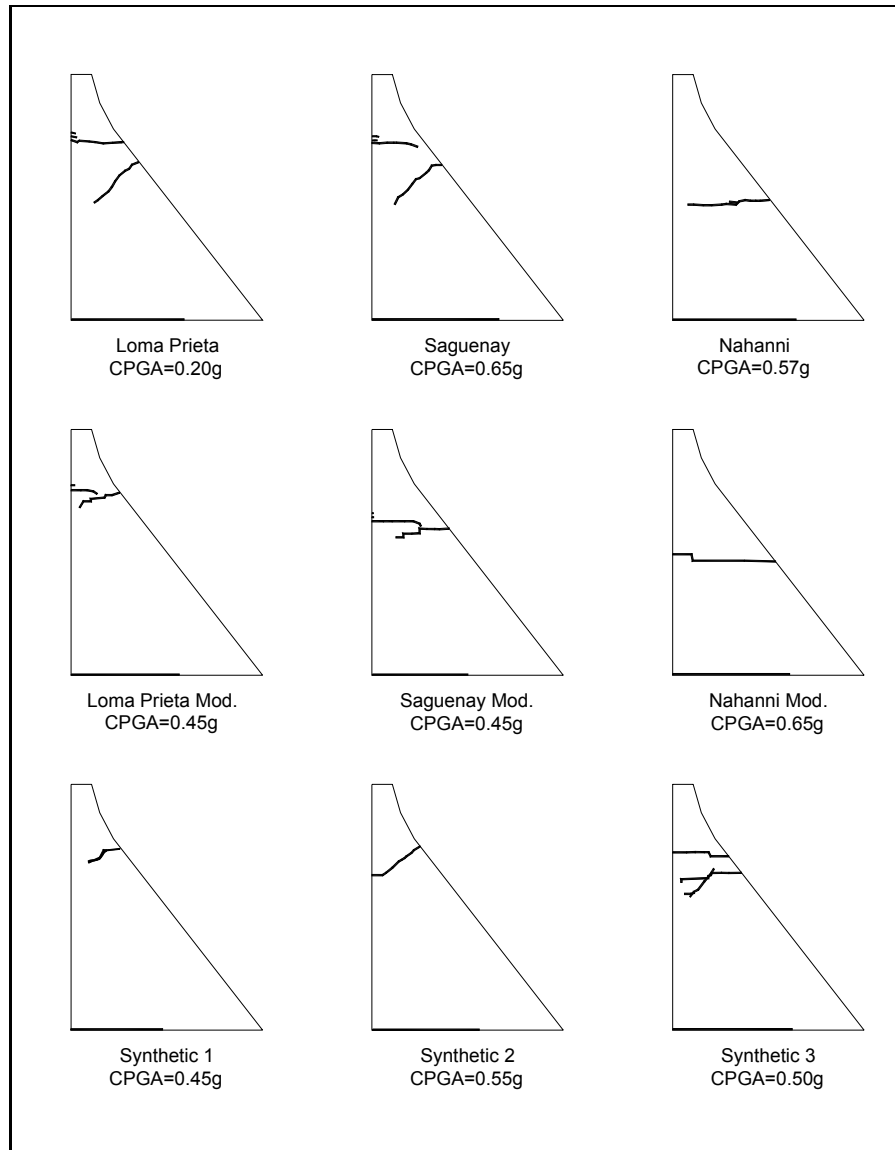


Figure 4-5. Probable cracking profiles of a typical gravity dam subjected to different types of earthquake ground motions (adapted from Leger and Leclerc 1996)

c. Performance criteria for linear analysis. The earthquake performance of gravity dams is evaluated on the basis of combined static and seismic stresses in accordance with the load combination cases in paragraph *d* below, demand-capacity ratios and the associated cumulative duration in *e* below, and presentation and interpretation of the results described in *f* below. The dam response to the MDE is considered to be within the linear elastic range of behavior with little or no possibility of damage if the computed demand-capacity ratios are less than or equal to 1.0. The dam will exhibit nonlinear response in the form of cracking of the concrete and/or opening of construction joints if the estimated demand-capacity ratios exceed 1.0. The level of nonlinear response or cracking is considered acceptable if demand-capacity ratios are less than 2.0 and limited to 15 percent of the dam cross-section surface area, and the cumulative duration of stress excursions beyond the tensile strength of the concrete falls below the performance curve given in Figure 4-6. Consideration should also be given to the relation between the fundamental period of the dam and peak of the earthquake response spectra. If lengthening of the periods of vibration due to nonlinear response behavior

causes the periods to move away from the peak of the spectra, then the nonlinear response would reduce seismic loads and improve the situation by reducing stresses below the values obtained from the linear time-history analysis. When these performance conditions are not met, or met only marginally with the nonlinear response increasing the seismic demand, then a nonlinear time-history analysis might be required to estimate the damage more accurately.

d. Load combination cases. Two-dimensional models of gravity dams should be evaluated for the vertical and one horizontal components of earthquake ground motion plus the effects of static loads. For each earthquake record, the static loads and earthquake components should be combined in accordance with Table 4-1. Three-dimensional models of gravity dams, when required, should be evaluated for three components of earthquake ground motion in accordance with Table 4-7.

e. Demand-capacity ratios. The demand-capacity ratios for gravity dams is defined as the ratio of the calculated principal stresses to tensile strength of the concrete. The tensile strength of plain concrete is obtained in accordance with 4-2b(1)(a). As discussed previously the demand-capacity ratio is limited to 2.0, thus permitting stresses up to twice the static or at the level of *dynamic apparent tensile strength* of the concrete.

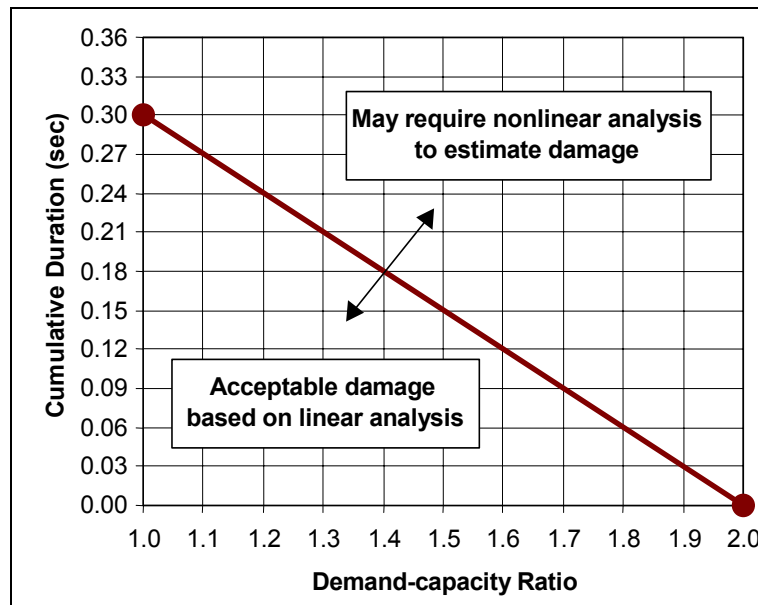


Figure 4-6. Performance curve for concrete gravity dams

Table 4-1 Load Combination Cases for Combining Static and Dynamic Stresses for 2-D Analysis			
Case	Seismic Loads		Static Loads (Stress)
	Vertical (V)	Stream Horizontal (H1)	
1 ¹	+	+	+
2	+	-	+
3	-	+	+
4	-	-	+

Note: The (+) and (-) signs indicate that the loads are multiplied by +1 or -1 to account for the most unfavorable earthquake direction.
¹ Case 1: Static + H1 + V

The cumulative duration in Figure 4-6 refers to the total duration of stress excursions beyond a certain level of demand-capacity ratio. For example, a cumulative duration of 0.21 sec at a demand-capacity ratio of 1.3 (Figure 4-6) indicates the total duration of stress excursions above the 1.3 times the tensile strength of the concrete. The cumulative duration beyond a certain level of demand-capacity ratio is obtained by multiplying number of stress values exceeding that level by the time-step used in the time-history analysis. As shown in Figure 4-6, the cumulative duration for gravity dams is set to 0.3 sec.

f. Presentation and performance evaluation. For performance evaluation of gravity dams described in *c* above, the following results from linear time-history analyses are required.

(1) Natural frequencies and mode shapes. Natural frequencies and natural modes of vibration provide important information on the dynamic characteristics of the dam, its degree of dynamic coupling or interaction with the impounded water, and its level of response to earthquake loading. A strong dynamic coupling with the impounded water indicates that more accurate representations of the dam-water interaction effects are required. Depending on whether the lower modes of the dam fall on the ascending or descending part of the earthquake response spectra, it can be inferred that nonlinear behavior would increase or decrease the seismic demand.

(2) Displacement histories. The magnitudes and time-histories of nodal displacements at critical locations such as the crest should be presented and evaluated. While displacement patterns provide a visual means of validating the results, displacement magnitudes are examined to ensure that they are small and that the overall stability of the dam is maintained.

(3) Maximum and minimum principal stresses. Maximum and minimum principal stresses due to static plus seismic loads should be determined and presented as contours or vector plots. In general vector plots are more useful than the contour plots because stress vectors provide both the magnitude and direction of principal stresses, thus can be used to predict probable direction of the tensile cracking. The maximum and minimum stress plots represent the largest tensile (positive) and the largest compressive (negative) stresses that occur in the dam generally at different times during the earthquake excitation.

(4) Demand-capacity ratios. The maximum principal stresses in (3) above could also be displayed as plots of the demand-capacity ratios by dividing the maximum stresses by the tensile strength and minimum stresses by the compressive strength of the concrete.

(5) Time-histories of critical principal stresses. Time-histories of the most critical maximum principal stresses identified in (3) above should be displayed and evaluated. Such time-histories are examined to determine the total duration of stress excursions beyond demand-capacity ratios of 1.0 to 2.0 for comparison with the performance curve in Figure 4-6. The total duration can simply be obtained by multiplying the number of stress values exceeding a stress level (or equivalent demand-capacity ratio) by the integration time-step used in the analysis. The magnitude of total duration indicates whether the peak stresses are merely spikes with little or no damage potential or they are of longer duration capable of producing significant damage.

(6) Concurrent principal stresses at the time of maximum stress. The maximum principal stresses in (3) above are not concurrent and generally occur at different time-steps during the earthquake excitation. They serve to identify the overstressed regions and locations of the critical principal stresses. From this information, time-steps at which the critical principal stresses reach their peak values are determined and used to obtain the corresponding concurrent or simultaneous principal stresses. The concurrent principal stresses should be displayed in the form of contours or vector plots and used to estimate the extent, location, and direction of probable tensile cracking following the general description provided in *a* above.

4-4. Arch Dams

Concrete arch dams are modeled and evaluated following the linear time-history analysis procedures outlined in Chapters 1 and 2. The results of analysis include peak values and time-histories of nodal displacements and element stresses. The analysis is repeated for three or more three-component sets of earthquake input acceleration time-histories. The results of each analysis are combined as described in this paragraph to account for the effects of static loads and phasing of the earthquake ground motion components. The magnitude, spatial extent, and spatial distribution of the combined stresses together with duration of stress excursions beyond the allowable values and an understanding of the possible nonlinear mechanism form the basis for earthquake performance evaluation of arch dams. In this paragraph probable nonlinear mechanism, modes of failure, and influence of earthquake ground motion characteristics on the level of damage are described first, followed by formulation of performance criteria and presentation and evaluation of results of linear time-history analysis.

a. Nonlinear behavior and modes of failure.

(1) Nonlinear behavior. Arch dams are generally built as cantilever monoliths separated by vertical contraction joints. Since contraction joints cannot transfer substantial tensile stresses in the arch direction, the joints can be expected to open and close repeatedly as the dam vibrates in response to severe earthquake ground motion. The contraction joint opening releases tensile arch stresses and transfers forces to the cantilevers. The increased cantilever stresses may exceed tensile strength of the lift lines (or horizontal joints), possibly resulting in crushing or horizontal cracking of the cantilevers. Potentially opened contraction joints and cracked lift joints may subdivide the monolithic arch structure into partially free cantilever blocks, capable of transmitting only compressive or frictional forces (Figure 4-7).

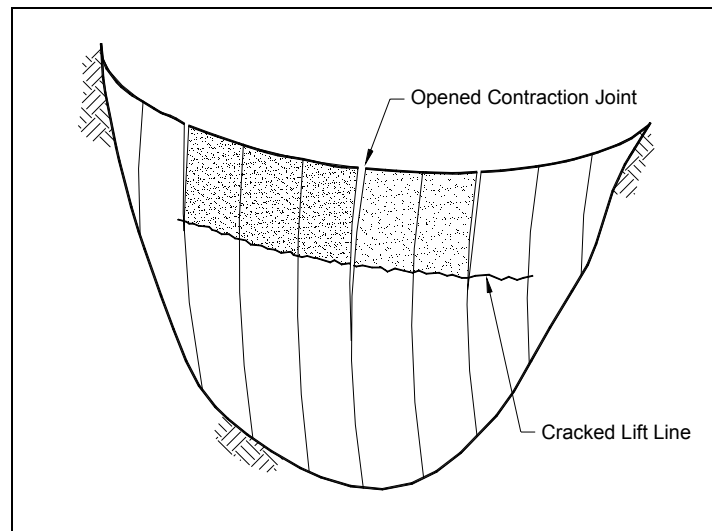


Figure 4-7. Contraction joint opening and lift line cracking in Arch dams

(2) Modes of failure. Any failure mode of the arch structure more likely would involve sliding stability of the partially free cantilevers. For small and moderate joint openings, the partially free cantilever blocks, bounded by opened joints, may remain stable through interlocking (wedging) with adjacent blocks. The extent of interlocking depends on the depth and type of shear keys and the amount of opening to be expected. Such concepts have similarities to Goodman and Shi's Block Theory (Goodman and Shi 1985) for the stability evaluation of rock masses: a continuous block, isolated by the intersection of discontinuities or free surfaces, can move only by sliding on one or two faces or by combined sliding and rotation. If potentially dangerous blocks can be shown to be incapable of moving because of friction, tapering, gravity, or orientation consideration, their stability is of no concern. A perfect shear key (i.e., rectangular shape) would permit only normal opening, but no sliding. Triangular or trapezoidal shear keys allow both opening and some sliding. Hence, the depth of the shear keys controls the maximum amount of joint opening for which adjacent blocks would remain interlocked; deeper shear keys permit larger joint openings. When the partially free cantilevers are treated as rigid blocks, the maximum joint opening with active interlocking can be estimated from rigid block geometry. Therefore, under nonlinear dynamic analysis, the magnitude of compressive stresses, the extent of joint opening or cracking, and the amplitude of non-recoverable movements of concrete blocks bounded by failed joints will control the overall stability of the dam, rather than the magnitude of calculated tensile stresses.

b. Influence of earthquake ground motion. The magnitude and characteristics of earthquake input motions and the way they are applied to the dam and foundation model have significant effects on the linear and especially nonlinear responses and must be evaluated carefully. For the linear elastic response analysis, the frequency content of the seismic input defined by the shape of the response spectrum plays a more significant role than any other parameter. For nonlinear analysis and linear analysis used for qualitative evaluation of damage, in addition to the frequency content, other ground motion characteristics such as duration, energy, and pulse sequencing become extremely important, and must be considered in selecting or developing acceleration histories. This paragraph illustrates the effects of ground motion characteristics on the response of two arch dams analyzed by the linear time-history method using six different sets of acceleration time-histories.

(1) Selected earthquake ground motions. For qualitative damage evaluation using linear time-history analysis, example arch dams were assumed to be located in the near field of a maximum earthquake event having a moment magnitude M_w of about 6-1/2. Five three-component sets of recorded acceleration time-histories from four recent earthquakes were selected. In addition, a three-component spectrum-compatible time-history derived using the 1971 Pacoima Dam record was also included. The smooth response spectra for the horizontal and vertical components of ground motion were constructed to be representative of median ground motions for an M_w 6-1/2 earthquake occurring at a distance of $R \approx 5$ km. The records considered are listed in Table 4-2 and the smooth response spectra are shown in Figure 4-8. The ground motions were scaled such that the sum of ordinates for the response spectra of each natural record would match the sum for the smooth response spectra in the period range of 0.1 to 0.4 sec. This period range was selected to contain the most significant modes of vibration for both example dams (i.e., all periods longer than 0.1 sec). The resulting scale factor for each record is listed in Table 4-2, and the response spectra for all records in the period range of 0.1 to 0.5 sec are compared in Figure 4-9. Time-histories of the larger horizontal component of the records are plotted in Figure 4-10. The figure clearly demonstrates the pulsive ("fling") type motions contained in the Pacoima Dam and Morgan Hill records.

Table 4-2
Near-Source Earthquake Records

Earthquake Record	Designated Name	Scale
Pacoima Dam, downstream record 1971 San Fernando earthquake, M_w 6.6, R = 2.8 km	Pacx	0.52
Spectrum-matched 1971 Pacoima Dam record	Pacb	1.00
Pacoima Dam, downstream record 1994 Northridge earthquake, M_w 6.7, R = 8 km	Pacn	1.13
Newhall, West Pico Canyon Boulevard 1994 Northridge earthquake, M_w 6.7, R = 7.1 km	U56	1.80
Coyote Lake Dam 1984 Morgan Hill earthquake, M_w 6.2, R = 0.1 km	Cld	0.64
Gilroy Array No. 1 1989 Loma Prieta earthquake, M_w 6.9, R = 11 km	Gly	0.81

(2) Description of arch dams. The geometry and finite element models of two arch dams, Dam-1 and Dam-2, analyzed for damage evaluation are given in Figure 4-11. The model of each dam includes three layers of solid elements through the dam thickness. The foundation models also use solid elements and are constructed on semicircles having a radius twice the dam height. The water level at Dam-1 is at 64 percent of the dam height and at Dam-2 is at the crest level. The dam-water interaction, therefore, is less significant for Dam-1 than it is for Dam-2. The lowest ten modes of Dam-1 have periods ranging from 0.23 to 0.09 sec and of Dam-2 from 0.34 to 0.10 sec.

(3) Earthquake response of Dam-1. This paragraph summarizes earthquake responses of Dam-1 to six sets of three-component earthquake ground motions discussed in (1) above. The computed natural periods for the 10 lowest modes of the dam are 0.233, 0.237, 0.161, 0.133, 0.128, 0.118, 0.110, 0.102, 0.096, and

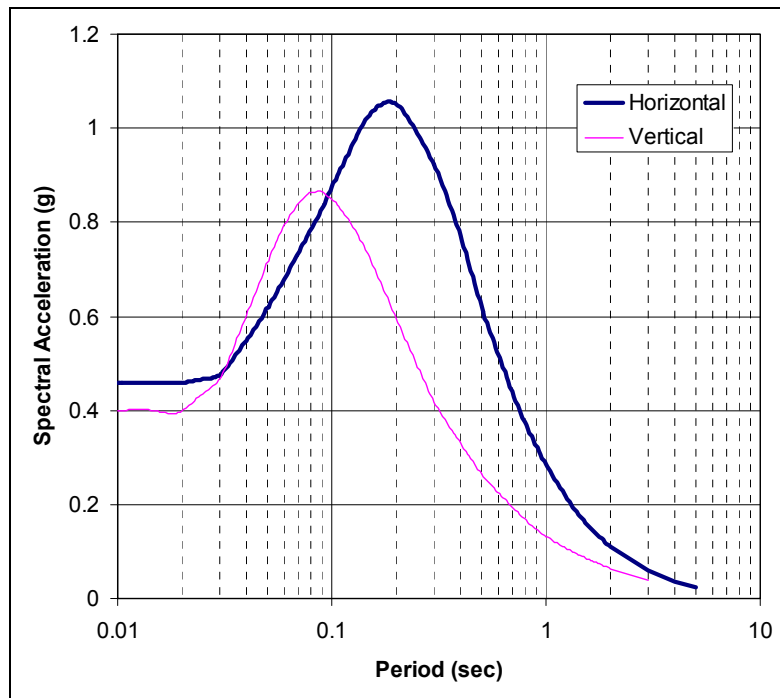


Figure 4-8. Horizontal and vertical smooth response spectra

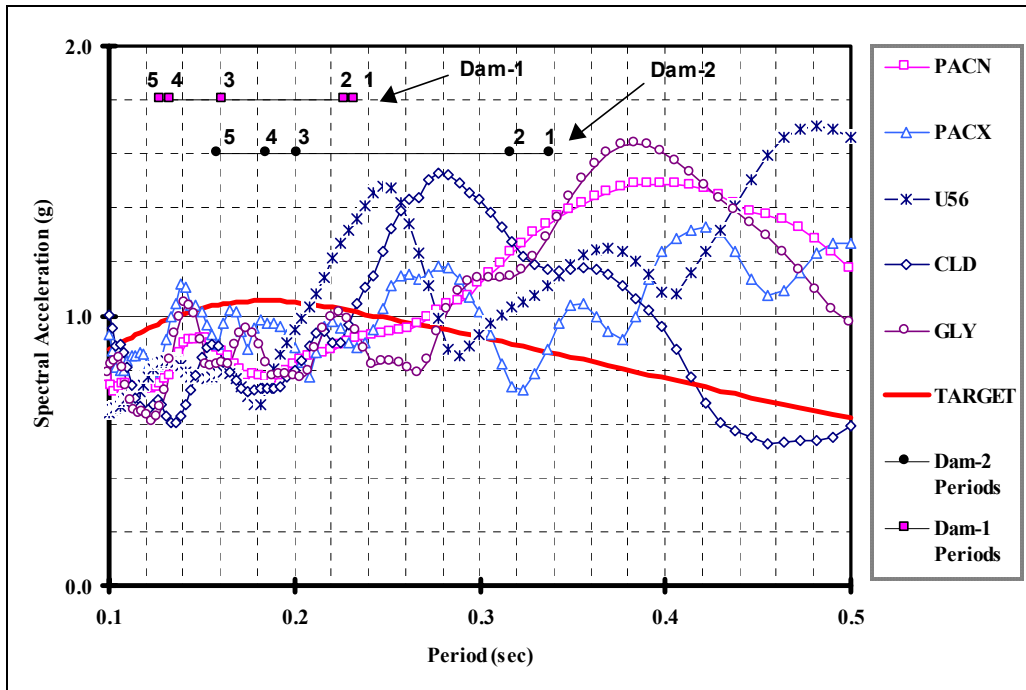


Figure 4-9. Response spectra of scaled records

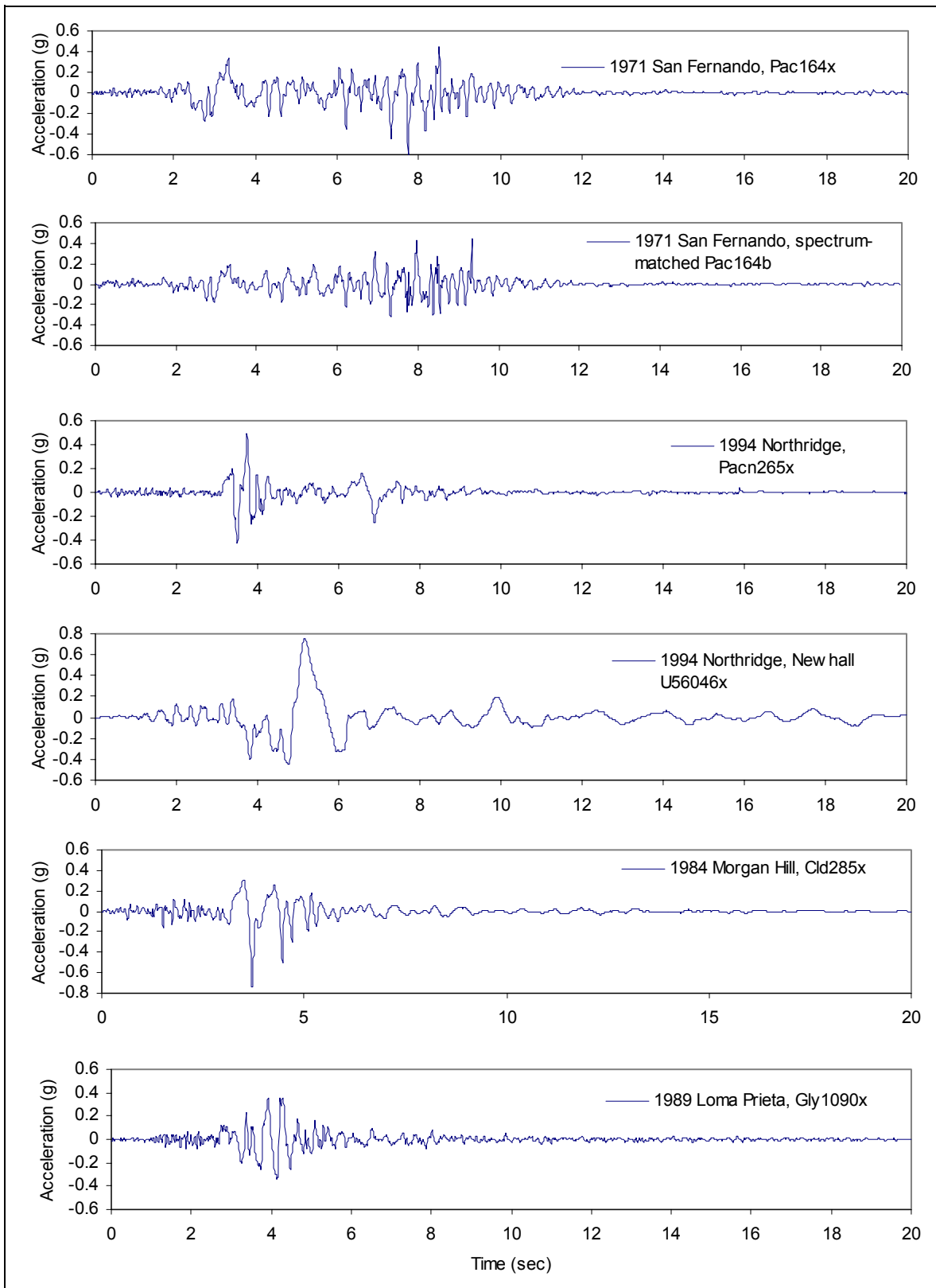


Figure 4-10. Scaled acceleration time-histories for near-source, $M_w \sim 6\text{-}1/2$ earthquake

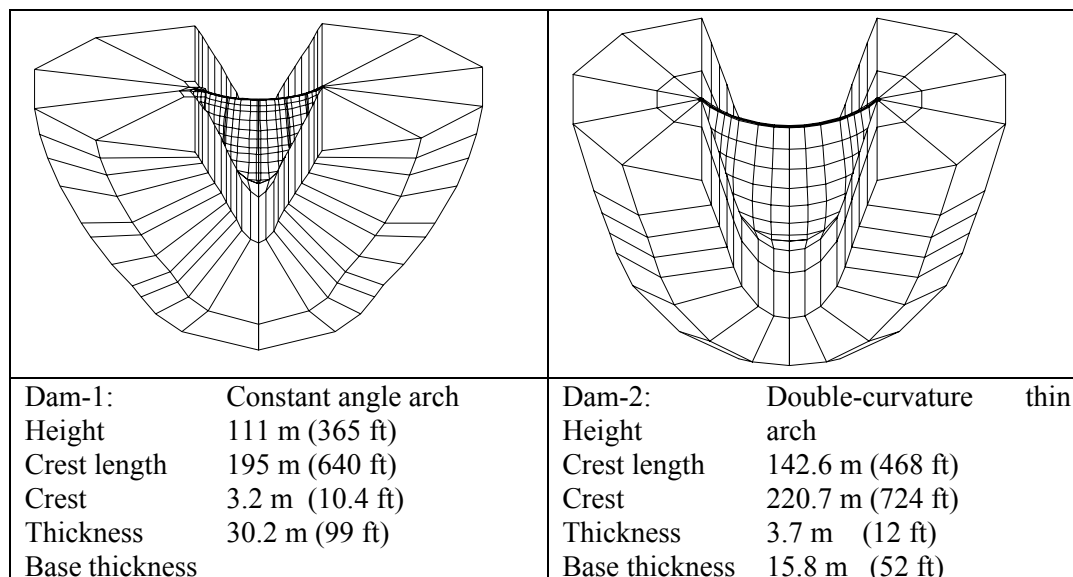


Figure 4-11. Finite element models and geometry data for example Dam-1 and Dam-2

0.088 sec, the first 5 of which are displayed in Figure 4-9 for comparison with response spectra of the earthquake input motions. Only spectral ordinates of U56 at the periods of Modes 1 and 2 exceed the values for the target and other spectra. The spectrum-compatible record (Pacb) induces the largest upstream-downstream displacements at the center and right 1/4 point of the crest. The 1994 Northridge Newhall record (U56) produces the largest vertical and cross-stream displacements at the right 1/4 point, center, and the left 1/4 point of the crest (Table 4-3). Time-histories of the midcrest displacements (Figure 4-12) for different records show significant differences, but the magnitude of peak displacements closely relates to the spectral ordinate values. None of the earthquake records produces both the arch and cantilever peak maximum stresses on both faces of the dam. Pacb produces the peak upstream arch and peak upstream cantilever stresses, Pacx induces the peak downstream arch stress, and U56 provides the peak downstream cantilever stress (Table 4-4). This is expected since several lower modes contribute to the dynamic stresses developed in the dam and the spectral ordinates of these modes are significantly different from one scaled record to another. The distributions of maximum stresses for all earthquake records are nearly the same and quite similar to that for Pacb shown in Figure 4-13. On the upstream face high tensile arch stresses occur in the upper central region of the dam, while on the downstream face they develop in the upper regions near 1/4-point locations. High tensile cantilever stresses occur in the upstream central region of the dam at about 1/4 of the dam height below the crest and on the downstream region toward the right abutment. The concurrent stress contours at the time of maximum arch stress (Figure 4-14) indicate that the simultaneous tensile arch stresses are essentially developed on the upstream central region and downstream 1/4-point locations of the dam. The corresponding concurrent cantilever stresses (right graphs in Figure 4-14) are mainly compressive on the upstream face with small tensile stresses on the upper part of the downstream face of the dam. The magnitude and concurrent stress distributions at the time of maximum arch stress suggest that joint opening, if any, would be minor, possibly involving the joints at the crown and 1/4-point locations. Time-histories of maximum stresses in Figures 4-15 and 4-16 show that time variation of stresses is quite different for each earthquake record and that the number of stress peaks beyond 500 psi is within 5 cycles for arch stresses and none for cantilever stresses. The cumulative duration of stress cycles beyond the tensile strength of the concrete discussed in *c* below generally meets the performance criteria for the linear elastic analysis.

Table 4-3
Dam-1 Maximum Displacements, inches

Ground Motion	Right ¼ Point			Center			Left ¼ Point		
	x	y	z	x	y	z	x	y	z
Pacx	0.58	1.15	0.17	0.33	1.80	0.20	0.57	1.20	0.19
Pacb	0.63	<u>1.52</u>	0.18	0.35	<u>2.05</u>	0.23	0.57	0.92	0.18
Pacn	0.46	<u>0.87</u>	0.10	0.28	<u>1.54</u>	0.13	0.53	1.10	0.12
U56	<u>0.66</u>	0.89	<u>0.27</u>	<u>0.46</u>	1.82	<u>0.35</u>	<u>0.80</u>	<u>1.28</u>	<u>0.23</u>
Cld	0.52	1.10	0.17	0.37	1.97	0.21	0.66	1.26	0.20
Gly	0.62	1.14	0.15	0.32	1.81	0.12	0.56	1.13	0.14

Note: Bold underlined values are the largest maximum displacements.

Table 4-4
Dam-1 Maximum Arch and Cantilever Stresses, psi

Earthquake Record	Arch		Cantilever	
	Upstream	Downstream	Upstream	Downstream
Pacx	698	<u>537</u>	406	238
Pacb	<u>784</u>	520	<u>440</u>	255
Pacn	558	392	222	134
U56	649	500	223	<u>274</u>
Cld	755	508	359	234
Gly	688	476	288	217

Note: Bold underlined values are the largest maximum stresses.

(4) Earthquake response of Dam-2. This paragraph describes earthquake responses of Dam-2 to six sets of three-component earthquake ground motions discussed in (1) above. The computed natural periods for the 10 lowest modes of the dam vary from 0.338 to 0.104 sec, the first 5 of which are displayed in Figure 4-9 for comparison with response spectra of the earthquake input motions. Compared to the target spectrum, all scaled records show higher spectral ordinates for Mode 1 and Mode 2 and lower for Modes 3 to 5, with the exception of Pacx whose spectral value for Mode-2 is lower. None of the earthquake records produces peak maximum values for all displacement components at all locations. The Gilroy record (Gly) induces the largest upstream-downstream displacement of 6.9 in. at the center of the crest, while other records produce peak vertical and cross-stream displacements, as highlighted in Table 4-5. Consistent with the input records, time-histories of the midcrest displacements vary significantly in terms of the wave forms (Figure 4-17). The magnitudes of peak radial displacements are about the same for all earthquake records, except for Gly, which is 60 to 70 percent higher due to the harmonic wave form of this record. None of the earthquake records produces both the arch and cantilever peak maximum stresses. While the Gilroy record produces the peak upstream and downstream arch stresses, the Northridge record (Pacn) produces the peak upstream and downstream cantilever stresses, as highlighted in Table 4-6. The distributions of maximum stresses are nearly the same for Pacx and Pacb but different for other records. This is expected since several lower modes contribute to the dynamic stresses developed in the dam and the spectral ordinates of these modes are significantly different from one scaled record to another. The maximum stress contours for Gly producing the largest arch stresses are shown in Figure 4-18. On the upstream face high-tensile arch stresses develop in the upper half of the central region of the dam, while on the downstream face they develop mostly in the 1/4-point locations but also in the upper central region. High-tensile cantilever stresses occur in the upstream middle region of the dam and in the upper abutment regions. The concurrent stress contours at the time of maximum arch stress (Figure 4-19) indicate that the simultaneous tensile arch stresses are developed on the upstream central region and downstream 1/4-point locations of the dam. The corresponding concurrent cantilever stresses (right graphs in Figure 4-19) are mostly compressive on both the upstream and downstream faces of the dam. The magnitude and concurrent stress distributions at the time of maximum arch stress suggest that joint opening would be significant. Figure 4-20 shows that the maximum arch stresses for all records are greater than 13.8 MPa (2,000 psi), indicating significant contraction joint opening. Time-histories of maximum cantilever stresses in Figure 4-21

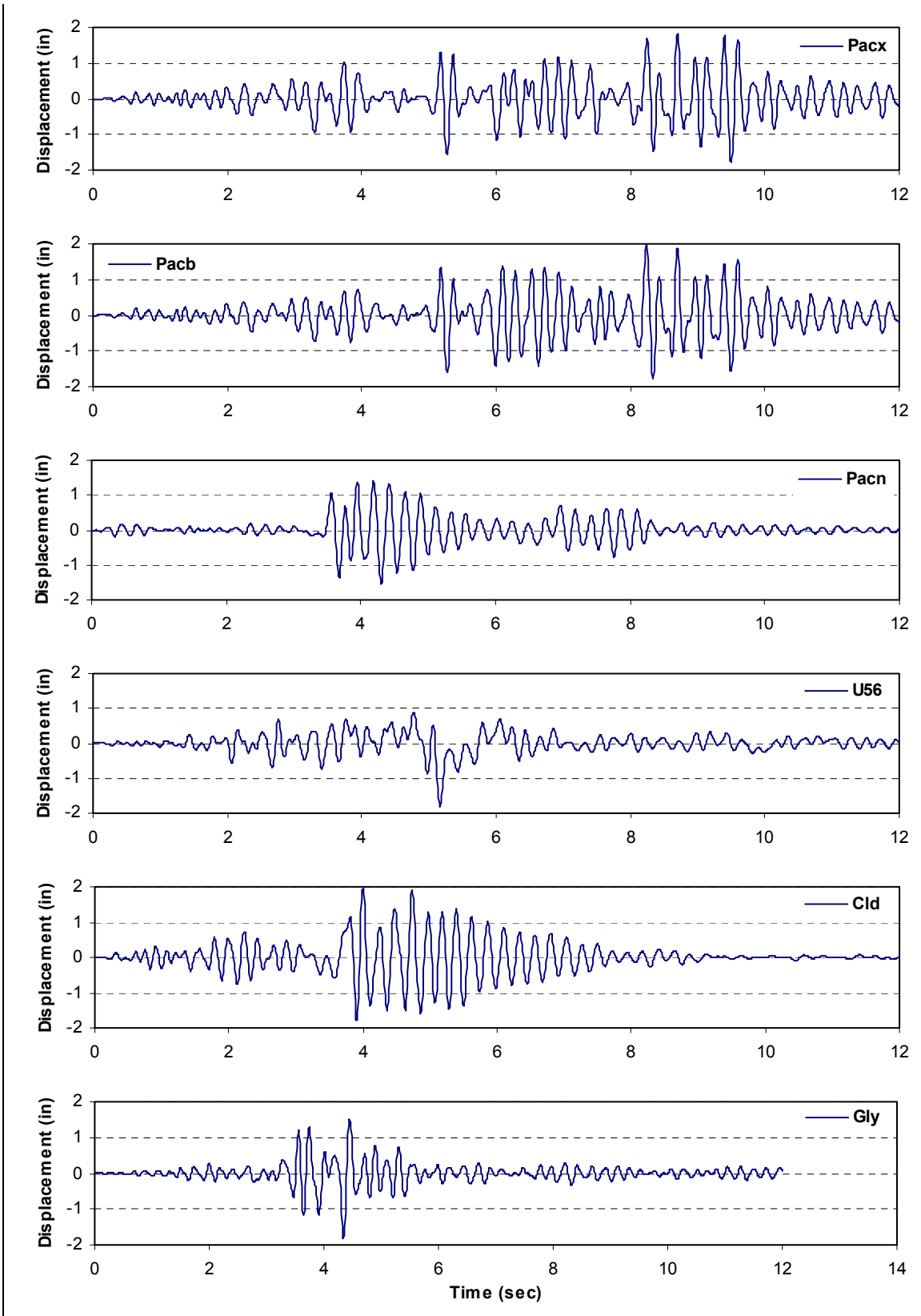


Figure 4-12. Time-histories of midcrest radial displacements for Dam-1



Figure 4-13. Envelope of maximum stresses due to spectrum-matched Pacb record (Dam-1)

Table 4-5
Dam-2 Maximum Displacements, inches

Ground Motion	Right ¼ Point			Center			Left ¼ Point		
	x	y	z	x	y	z	x	y	z
Pacx	1.19	1.25	0.25	0.56	4.03	0.31	1.08	2.16	0.25
Pacb	0.89	1.03	0.18	0.39	4.04	0.28	0.96	1.70	0.20
Pacn	1.51	1.49	0.11	0.61	4.38	0.17	0.78	1.96	0.21
U56	1.17	1.13	0.20	0.54	4.21	0.33	0.83	1.28	0.21
ClD	1.26	1.37	0.22	0.46	4.08	0.31	0.76	1.43	0.23
Gly	1.12	1.05	0.25	0.40	6.94	0.23	1.07	1.57	0.27

Table 4-6
Dam-2 Maximum Tensile Stresses, psi

Earthquake Record	Arch		Cantilever	
	Upstream	Downstream	Upstream	Downstream
Pacx	2,088	1,697	895	576
Pacb	2,099	1,415	650	461
Pacn	2,360	2,117	1,028	639
U56	2,019	1,891	741	424
CLD	2,315	1,890	975	504
GLY	2,917	2,508	748	636

are quite different for each earthquake record. The maximum cantilever stresses, even without further increase due to contraction joint opening, are about 6.9 MPa (1,000 psi). At such high stress levels it is expected that the cracking of the lift lines would also be significant. The cumulative duration of stress cycles beyond the tensile strength of the concrete discussed in *c* below markedly exceeds the performance criteria for the linear elastic analysis.

c. Performance criteria for linear analysis. The earthquake performance of arch dams is evaluated on the basis of combined static and seismic stresses in accordance with the load combination cases in *d* below,

demand-capacity ratios and the cumulative inelastic duration in *e* below, and presentation and interpretation of

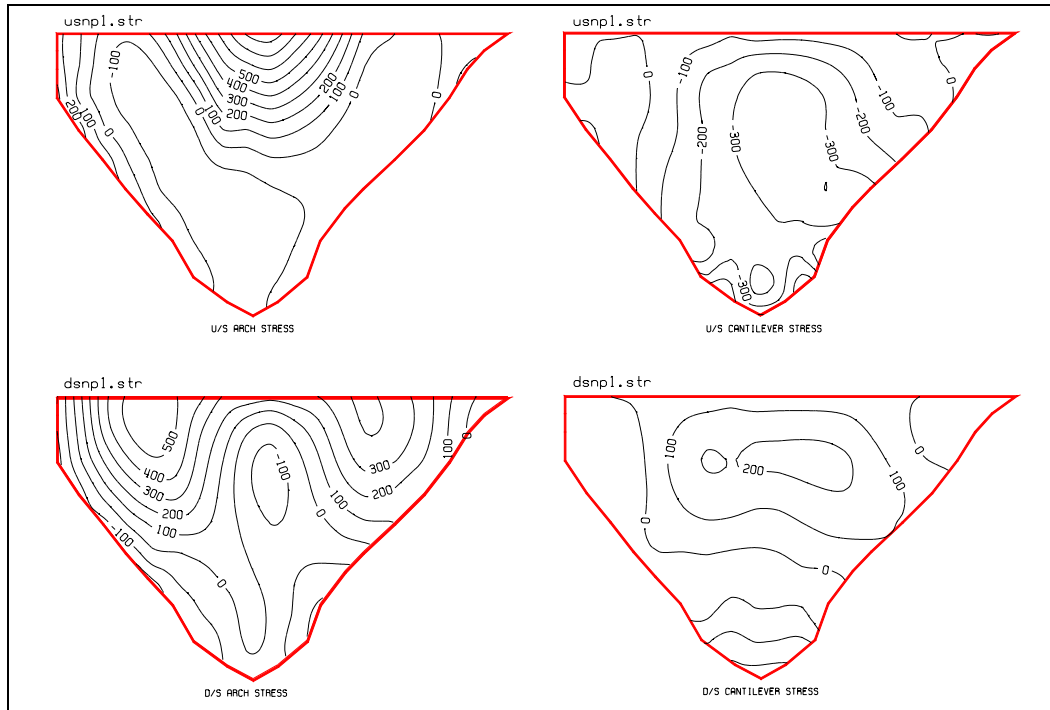


Figure 4-14. Concurrent stresses at the time of maximum arch stress due to spectrum-matched Pacb record (Dam-1)

results described in *f* below. The dam response to the MDE is considered to be within the linear elastic range of behavior with little or no possibility of damage if computed demand-capacity ratios are less than or equal to 1.0. Considering that the ability of contraction joints to resist tension is limited, the joints may still open even if demand-capacity ratios are less than or equal to 1.0. The amount of contraction joint opening at a demand capacity ratio ≤ 1 , however, is expected to be small with negligible or no effects on the overall stiffness of the dam. The dam is considered to exhibit nonlinear response in the form of opening and closing of contraction joints and cracking of the horizontal joints (lift lines) if the estimated demand-capacity ratios exceed 1.0. The level of nonlinear response or opening and cracking of joints is considered acceptable if the demand capacity ratio < 2 , overstressed region is limited to 20 percent of the dam surface area, and the cumulative inelastic duration falls below the performance curve given in Figure 4-22. The relation between the fundamental period of the dam and peak of the response spectra should also be considered to determine whether the nonlinear response behavior would increase or decrease the seismic demand. If these performance criteria are not met, or met marginally with increasing demand due to nonlinear behavior, then a nonlinear analysis would be required for more accurate estimate of the damage.

d. Load combination cases. Three-dimensional analysis of arch dams should be evaluated for three or more sets of three-component earthquake ground motions. For each set of three-component earthquake ground motions the static loads and earthquake ground motion components should be combined in accordance with Table 4-7.

e. Demand-capacity ratios. The demand-capacity ratio for arch dams is defined as the ratio of the calculated arch or cantilever stress to tensile strength of the concrete. The tensile strength of the concrete is measured by the uniaxial splitting in accordance with American Society for Testing and Materials (ASTM) C496. Although tensile strength of concrete is affected by the rate of seismic loading, the acceptance criteria in *c*

above employ the static tensile strength in computation of the demand-capacity ratios. The reason for this is to account for the lower strength of the lift lines and provide some level of conservatism in estimation of damage

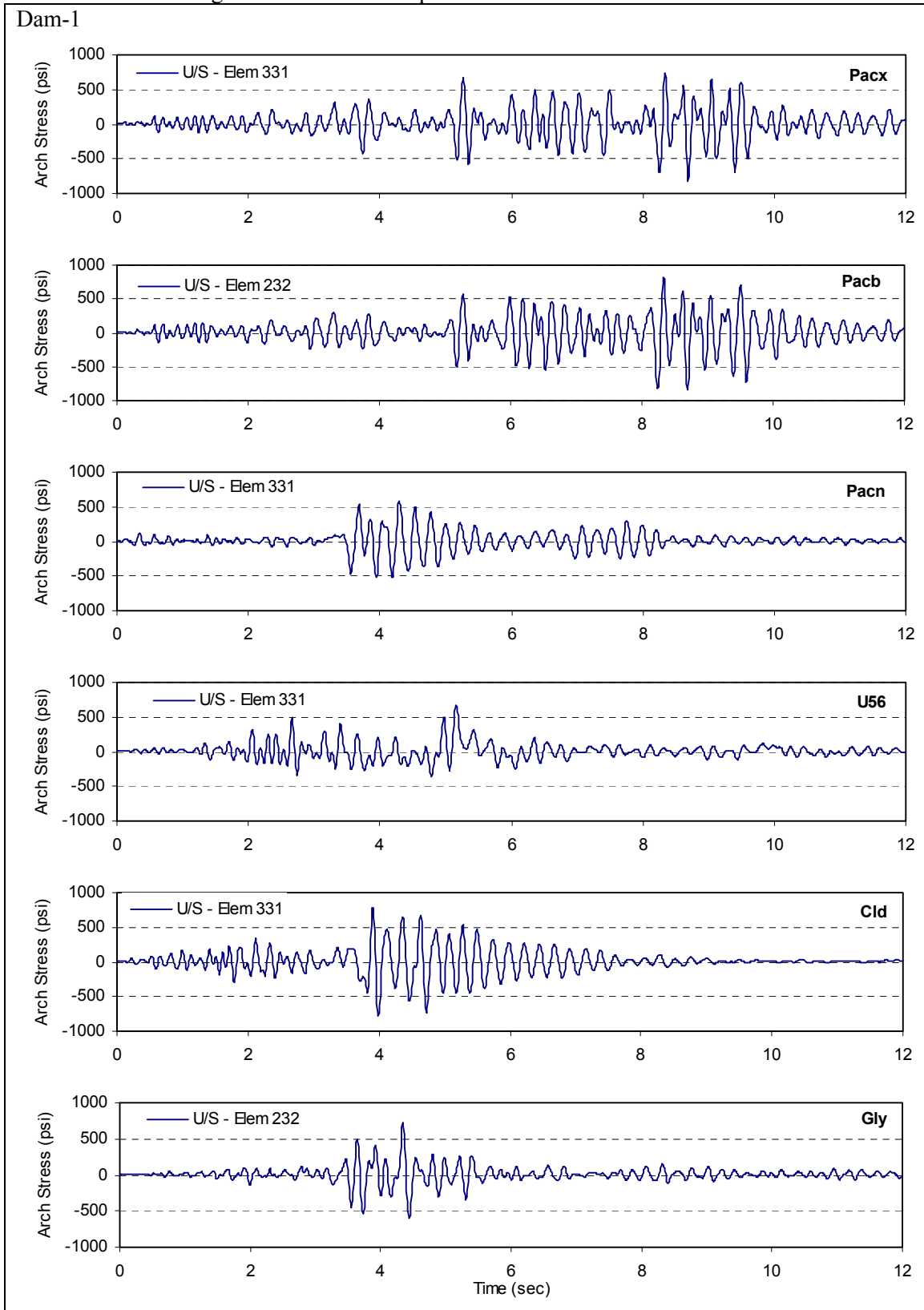


Figure 4-15. Time-history of maximum arch stresses for Dam-1

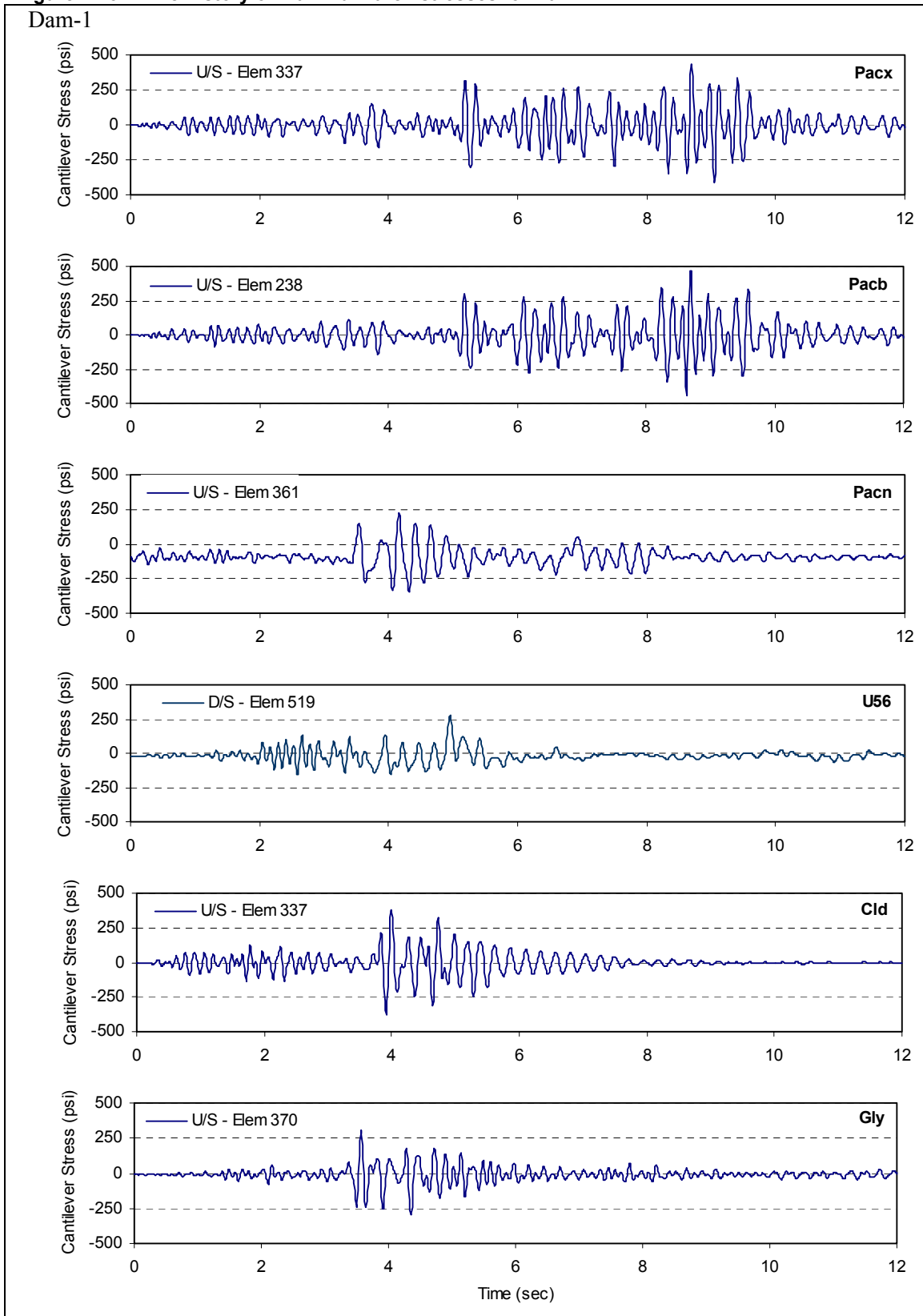


Figure 4-16. Time-histories of maximum cantilever stresses for Dam-1

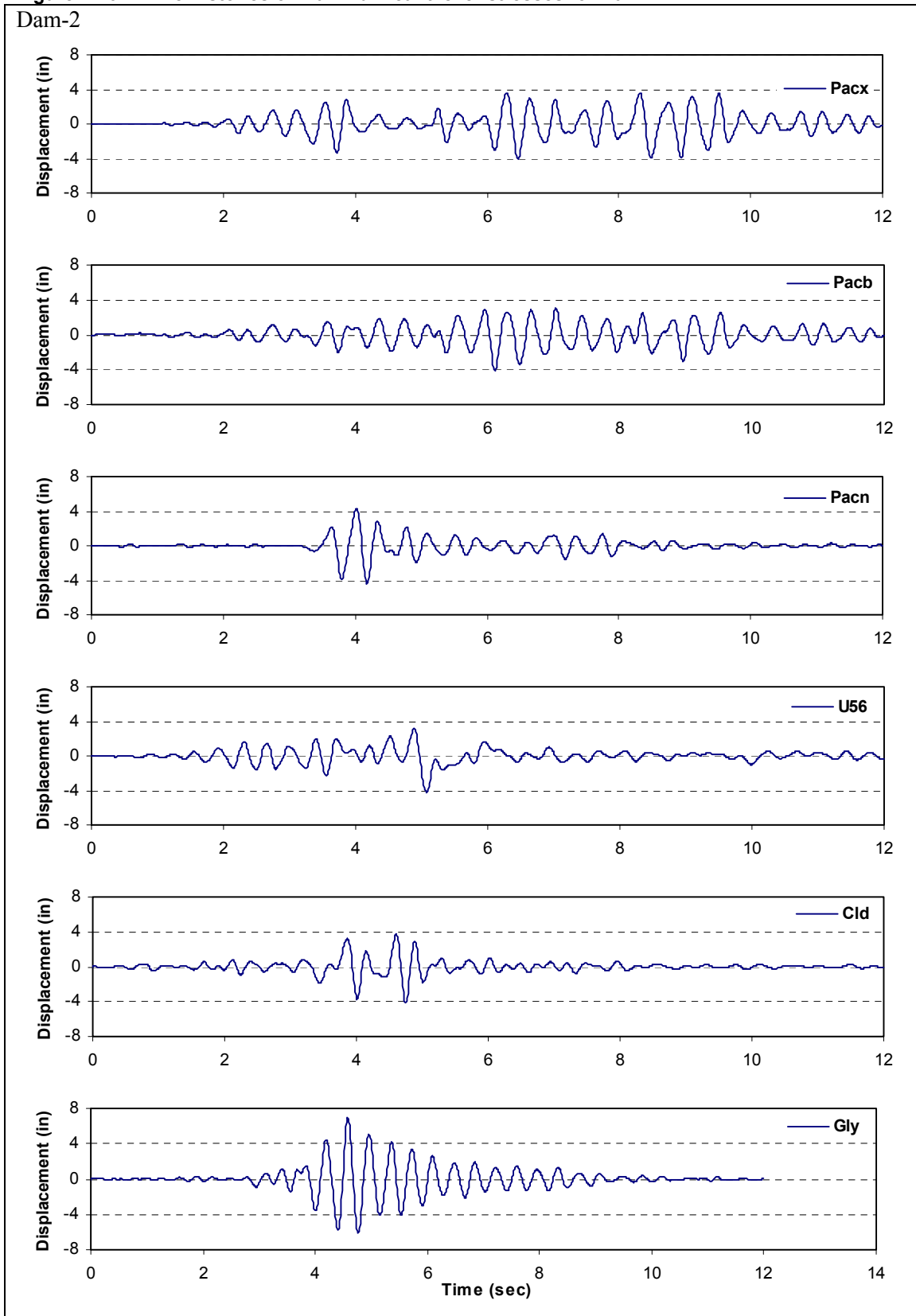


Figure 4-17. Time-histories of midcrest radial displacements for Dam-2

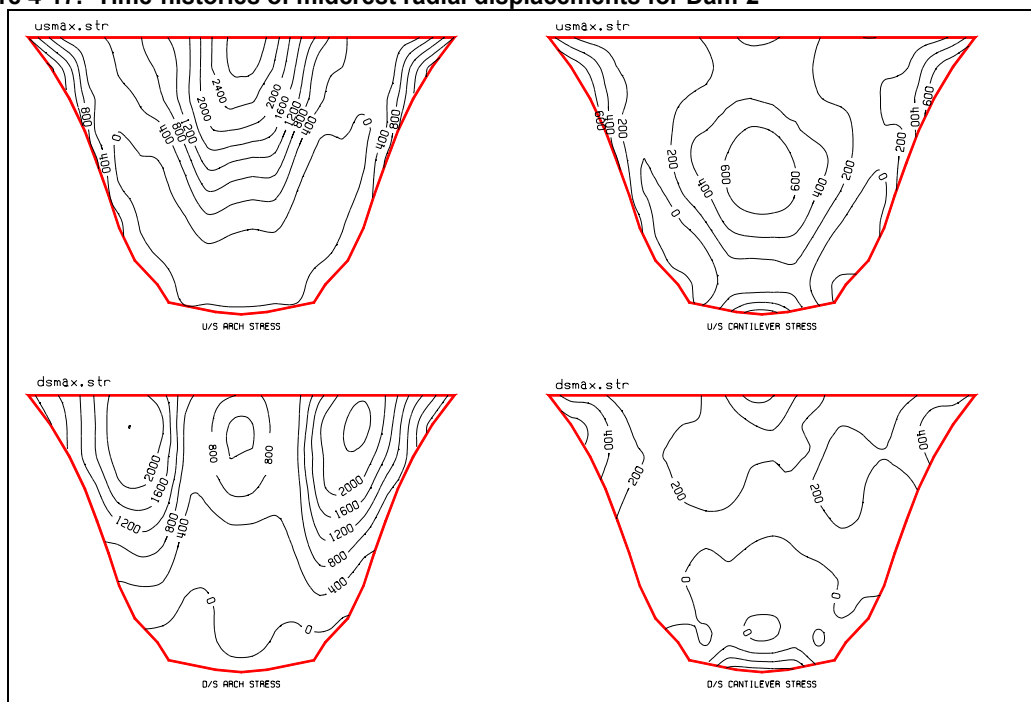


Figure 4-18. Envelope of maximum stresses due to Gilroy record (Dam-2)

using the results of linear elastic analysis. A demand-capacity ratio of 2 allows stresses up to twice the static tensile strength of the concrete or to the level of dynamic apparent tensile strength, as long as the overstressed region is less than 20 percent of the dam surface area. The cumulative duration beyond a certain level of demand-capacity ratio is obtained by multiplying number of stress values exceeding that level by the time-step of the time history analysis. The cumulative inelastic duration in Figure 4-22 refers to the total duration of all stress excursions beyond a certain level of demand-capacity ratio. The cumulative inelastic duration for the example Dam-1 and Dam-2 is presented in Figures 4-23 and 4-24, respectively. The results for Dam-1 show that demand-capacity ratios for all earthquake input records are less than 2 and that the cumulative inelastic duration at all demand-capacity ratios falls below the acceptance curve. On these bases and as discussed in *b(3)* above, Dam-1 responses to the selected earthquake ground motions exhibit negligible nonlinear response in the form of contraction joint opening and closing. The linear time-history method of analysis is therefore acceptable for Dam-1. The results for Dam-2 show that demand-capacity ratios for all earthquake input exceed 2 and that the cumulative inelastic duration, especially for Pacx, Pacb, and Gly, is substantially greater than the acceptance level. This suggests that the selected records cause significant and repeated opening and closing of the contraction joints and that Dam-2 should be analyzed using the nonlinear time-history analysis.

f. Presentation and evaluation. For performance evaluation of arch dams the following results from the linear time-history analysis are required.

(1) Natural frequencies and mode shapes. Natural frequencies and mode shapes of the arch dam-water-foundation system are examined to gain insight into the dynamic characteristics of the dam, its dynamic coupling with the impounded water, and its level of response to earthquake loading. Proximity of the fundamental resonant frequency of the impounded water to fundamental frequency of the dam indicates a strong coupling between the dam and water, thus requiring a more refined dam-water interaction analysis

described in Chapter 2. The frequency range of significant lower modes of vibration should be determined and used in spectrum scaling of the natural earthquake records for dynamic analysis as described in *b(1)* above. The presence of lower modes in the ascending slope of the earthquake response spectra shows an increase in the

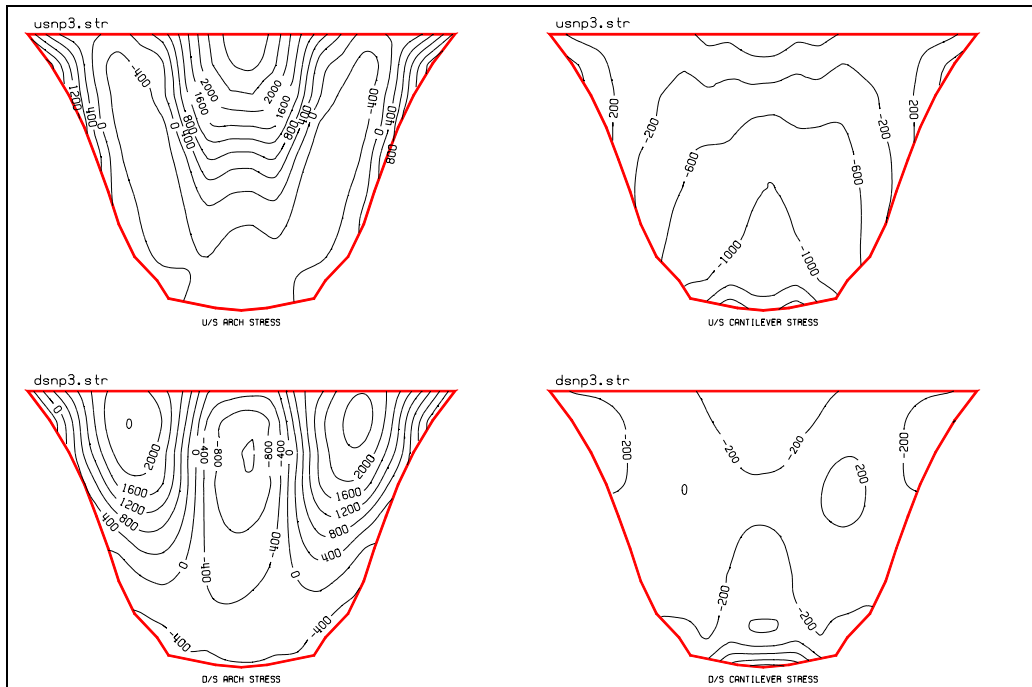


Figure 4-19. Concurrent stresses at the time of maximum arch stress due to Gilroy record (Dam-2)

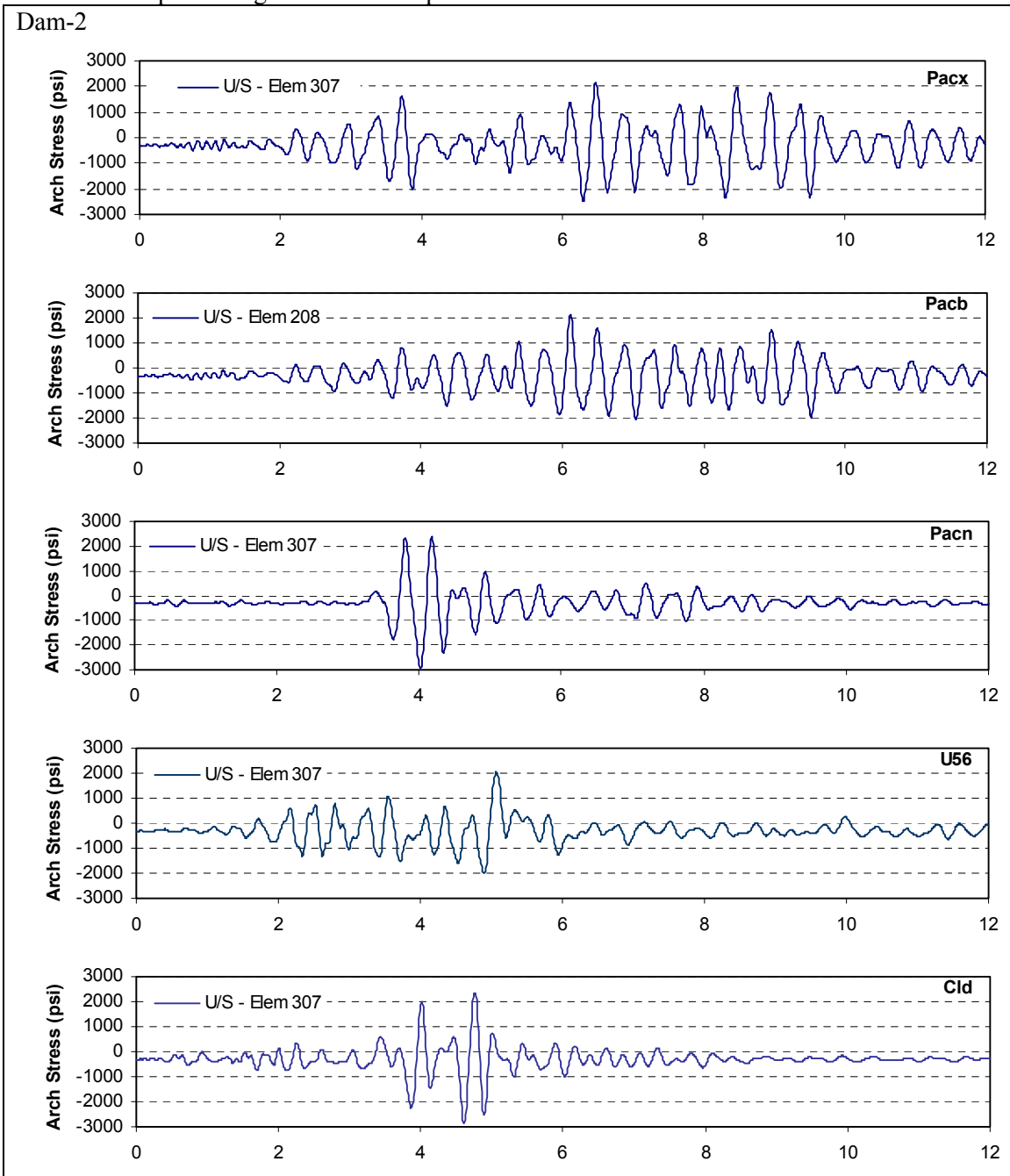
seismic demand if the dam experiences nonlinear response, while the presence of the same in the descending slope indicates reduction of seismic forces.

(2) Displacement histories. The magnitudes and time-histories of nodal displacements at the crest and lower elevations should be presented and examined. Even though displacement magnitudes are not directly used in the performance criteria, their patterns provide a visual means of validating the results and their magnitudes can be employed to assess the overall stability of the dam.

(3) Maximum and minimum stress contours. The maximum and minimum arch and cantilever stresses on the upstream and downstream faces of the dam should be displayed as contour plots and evaluated. The maximum arch and cantilever stress contours show the largest static plus dynamic tensile (positive) stresses that may occur at any location in the dam during the earthquake ground shaking (Figures 4-13 and 4-18). These contours are used to identify critical regions where tensile stresses exceed the tensile or cracking strength of the concrete. Only these regions need to be examined for possible damage. Similarly, contours of the minimum stresses indicate the largest compressive (negative) arch and cantilever stresses that may develop in the dam. The magnitudes of extreme compressive stresses should be compared with the allowable compressive stress to ensure that they meet the required factors of safety. It should be obvious that the maximum and minimum stresses at different locations generally occur at different instants of time and thus are not concurrent.

(4) Time-histories of critical arch and cantilever stresses. Time-histories of the most critical arch and cantilever stresses identified in (3) above should be displayed and evaluated. For each critical arch or cantilever stress point, a pair of stress time-histories, one for the critical point and another for a similar point

on the opposite face of the dam, should be provided. An examination of an arch or cantilever stress pair shows whether the dam undergoes the flexural bending, extension, or a combination of the bending and extension. A pure bending exposes only one-half of the dam cross section to tension, while a pure extension shows the whole section is experiencing tension or compression.



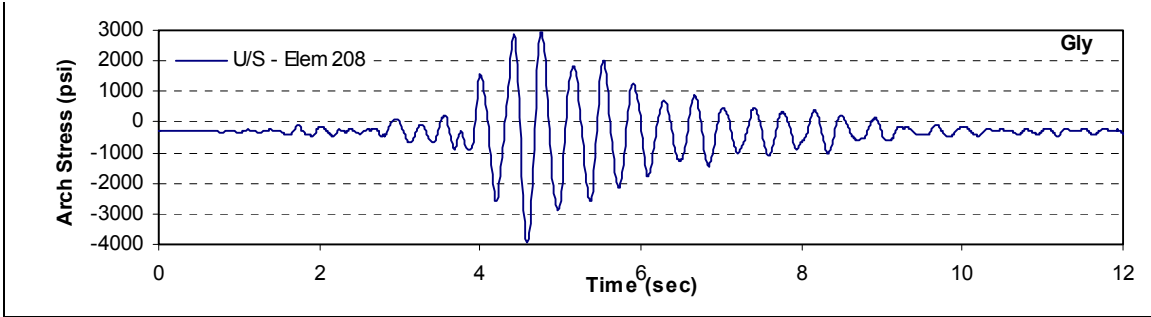
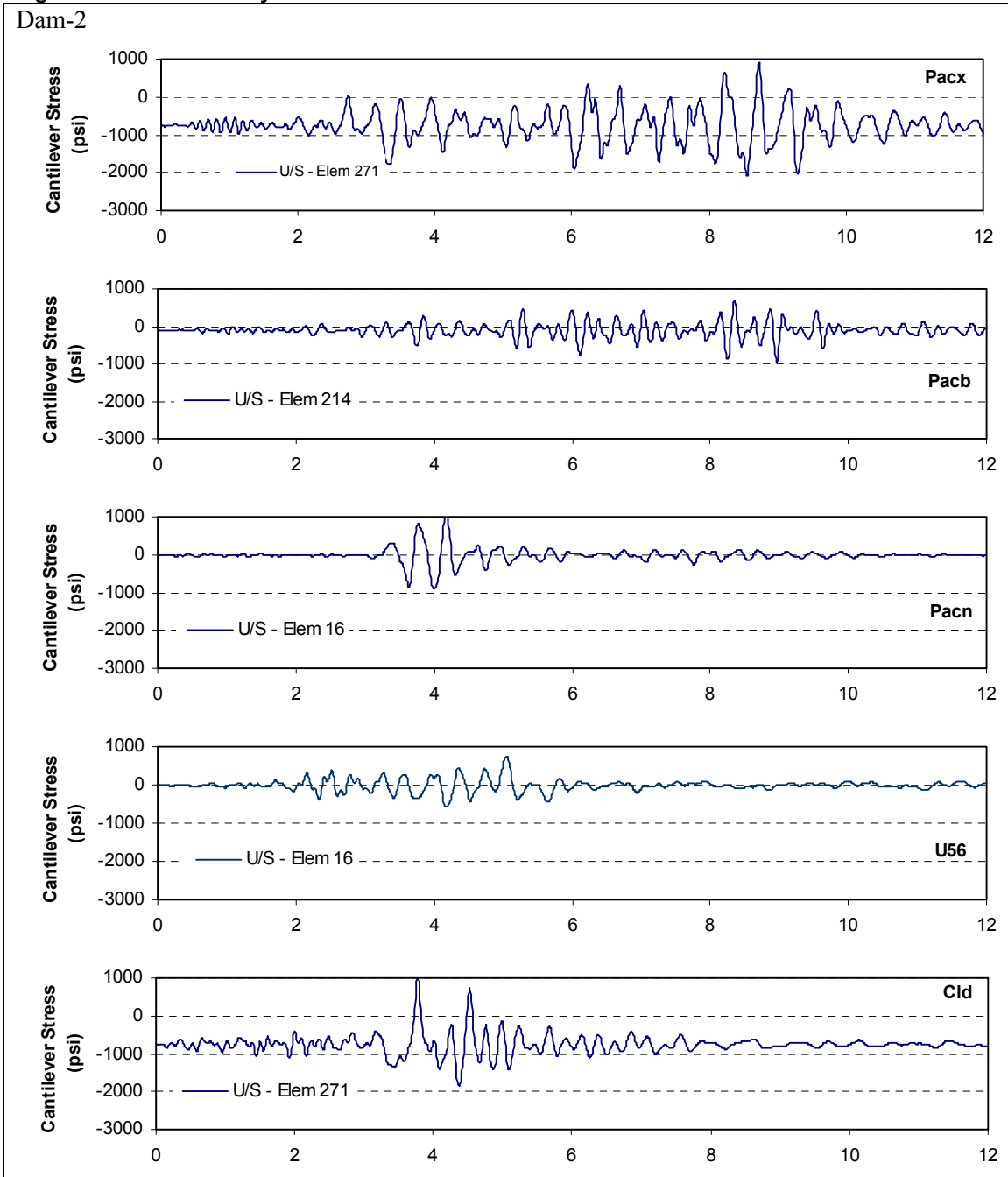


Figure 4-20. Time-history of maximum arch stresses for Dam-2



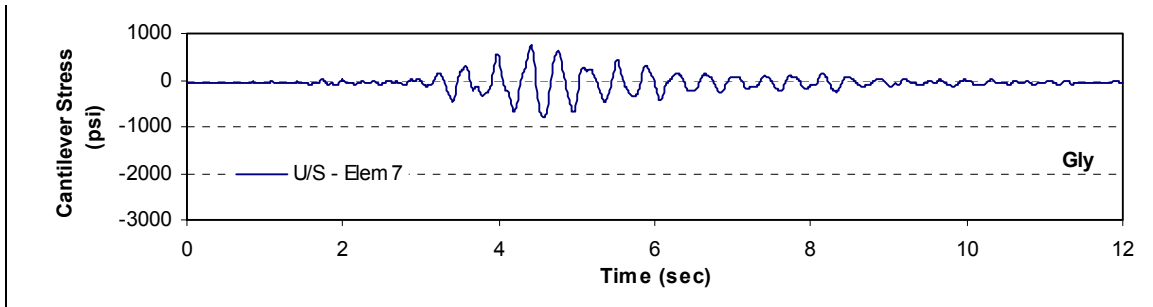


Figure 4-21. Time-history of maximum cantilever stresses for Dam-2

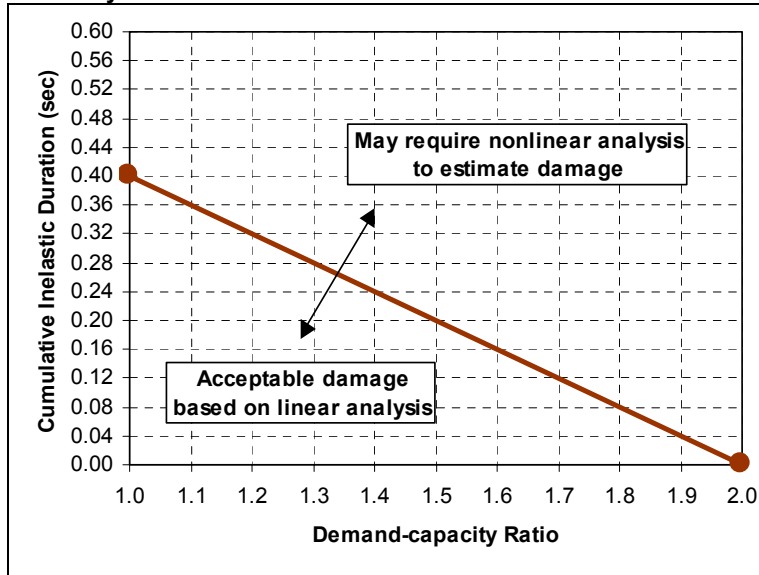


Figure 4-22. Performance curve for linear elastic analysis of arch dams

Table 4-7
Load Combination Cases for Combining Static and Dynamic Stresses for Multicomponent Excitation

Case	Seismic Loads			Static Loads
	Cross-stream Horizontal (H1)	Vertical (V)	Stream Horizontal (H2)	
1 ¹	+	+	+	+
2	+	+	-	+
3	+	-	+	+
4	+	-	-	+
5	-	+	+	+
6	-	+	-	+
7	-	-	+	+
8	-	-	-	+

Note: The (+) and (-) signs indicate the loads are multiplied by +1 or -1 to account for the most unfavorable earthquake direction.
¹ Case-1: Static + H1 + V + H2

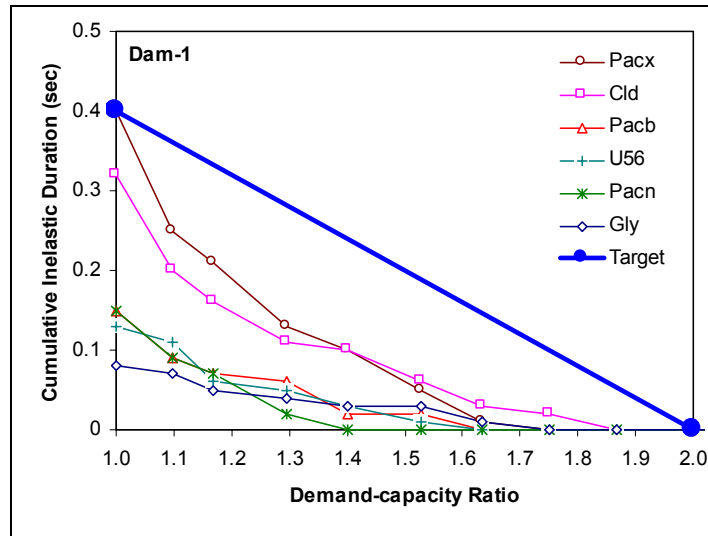


Figure 4-23. Performance assessment of example Dam-1

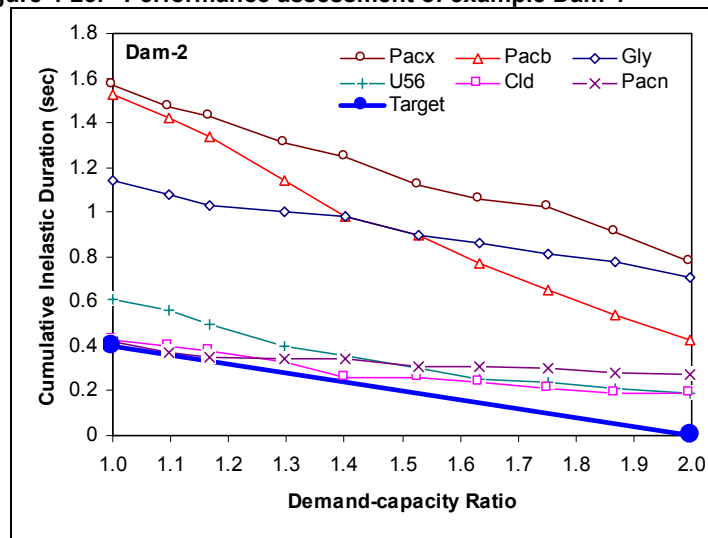


Figure 4-24. Performance assessment of example Dam-2

(5) Concurrent stresses at the time of maximum stresses. The envelopes of maximum stresses in (3) above serve to identify the overstressed regions, critical stress points, and the associated time-histories. From the time-histories of the critical arch and cantilever stresses, the times at which the critical stresses reach their peak values can be determined. The times of maximum arch and maximum cantilever stresses are then used to retrieve simultaneous stress values and prepare concurrent or snapshot stress contours (Figures 4-14, 4-19). The concurrent stresses are evaluated similar to the envelope maximum stresses, except that they represent stress values and are not necessarily all tension.

(6) Demand-capacity ratios. The maximum arch and cantilever stresses in (3) above could also be displayed as plots of the demand-capacity ratios by dividing the computed stresses by the tensile strength of the concrete.

4-5. Navigation Locks

A typical chamber monolith may be analyzed adequately using a 2-D model of the monolith in the cross-stream direction. Dynamic analyses of a miter gate monolith, however, usually require 3-D models or the use of two separate 2-D models in the cross-stream and the upstream-downstream directions. This paragraph discusses presentation and performance evaluation methodology for a miter gate monolith analyzed using 2-D SSI models (Geomatrix 1999). The 2-D cross-stream model of the monolith is approximated by a smeared model, in which the effects of culverts and corrugated pipes are taken into account using appropriate adjustments of the mass and elastic modulus of the concrete. The 2-D model of the monolith in the upstream-downstream direction is also developed the same way by appropriate smearing of the mass and elastic modulus of the concrete and collapsing of the entire monolith into a unit-thick slice. The cross-stream model is analyzed for the vertical and cross-stream components and the upstream-downstream model for the vertical and upstream-downstream components of the MDE ground motion. The results of such analyses include peak values and time-histories of pile forces and moments, lock stresses, and lock section forces and moments at selected critical sections, as well as pile and lock deflections. The pile forces and moments and concrete section forces from each model are then combined to obtain the resulting demands for the design and/or evaluation of the structure, as discussed in the following subparagraphs.

a. Performance criteria. The earthquake performance of reinforced concrete navigation locks is evaluated on the basis of demand-capacity ratios computed for the foundation piles and the concrete sections. The basic approach is to perform linear time-history analysis (with equivalent linear soil modulus) using the load combination cases defined in paragraph 4-5*b* and then compute demand-capacity ratios following procedures described in paragraphs 4-5*c* and 4-5*d* to identify the magnitude and distribution of nonlinear response in various components of the structure. If all computed demand-capacity ratios are less than or equal to 1.0, then the lock structure and piles are expected to respond elastically with no damage. Otherwise demand-capacity ratios of greater than 1.0 show the structure will experience nonlinear behavior in the form of yielding of steel members and cracking or crushing of the concrete. In linear time-history analysis the level of damage or nonlinear behavior will be acceptable if the yielding and associated cumulative yield duration fall below the performance curves provided in Figures 4-25 and 4-26. Regions above the performance curves indicate that the linear time-history analysis is no longer valid and that nonlinear analysis should be employed to assess the damage. The performance curves are given for “Extreme Allowable,” “Minimum Yield,” and “Expected Yield” cases described in paragraph 4-5*c*. In the case of “Minimum Yield,” the performance criteria indicate that yielding should be limited to less than 56 percent of piles and that the peak demand-capacity ratio should not exceed 1.45. The corresponding cumulative yield duration for demand-capacity ratios greater than 1 and 1.45 should be less than 1.52 and 0.02 sec, respectively (Tables 4-8 and 4-9).

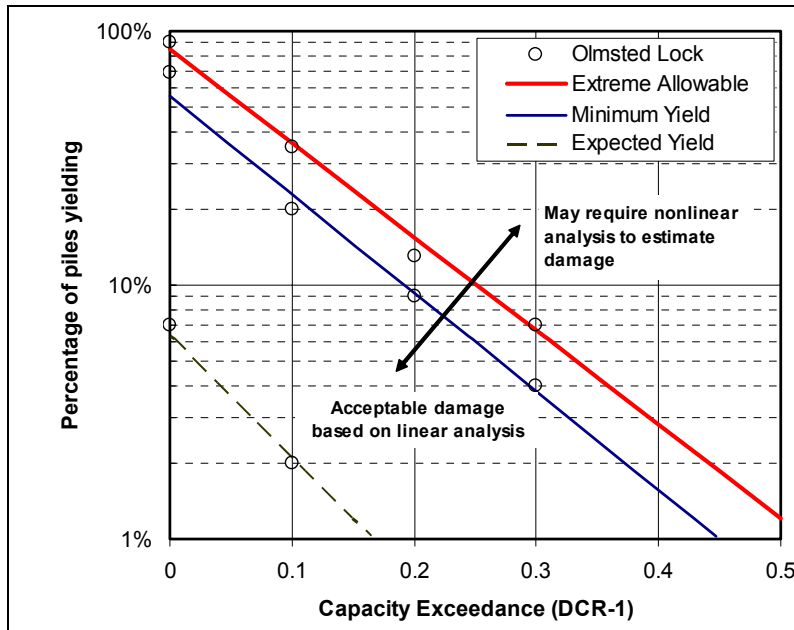


Figure 4-25. Acceptable percentage of pile yielding as a function of demand-capacity ratio levels in linear time-history analysis

b. Load combination cases. Two-dimensional cross-stream and upstream-downstream models of the miter gate monolith are designed or evaluated for two horizontal and vertical excitations plus the effects of usual static loads as described in paragraph 1-6d. Each component of the earthquake input is assumed to have a phasing equal to zero or 180 deg in order to identify the most critical earthquake direction that would give the largest structural response. According to this simple procedure, a total of eight combination cases would be required when all three components of the earthquake input are considered, as listed in Table 4-10.

c. Pile interaction factors (demand-capacity ratios). Performance of the pile-foundation under the MDE loading combination is evaluated using interaction factors or demand-capacity ratios computed in accordance with Equation 4-1.

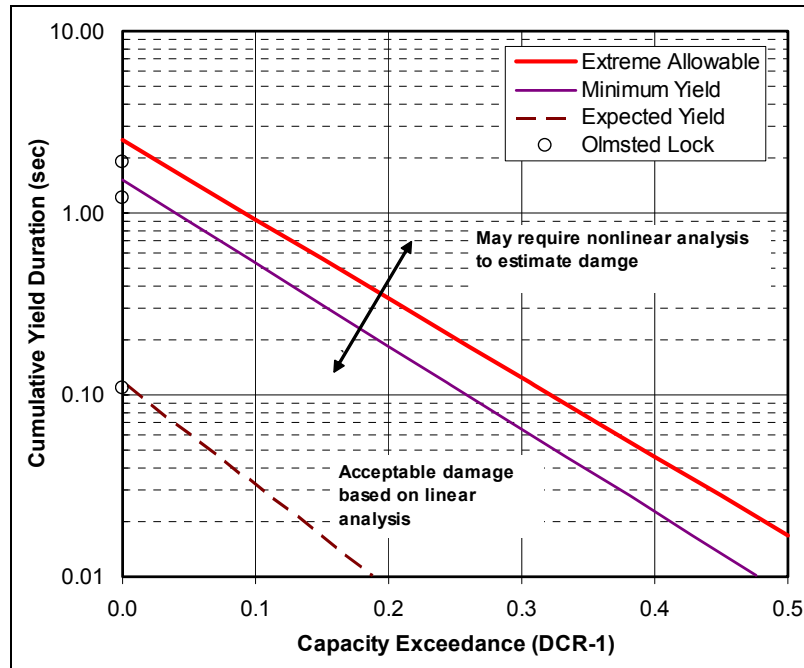


Figure 4-26. Acceptable cumulative yield duration as a function of demand-capacity ratio levels in linear time-history analysis

Table 4-8
Peak Allowable Percentages of Piles Exceeding Various Level of Interaction Factors

Level of Interaction Factor	Extreme Allowable		Minimum Yield 248 MPa (36 ksi)		Expected Yield 303 MPa (44 ksi)	
	Load Combination Case	Percent	Load Combination Case	Percent	Load Combination Case	Percent
1.0	Most Critical	85	Most Critical	56	Most Critical	6
1.1	Most Critical	36	Most Critical	24	Most Critical	2
1.2	Most Critical	16	Most Critical	9		
1.3	Most Critical	7	Most Critical	4		
1.4	Most Critical	3	Most Critical	<2		
1.5	Most Critical	1				

Table 4-9
Peak Allowable Cumulative Yield Duration at Which Pile Interaction Factors Exceed Unity

Level of Interaction Factor	Extreme Allowable		Minimum Yield 248 MPa (36 ksi)		Expected Yield 303 MPa (44 ksi)	
	Load Combination Case	Duration sec	Load Combination Case	Duration Sec	Load Combination Case	Duration sec
1.0	Most Critical	2.5	Most Critical	1.52	Most Critical	0.11
1.1	Most Critical	0.92	Most Critical	0.56	Most Critical	0.03
1.2	Most Critical	0.34	Most Critical	0.18	Most Critical	< 0.01
1.3	Most Critical	0.12	Most Critical	0.07		-
1.4	Most Critical	0.04	Most Critical	0.02		-
1.5	Most Critical	0.02		-		-

Table 4-10
Load Combination Cases for Combining Static and Dynamic Interaction Factors for Multicomponent Excitation

Case	Seismic Loads			Static Loads (Moment / Axial Load)
	Cross-stream Horizontal (H1)	Vertical (V)	Stream Horizontal (H2)	
1 ¹	+	+	+	+
2	+	+	-	+
3	+	-	+	+
4	+	-	-	+
5	-	+	+	+
6	-	+	-	+
7	-	-	+	+
8	-	-	-	+

Note: + = seismic input is multiplied by +1 (zero phase)
 - = seismic input is multiplied by -1 (180-deg phase)
¹ Case-1: Static + H1 + V + H2

$$I_p = \left(\frac{f_a}{F_a} + \frac{m_x}{M_x} + \frac{m_y}{M_y} \right)_{static} + \left(\frac{f_a}{F_a} + \frac{m_x}{M_x} + \frac{m_y}{M_y} \right)_{dynamic} \quad (4-1)$$

where

I_p = pile interaction factor

f_a, m_x, m_y = the axial force and bending moments (force and moment demands) computed either from the static or dynamic analysis

F_a = allowable axial force (force capacity) for combining with allowable moment (moment capacity)

M_x, M_y = allowable moments (moment capacities), respectively, about the strong and weak axes of the pile

For a complete performance evaluation of the piles the three performance cases in Table 4-11 may be considered. The “Extreme Allowable” case is based on EM 1110-2-2906, which requires a factor of safety (FS) of 1.15 for the extreme loading combination and an ASTM A36 for the yield strength. The “Extreme Allowable” case with an FS of 1.15 is considered appropriate when the SPSI effects are modeled approximately and the earthquake input is developed using standard or empirical relationships. However, the use of yield strength (i.e., FS = 1) in computing pile capacities can be justified if dynamic SPSI analyses are employed and extensive geotechnical and site-specific seismic hazard studies are performed. In the absence of measured data a minimum yield strength of 248 MPa (36 ksi) and an FS of 1.0 should be used. This performance case is called “Minimum Yield” case. In situations where testing of steel piles consistently indicates yield strengths of greater than 248 MPa (36 ksi), the average measured yield strength may be employed in the final evaluation. The performance condition based on the expected yield strength is called “Expected Yield” case.

Case	Condition	Yield Strength	Factor of Safety (FS)
I	Extreme Allowable	Nominal: 248 MPa (36 ksi)	1.15
II	Minimum Yield	Nominal: 248 MPa (36 ksi)	1.0
III	Expected Yield	Measured: 303 MPa (44 ksi)	1.0

d. *Allowable pile deflection.* The allowable pile lateral deflection is determined by a separate analysis of the pile-soil system incorporating measured data from the pile load tests (U.S. Army Engineer District, Louis-

ville, 1994b). The allowable deflection or “deflection capacity” is usually selected as a fraction of the pile head deflection that initiates first yielding of the pile. In determining the allowable deflection value, consideration should be given to rebounding of the pile. The study by U.S. Army Engineer District, Louisville (1994b) indicates that as long as the piles do not reach yield condition, a 50 percent rebound of the pile can be expected.

e. Interaction diagrams (demand-capacity ratios) for concrete sections. The axial force-bending moment interaction diagram, plotted in terms of ultimate axial loads as ordinates and ultimate moments as abscissas, characterizes the strength of a reinforced concrete section. Interaction diagrams therefore provide a means for comparing the required strengths (force demands) due to the loading combination cases defined in paragraph 4-5*b* with the design strengths (force capacities) of reinforced concrete sections. The nominal strength and design strength of a reinforced concrete section can be determined using the CORPS library program CSTAR for reinforced concrete design and investigation. For a given section the force capacities are determined from the intersection of the design strength curve with a line drawn from the origin to the required axial force-moment pair computed for the section.

f. Presentation and performance evaluation.

(1) Pile deflections. Pile deflections refer to relative dynamic displacements between pile head and pile tip. The maximum vertical and horizontal pile deflections resulting from the applied loads should be limited to allowable values to ensure integrity of the structure.

(2) Pile forces and moments. Pile axial forces and bending moments are used in accordance with Equation 4-1 to compute pile interaction factors in time domain for the eight combination cases of the static and seismic loads listed in Table 4-10. For each performance criteria case shown in Table 4-11, the resulting time-histories of interaction factors should be processed and presented according to the following list to facilitate performance evaluation and estimation of probable damage:

(a) Peak dynamic pile forces and moments.

(b) Pile forces and moments for static, static plus dynamic values at peak moment, static plus dynamic values at peak axial, and static plus dynamic values at peak shear.

(c) Pile forces and moments for static plus peak dynamic values.

(d) Table of peak interaction factors and associated forces and moments corresponding to the most critical load combination.

(e) Graph of peak interaction factors for the most critical load combination (Figures 4-27 to 4-29).

(f) Time-history of interaction factors for the most critical piles (Figure 4-30).

(g) Duration or number of time-steps that the interaction factors for each pile exceed unity.

(h) Time-history plots of the percentages of piles having an interaction factor (DCR) exceeding 1.0, 1.1, 1.2, and 1.3.

(i) Table of peak percentages of piles having an interaction factor exceeding 1.0, 1.1, 1.2, and 1.3 (Table 4-12)

(j) Table of peak duration at which pile interaction factors exceed unity (Table 4-13).

Extreme Allowable Case

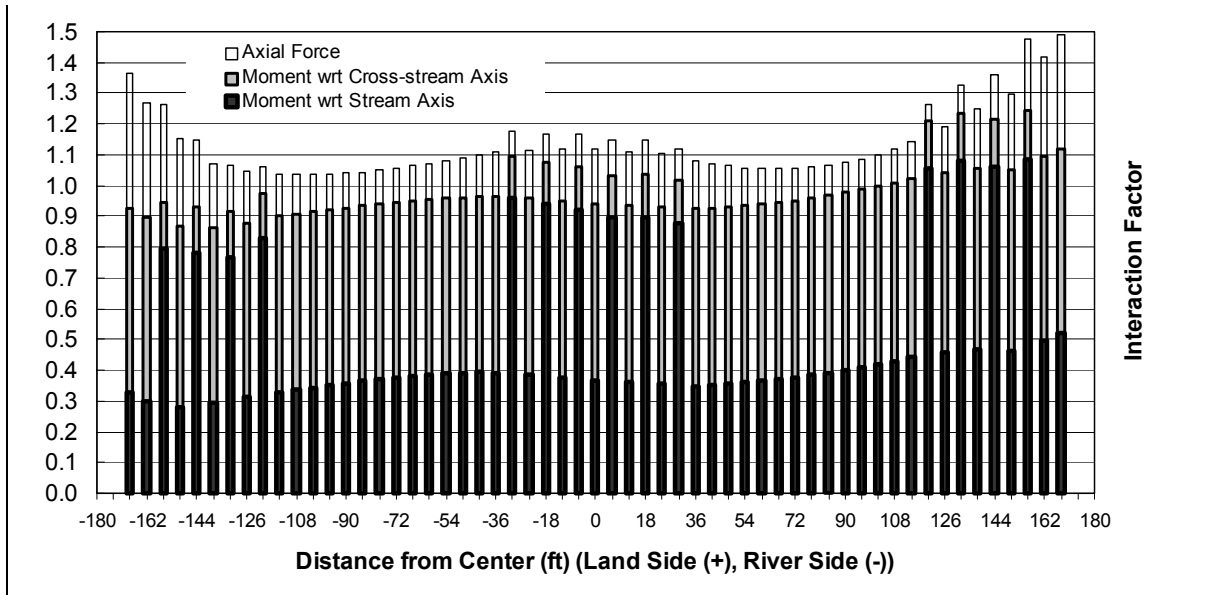


Figure 4-27. Combined static and dynamic interaction factors for H-piles under lower miter gate monolith subjected to MDE; extreme allowable case, FS = 1.15; distance to downstream face = 17 m (56.74 ft)

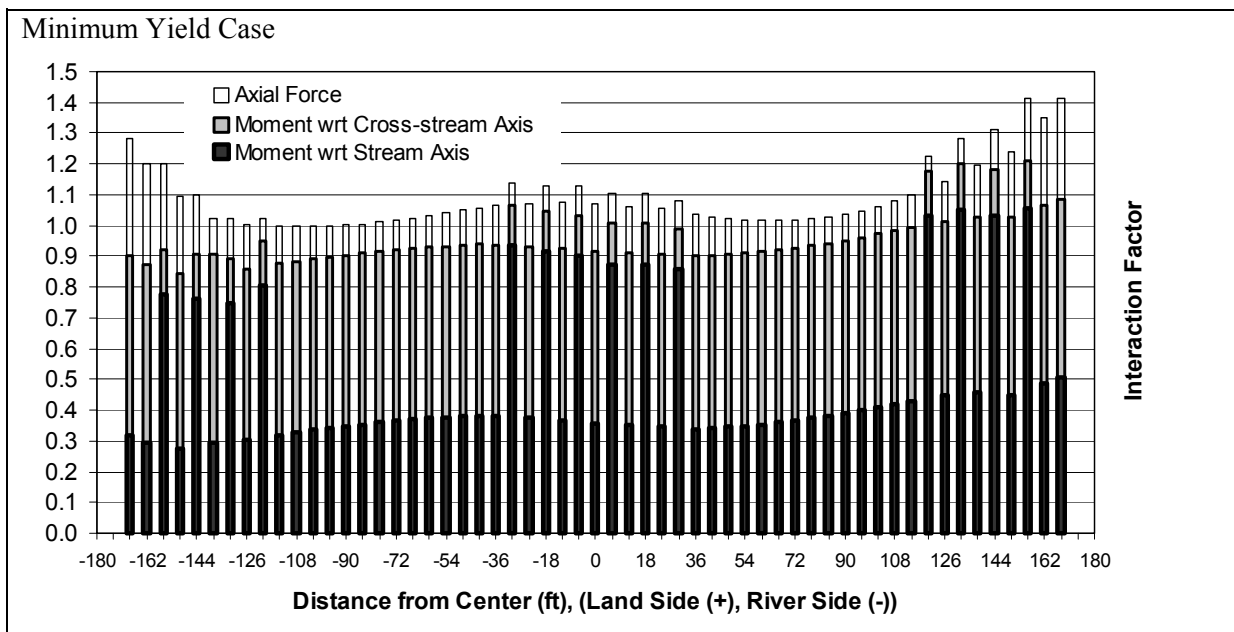


Figure 4-28. Combined static and dynamic interaction factors for H-piles under lower miter gate monolith subjected to MDE; minimum yield case, FS = 1.0; distance to downstream face = 17 m (56.74 ft)

The evaluation process starts with comparison of peak pile forces and moments ((b) and (c) above), acting individually, with the allowable values set forth in EM 1110-2-2906. The combined axial forces and bending moments are assessed using the interaction factors and information described under (d) to (j) above. For three

Expected Yield Case

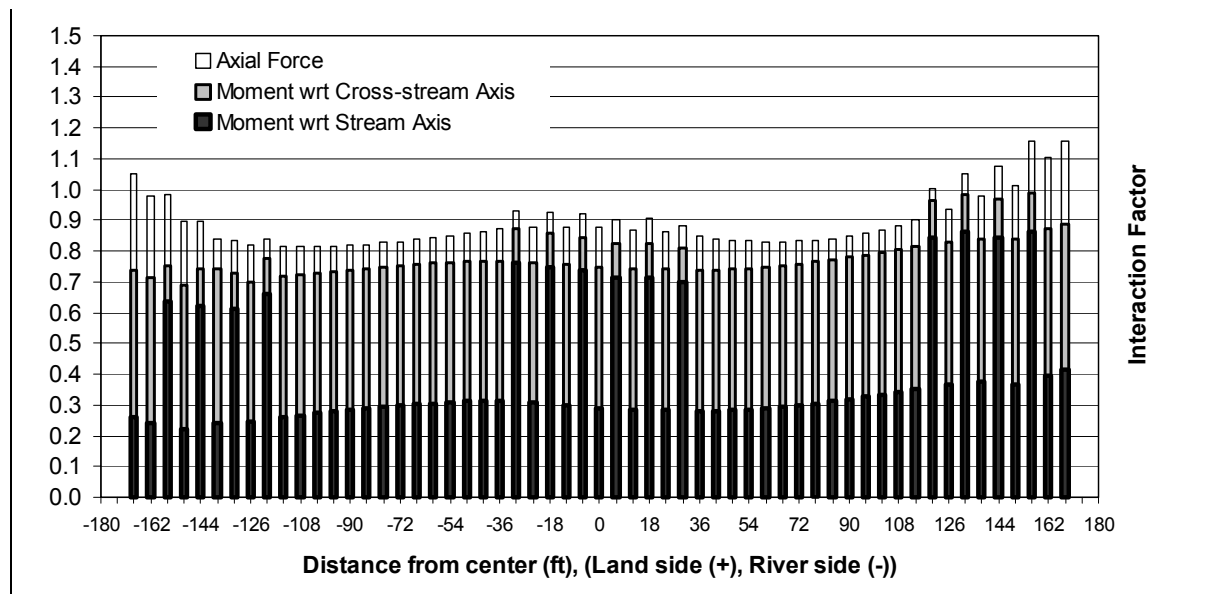


Figure 4-29. Combined static and dynamic interaction factors for H-piles under lower mitergate monolith subjected to MDE; expected yield case, FS = 1.0; distance to downstream face = 17 m (56.74 ft)

performance cases of Extreme Allowable, Minimum Yield, and Expected Yield, the graphs of peak interaction factors (Figures 4-27 to 4-29) provide a snapshot of the peak demand-capacity ratios (interaction factors) that each pile might experience at some instant of time during the earthquake shaking. In the Extreme Allowable Case, if all demand-capacity ratios are less than or equal to unity, all piles remain elastic and satisfy the required factor of safety (FS = 1.15). No further evaluation of piles is therefore necessary. Otherwise some piles might yield, requiring an evaluation on the basis of the minimum or expected yield strength of the pile (i.e., FS = 1) in accordance with paragraph 4-5c. In either case demand-capacity ratios ≤ 1 indicate a satisfactory performance with no need for additional evaluation. Otherwise percentage of piles whose combined demand-capacity ratios exceeding 1.0, 1.1, 1.2, and 1.3 (Figures 4-31 to 4-33) and the corresponding duration of demand-capacity ratio cycles whose values exceed each of these levels should be determined and compared with the performance curves. For comparison percentage of piles showing yielding and the corresponding cumulative yield duration for the Olmsted lower miter gate monolith are shown on the performance curves and summarized in Tables 4-12 and 4-13.

(3) Lock deflections and stresses. Dynamic displacements at the top and base of the lock walls should be computed and the relative displacements between the top and the base determined. The computed peak relative displacements should be within 0.1 percent of the lock height in order to limit the damage.

(4) Lock section forces and moments. Time-histories of dynamic forces and moments at selected concrete sections (Figure 4-34) are combined with the corresponding static forces and moments. Displayed as scatter plots, the resulting force demands are directly compared with the axial force-bending moment interaction diagrams discussed in *e* above. Figures 4-35 and 4-36 are examples of such scatter plots for Sections 1 and 4 (see Figure 4-33) of the Olmsted lower miter gate monolith for four loading combinations discussed in *b* above. The results indicate that the peak demand-capacity ratios for Section 1 are equal to unity and for Section 4 are much less than unity, an indication that the response of the monolith is essentially elastic or nearly elastic. Should the demand-capacity ratios for the concrete sections exceed unity, the performance criteria in *a* above must be followed to assess the severity of nonlinear response or damage.

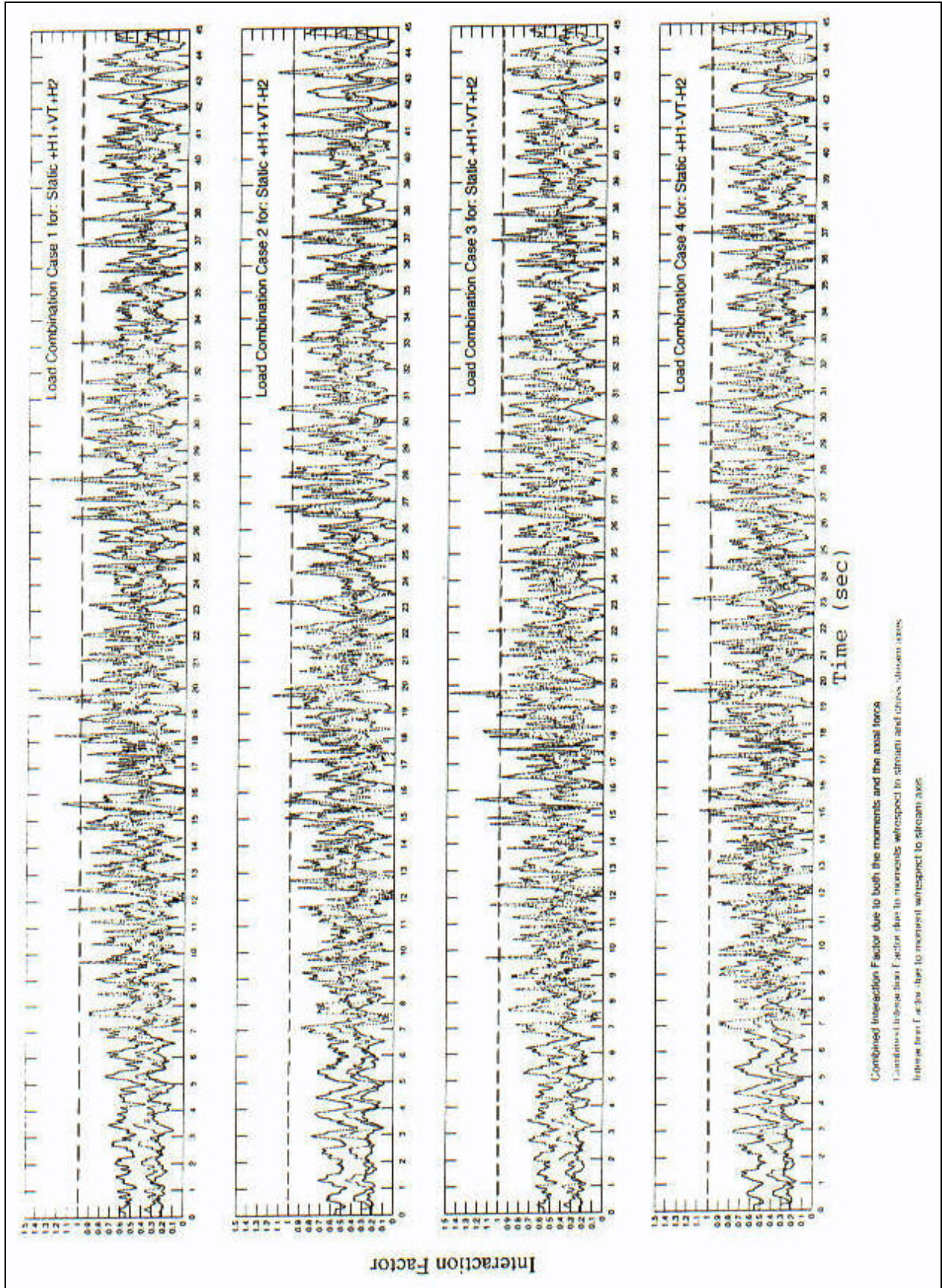


Figure 4-30. Time-history of interaction factors for the most critical piles

Table 4-12
Peak Percentages of Piles Exceeding Various Levels of Interaction Factors

Level of Interaction Factor	Extreme Allowable		Minimum Yield		Expected Yield	
	Load Combination Case	Percent	Load Combination Case	Percent	Load Combination Case	Percent
1.0	3	91	3	69	3	7
1.1	3	35	3	20	3	2
1.2	3	13	3	9	-	-
1.3	6	7	3	4	-	-

Table 4-13
Peak Accumulated Duration at Which Pile Interaction Factors Exceed Unity

Level of Interaction Factor	Extreme Allowable		Minimum Yield		Expected Yield	
	Load Combination Case	Duration sec	Load Combination Case	Duration sec	Load Combination Case	Duration sec
1.0	3	1.90	3	1.21	6	0.11

4-6. Free-Standing Intake Towers

The approximate level of earthquake damage in free-standing intake towers can be assessed using the linear time-history analysis procedures. A typical free-standing intake tower is modeled and evaluated as a 2- or 3-D cantilever column with appropriate stiffness, lumped masses, and damping. As outlined in Chapter 2, the lumped masses include the surrounding and contained water as well as the self-weight of the structure. The dynamic response is obtained for a minimum of three sets of site-specific earthquake-ground-acceleration time-histories as the input. Each set includes one vertical and two orthogonal horizontal components. For free-standing intake towers, the effects of vertical component of ground motion can usually be ignored, unless the tower exhibits significant rocking response. The results of analysis include peak values and time-histories of displacements and element forces. Other parameters of importance to damage assessment include demand-capacity ratios, cumulative duration of force excursions above the strength capacity, and the length of tower over which the strength capacity is exceeded. The procedure for estimation of the probable level of damage for free-standing intake towers was formulated using the results from linear time-history analyses of an example intake tower subjected to four different sets of earthquake ground motions. The accuracy of the procedure was verified by several nonlinear time-history analyses, which employed an elastic-plastic moment-rotation relationship for the structural members.

a. Nonlinear behavior and modes of failure. Figure 4-37 provides some examples of probable modes of failure for free-standing intake towers due to overstressing and structural instability conditions. Different combinations and sequence of failure modes shown in Figure 4-37a, b, c, and d are also conceivable. The desired mode of behavior is the moderate flexural yielding of the base region, which controls the strength, inelastic deformation, and energy dissipation capability of the tower during the earthquake shaking. This is because concrete structures with adequate reinforcement and detailing exhibit more ductile behavior in bending than in shear due to yielding of the flexural reinforcements. The behavior of reinforced concrete walls, with seismic response behavior similar to that of towers, indicates that the largest energy dissipation with the smallest strength degradation is feasible through flexural hinging but not shear (Paulay and Priestley 1992). This superior performance therefore makes the bending the most desirable mode of nonlinear behavior (Figure 4-37a). By contrast, shear failures tend to be nonductile, and can often lead to severe damage and even collapse of the structure. Failure modes such as diagonal tension/compression cracks (4-33b), shear or bond failure along the construction joints and anchorage (4-33c), and rocking (4-33d) are undesirable due to small energy dissipation and rapid strength degradation and should be avoided whenever possible. The shear forces, therefore, are not permitted to exceed the shear capacities of the members. Modes of failure and nonlinear response of intake towers depend largely on the arrangement and the amount of vertical and shear reinforcements (Dove 1998).

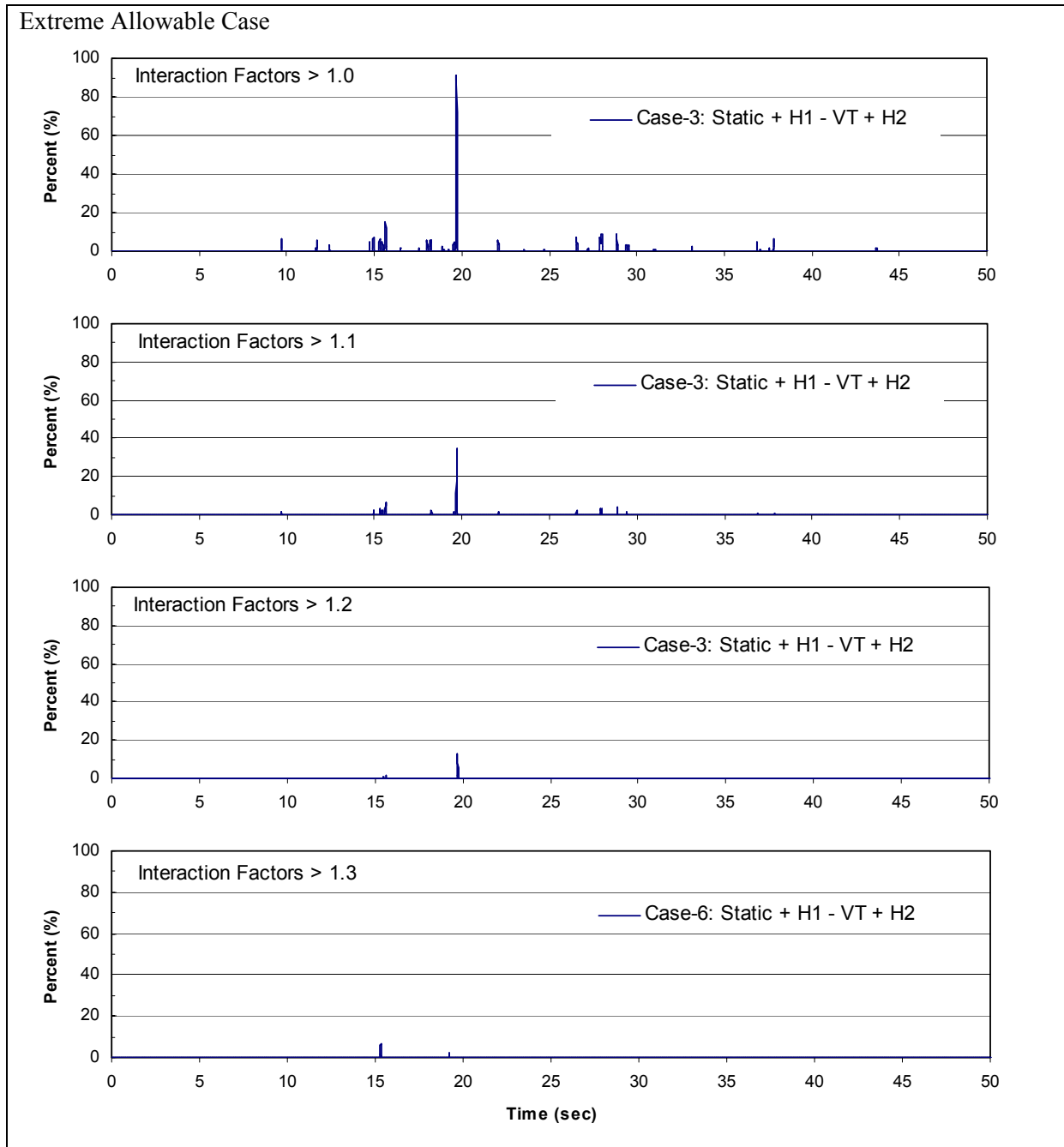


Figure 4-31. Peak percentage of H-piles whose combined interaction values exceed 1.0, 1.1, 1.2, and 1.3; extreme allowable case; lower miter gate monolith for MDE

In nonlinear analyses, the effects of reinforcements should be modeled appropriately in order to capture the most likely mode of behavior. For example, lightly reinforced concrete towers may offer limited ductility with prevailing sliding and/or overturning modes of failure (Figure 4-37c and d).

b. Influence of earthquake ground motion. The magnitude and characteristics of earthquake ground motions can significantly affect the dynamic response and the level of damage that could occur in an intake

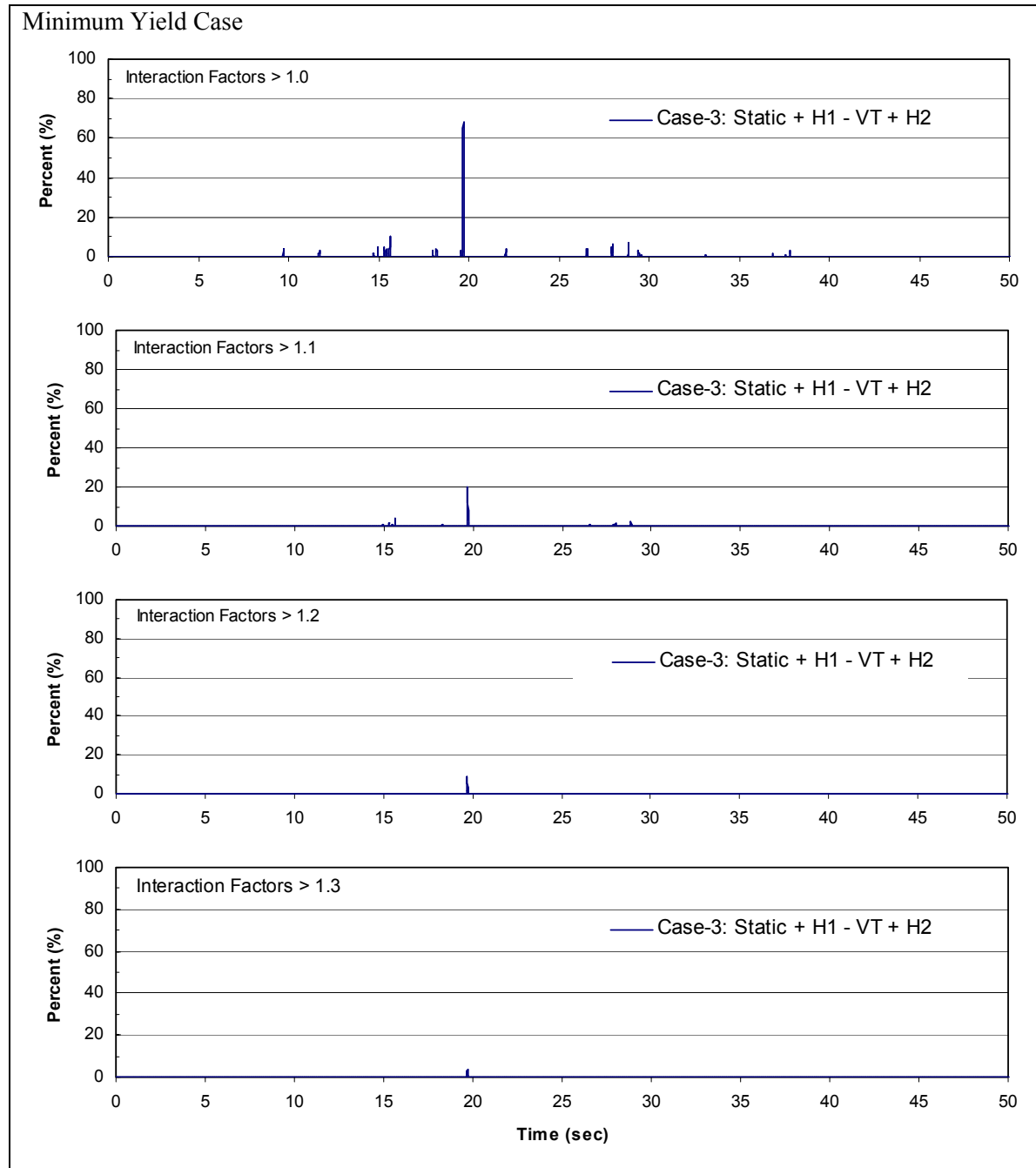


Figure 4-32. Peak percentage of H-piles whose combined interaction factor values exceed 1.0, 1.1, 1.2, and 1.3; minimum yield case; lower miter gate monolith for MDE

tower. The probable level of damage for the example intake tower was therefore evaluated for four sets of recorded acceleration time-histories selected from four different earthquake events having a moment magnitude M_w in the range of 6.0 to 6.9. As shown in Table 4-14, the style of faulting also varied for each event and included a strike-slip, an oblique, or a reverse fault. In general, recordings from these earthquakes showed differences in the frequency content, duration, energy content, and pulse sequencing, all of which were considered in the formulation of damage criteria discussed in *c* below.

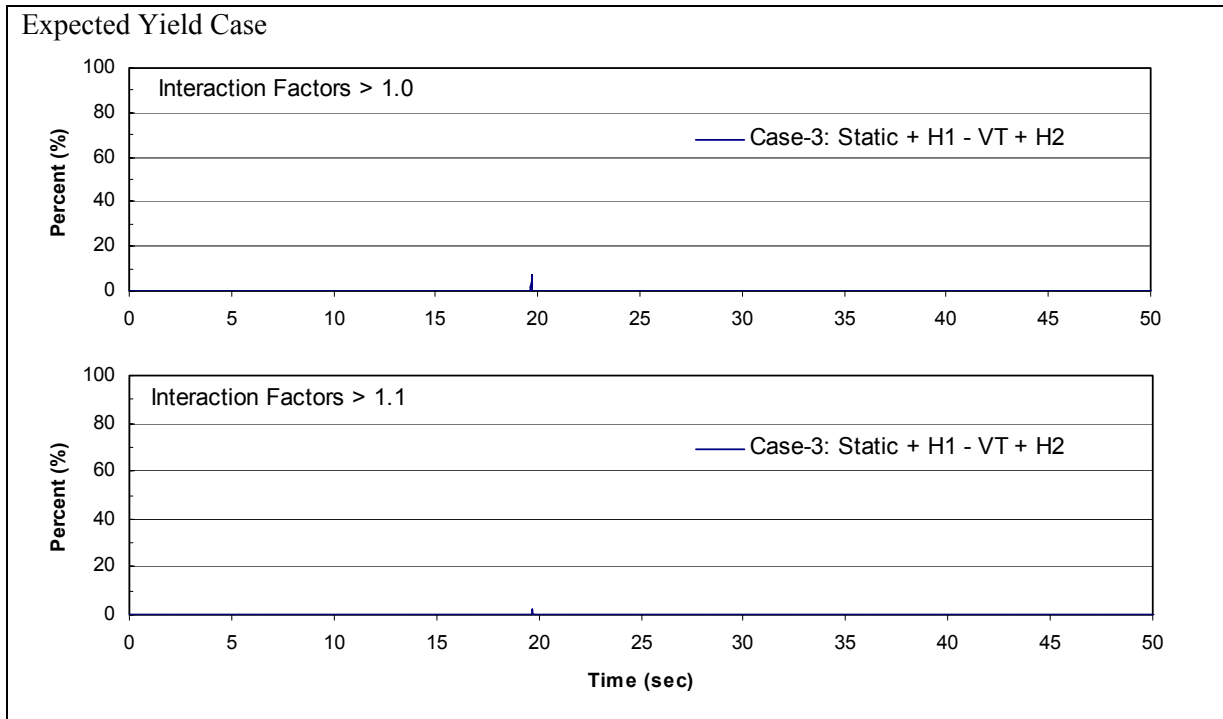


Figure 4-33 Peak percentage of H-piles whose combined interaction factor values exceed 1.0 and 1.1; expected yield case; lower miter gate monolith for MDE

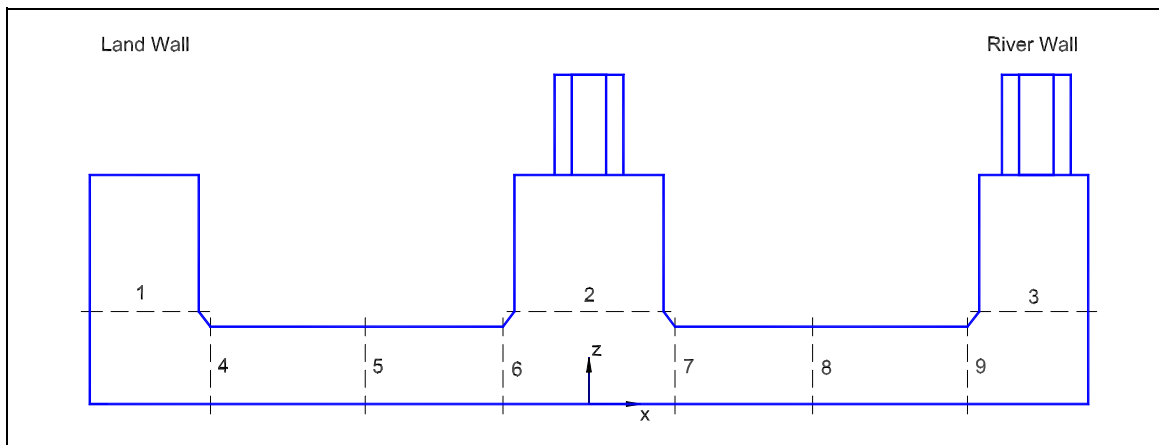


Figure 4-34. Critical lock sections for assessment of forces and moments

(1) Selected earthquake ground motions. Table 4-14 lists the four earthquake ground motion records with their corresponding characteristics and the scaling factors used in this study. These natural records were scaled such that the average of ordinates for the response spectra of all four records would match a smooth design response spectrum in the period range of 0.03 to 0.6 sec important to the example problem. The smooth design response spectrum was developed representative of the median ground motions corresponding to an earthquake M_w 6.5 at a distance of 5 km. Figures 4-38 and 4-39 provide comparisons between the smooth response spectrum with response spectra of the scaled primary and secondary natural records. Time-histories of the scaled records are displayed in Figures 4-40 to 4-43.

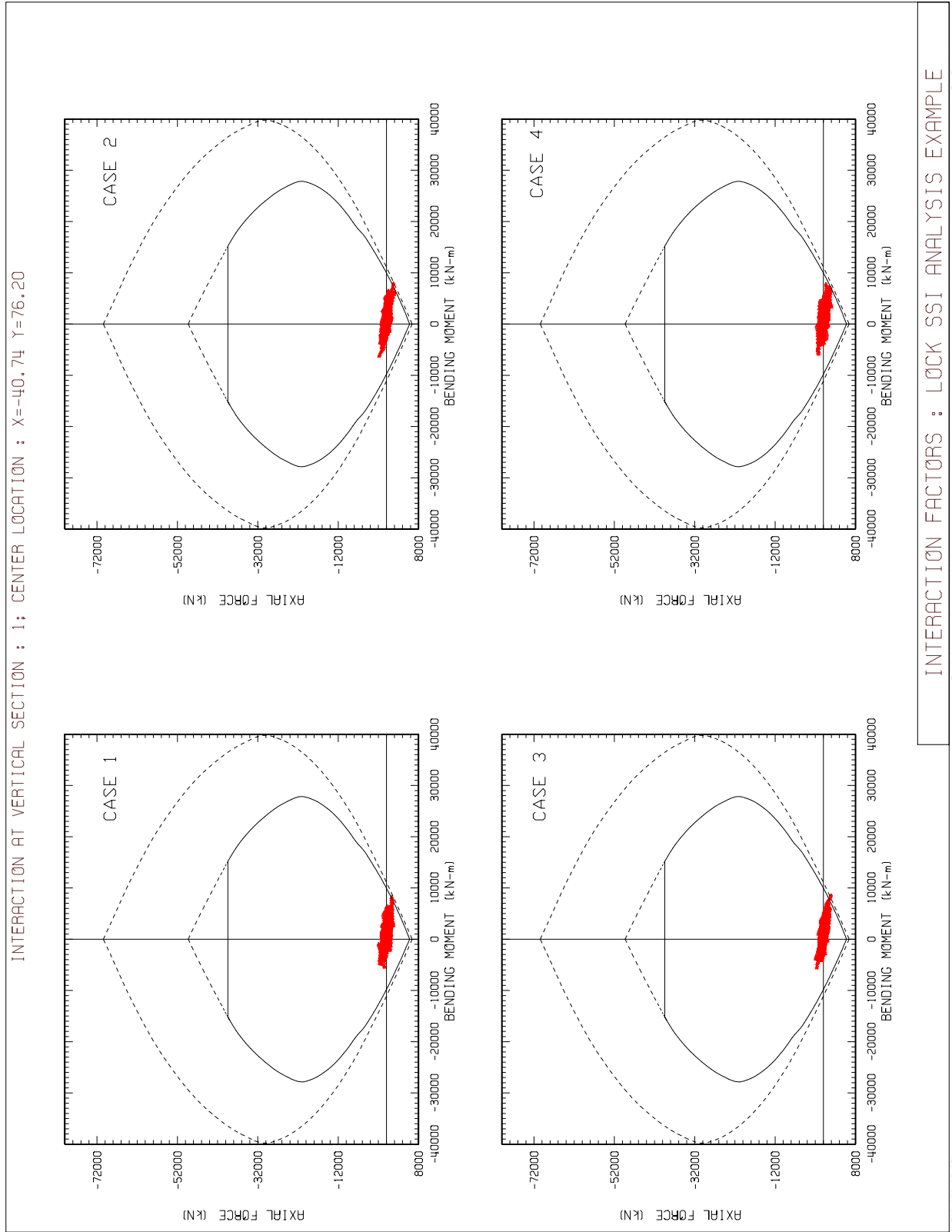


Figure 4-35. Axial force versus bending moment of concrete Section 1

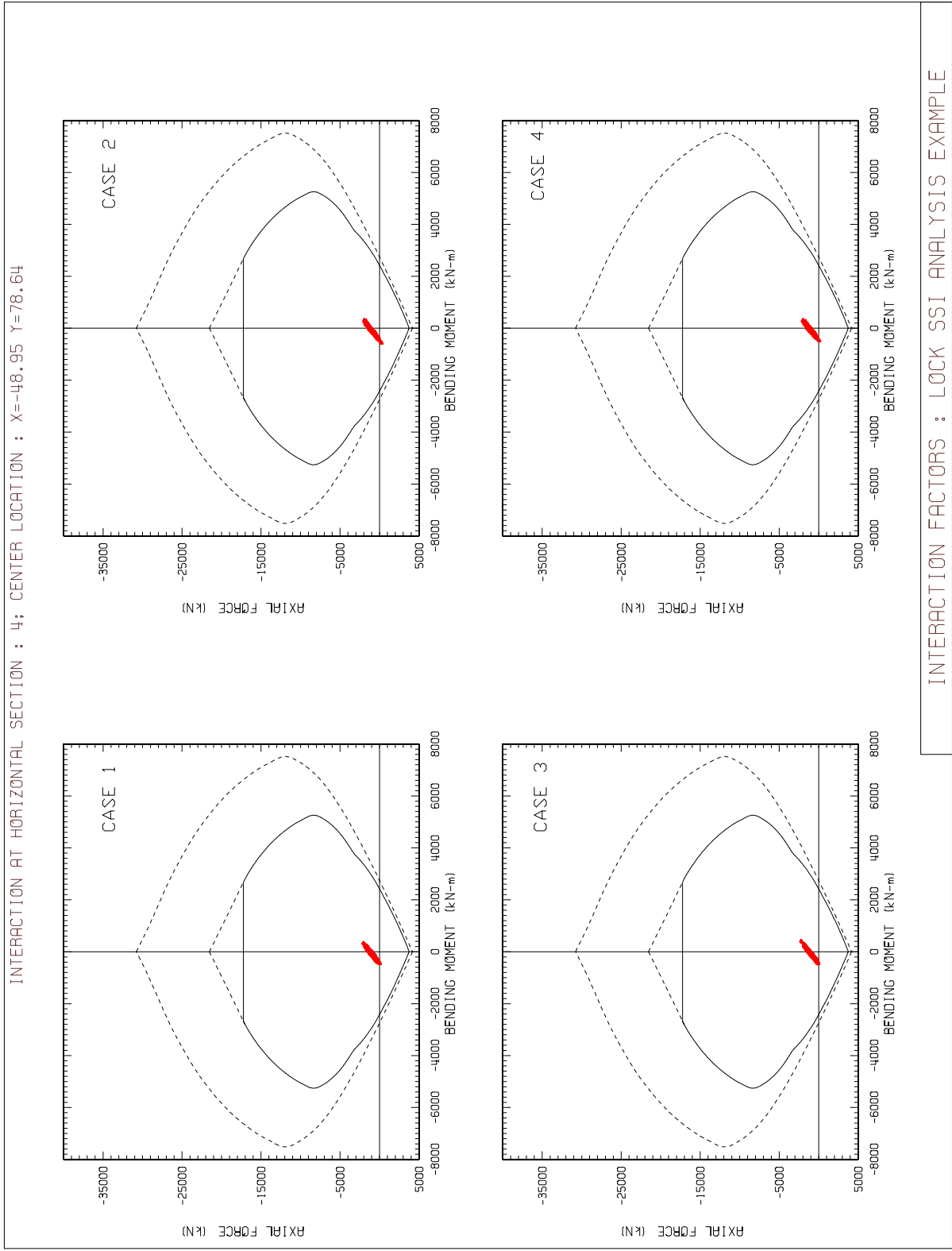


Figure 4-36. Axial force versus bending moment of concrete Section 4

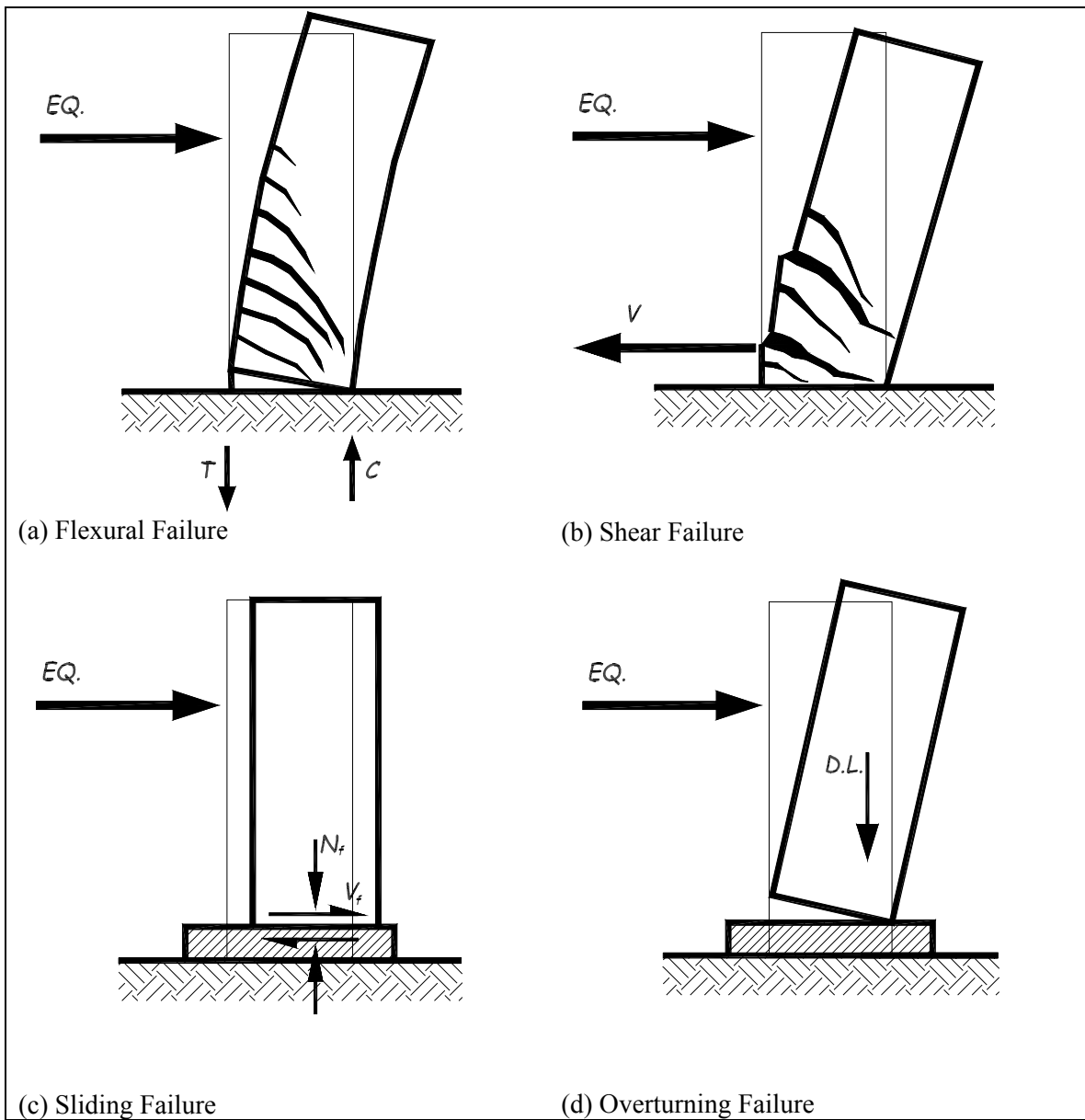


Figure 4-37. Probable modes of failure for free-standing towers where *EQ.* = lateral earthquake load, *T* = tensile base reaction force, *C* = compressive base reaction force, *V* = base shear, *N_f* = normal force at the base, *V_f* = shear friction, and *D.L.* = dead load

Time-History No.	Earthquake Record	<i>M_w</i>	Style of Faulting	Distance, km	Scaling Factor
1	Cholame #8, 1966 Parkfield	6.1	Strike-Slip	9.2	1.7962
2	Garvey Reservoir, 1987 Whittier Narrows	6.0	Reverse	12.1	0.8987
3	Gavilan College, 1989 Loma Prieta	6.9	Oblique	11.2	1.3596
4	Pacoima Dam, 1971 San Fernando	6.6	Reverse	2.8	0.4915

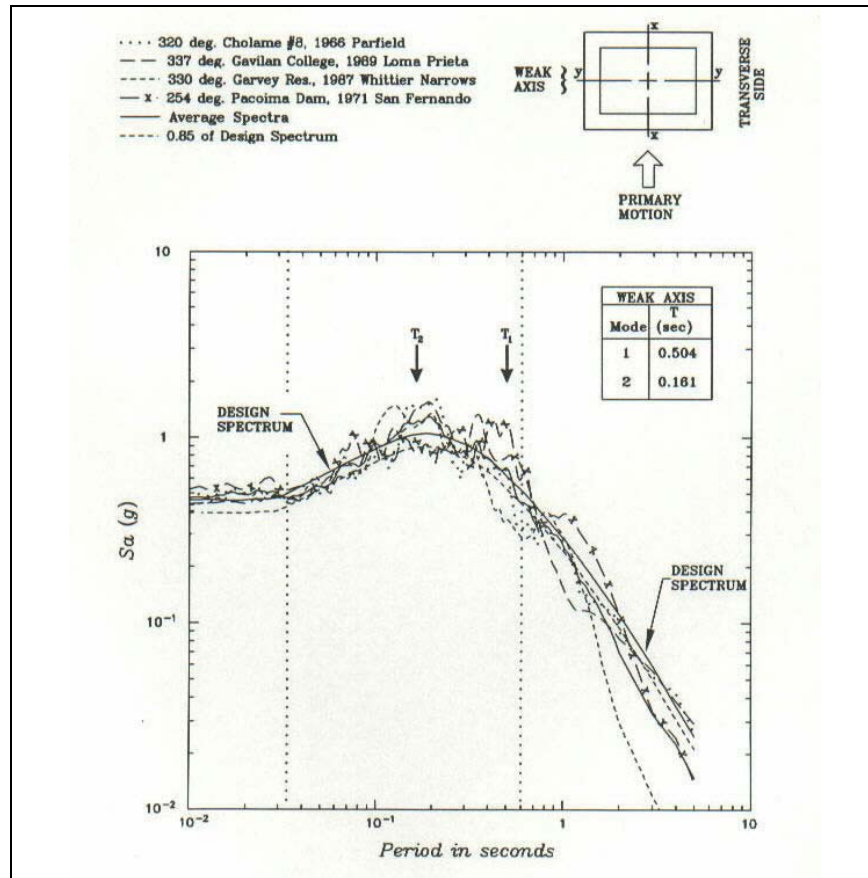


Figure 4-38. Horizontal design spectrum and the four scaled natural time-histories of the primary set with 5 percent damping

(2) Description of example intake tower. The geometry of the example free-standing intake tower is shown in Figure 4-44. The tower is 60.96 m (200 ft) high with base dimensions of 14.63 m by 11.28 m (48 ft by 37 ft). The wall thickness decreases in five steps from 1.83 m (6.0 ft) at the base to 0.61 m (2.0 ft) at the top. The water surface is at elevation 1,016.81 m (3,336 ft) corresponding to outside and inside water depths of 41.45 m (126 ft) and 39.62 m (130 ft), respectively. The material parameters of the concrete and reinforcing steel are summarized in Table 4-15. The transverse and longitudinal nominal and cracking moments and the shear capacities are listed in Table 4-16. To keep the analysis and damage formulation simple the following assumptions were made:

Tower elements do not reach their shear or axial load capacity.

Rocking or sliding modes of failure are not considered.

The vertical component of the earthquake ground motions is ignored.

The effects of gravity load are not included in the dynamic analysis.

(3) Linear time-history earthquake response. The earthquake response of the tower was computed for all four earthquake ground motions described in (1) above. The time-history analysis was carried out separately for excitation in the transverse and longitudinal directions. In each direction, the 10 lowest modes of vibration

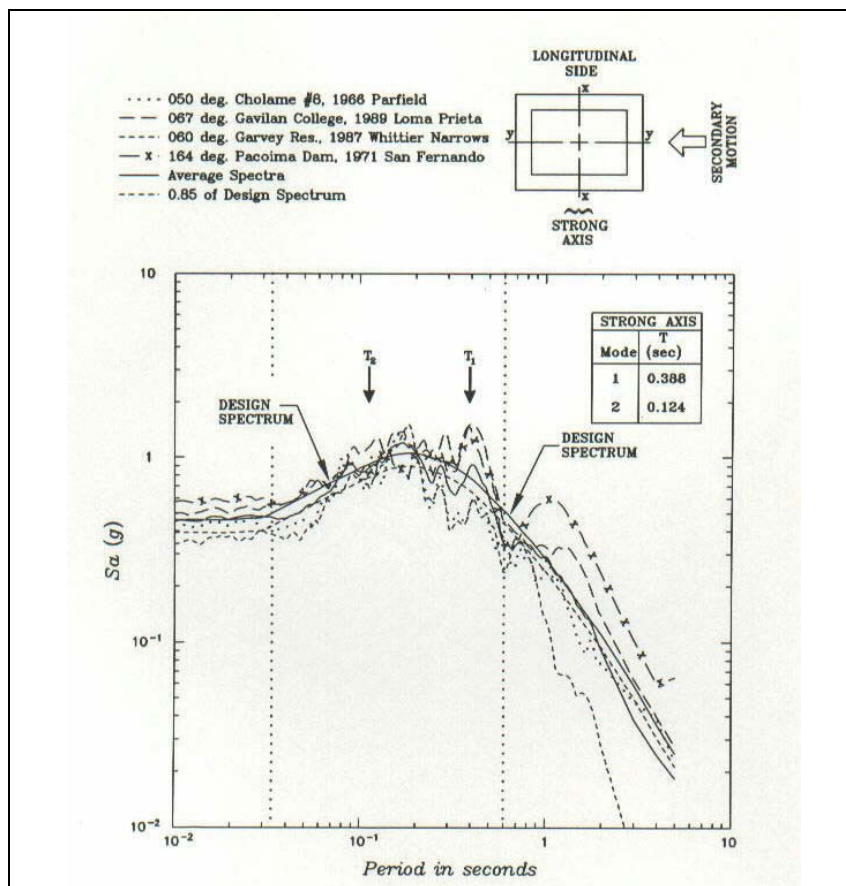


Figure 4-39. Horizontal design spectrum and the four scaled natural time-histories of the secondary set with 5 percent damping

with a modal damping ratio of 5 percent were considered in computation of the dynamic response. The periods of the five lowest transverse modes of vibration ranged from 0.529 to 0.034 sec. For the longitudinal direction, the periods of the five lowest modes were in the range of 0.041 to 0.026 sec. Table 4-17 summarizes maximum lateral displacements at the top of the tower and maximum bending moments and shear forces at the base of the tower. Figures 4-45 to 4-52 present time-histories of displacements, shears V_x and V_y , and bending moments M_x and M_y for the selected earthquake ground motions. The results show that the shear capacity is not reached but the bending moment capacity of the tower is exceeded for all four earthquake records, an indication that some nonlinear behavior and damage could be expected, as discussed next in *c* below.

c. Damage criteria for linear time-history analysis. The damage for lightly reinforced free-standing intake towers is evaluated on the basis of demand-capacity ratios described in *f* below. The basic procedure is to perform linear time-history analysis with appropriate amount of damping to obtain bending moment demand-capacity ratios for all tower elements. Initially a damping ratio of 5 percent is used. If the computed demand-capacity ratios are less than or equal to 1.0, the tower is considered to respond essentially within the linear elastic range with negligible or no damage. For MDE earthquake ground motions, however, it is likely that demand-capacity ratios will exceed 1.0, indicating that the tower would suffer some damage. In this situation, the damping for the linear analysis should be increased to 7 percent if demand-capacity ratios are approaching 2 and to 10 percent if they exceed 2. After adjustment for the damping, the damage is considered moderate and acceptable if the following conditions are met:

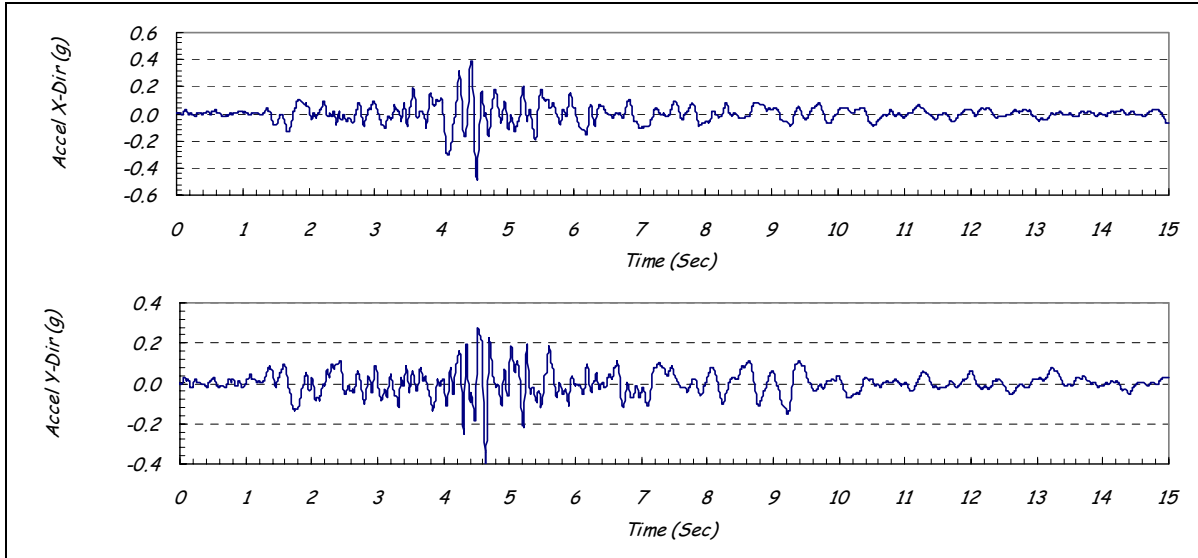


Figure 4-40. Cholame #8, 1966 Parkfield Earthquake (scaled by 1.7962)

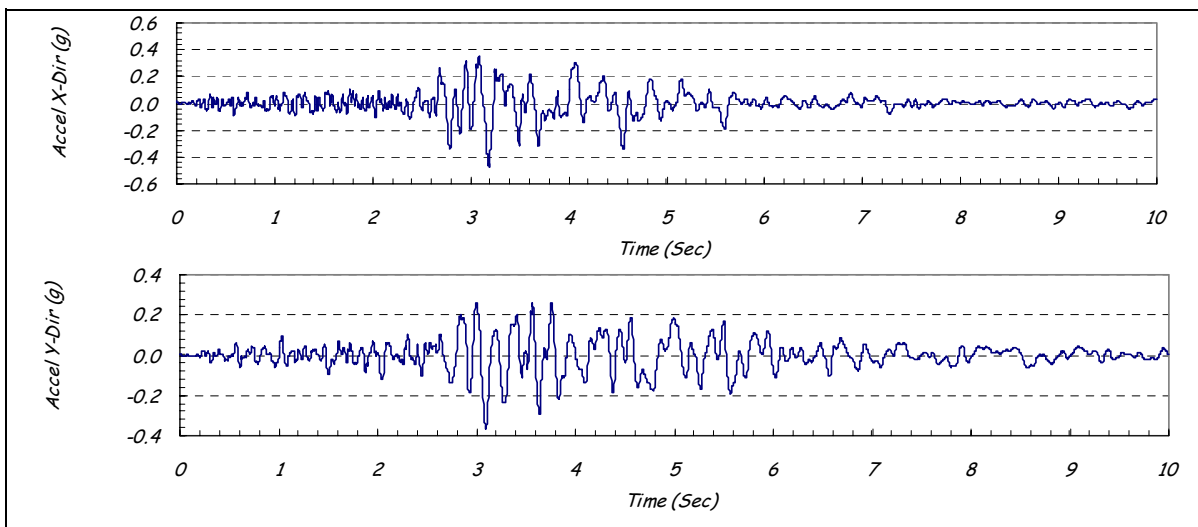


Figure 4-41. Garvey Reservoir, 1987 Whittier Narrows Earthquake (scaled by 0.8987)

- Bending moment demand-capacity ratios computed on the basis of linear time-history analysis remain less than 2.
- Cumulative duration of bending-moment excursions above demand-capacity ratios of 1 to 2 fall below the acceptance curve given in Figure 4-53.
- The extent of yielding along the height of tower (i.e., plastic hinge length for demand-capacity ratios of 1 to 2) is limited and falls below the acceptance curve.

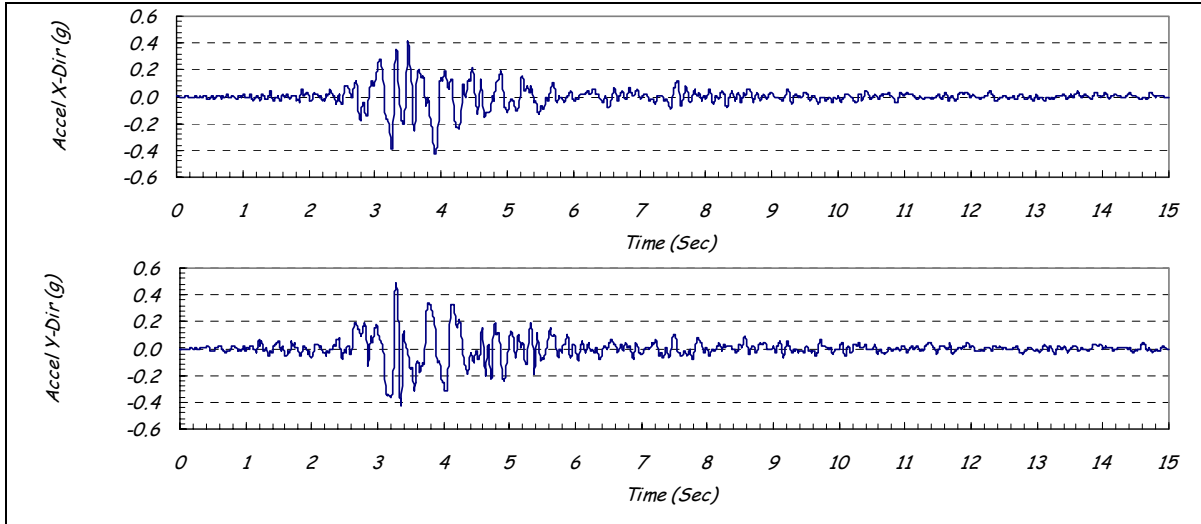


Figure 4-42. Gavilan College, 1989 Loma Prieta Earthquake (scaled by 1.3596)

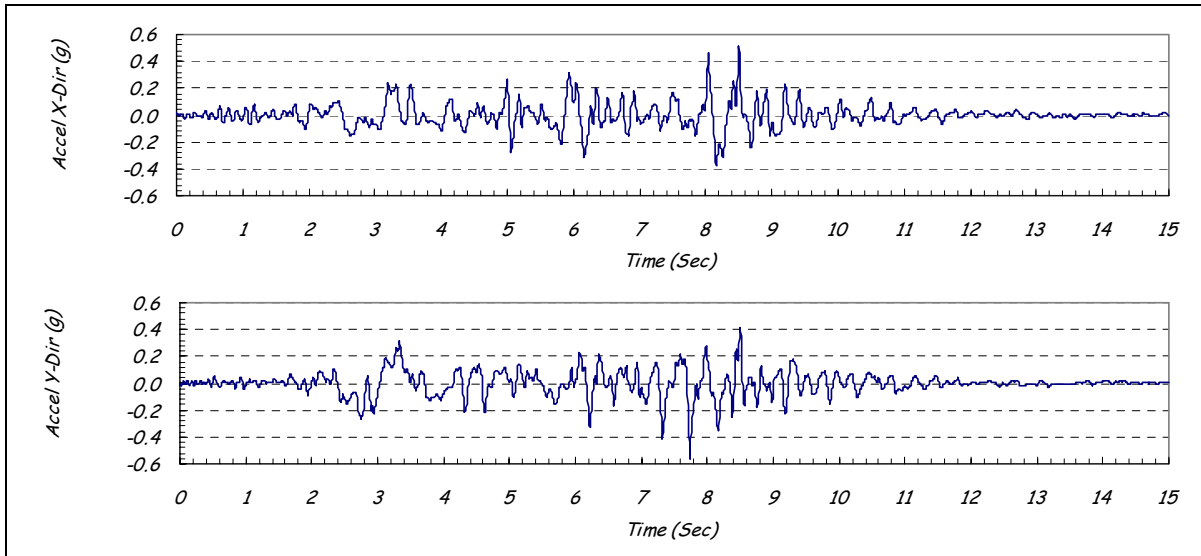


Figure 4-43. Pacoima Dam, 1971 San Fernando Earthquake (scaled by 0.4915)

The acceptance criteria state that as long as demand-capacity ratios are less than 2 and the cumulative inelastic duration and yielded height ratios fall below the acceptance curves, the level of damage will be moderate and can be approximated by the linear analysis procedures. If demand-capacity ratios exceed 2.0 or the cumulative duration and the yield lengths rise above the acceptance curves, the damage is considered to be severe and should be assessed using nonlinear analysis procedures. The term cumulative inelastic duration is defined as the total time of bending moment excursions above a particular capacity corresponding to demand-capacity ratios of 1 to 2. As shown in Figure 4-53, the cumulative inelastic duration for free-standing towers varies from 0.75 to 0.0 sec for demand-capacity ratios of 1 and 2, respectively. The yield height ratio refers to the yielded length of tower normalized with respect to the tower height. To keep the damage to a moderate level, the yield length should be less than one-third of the tower height, as shown in Figure 4-53.

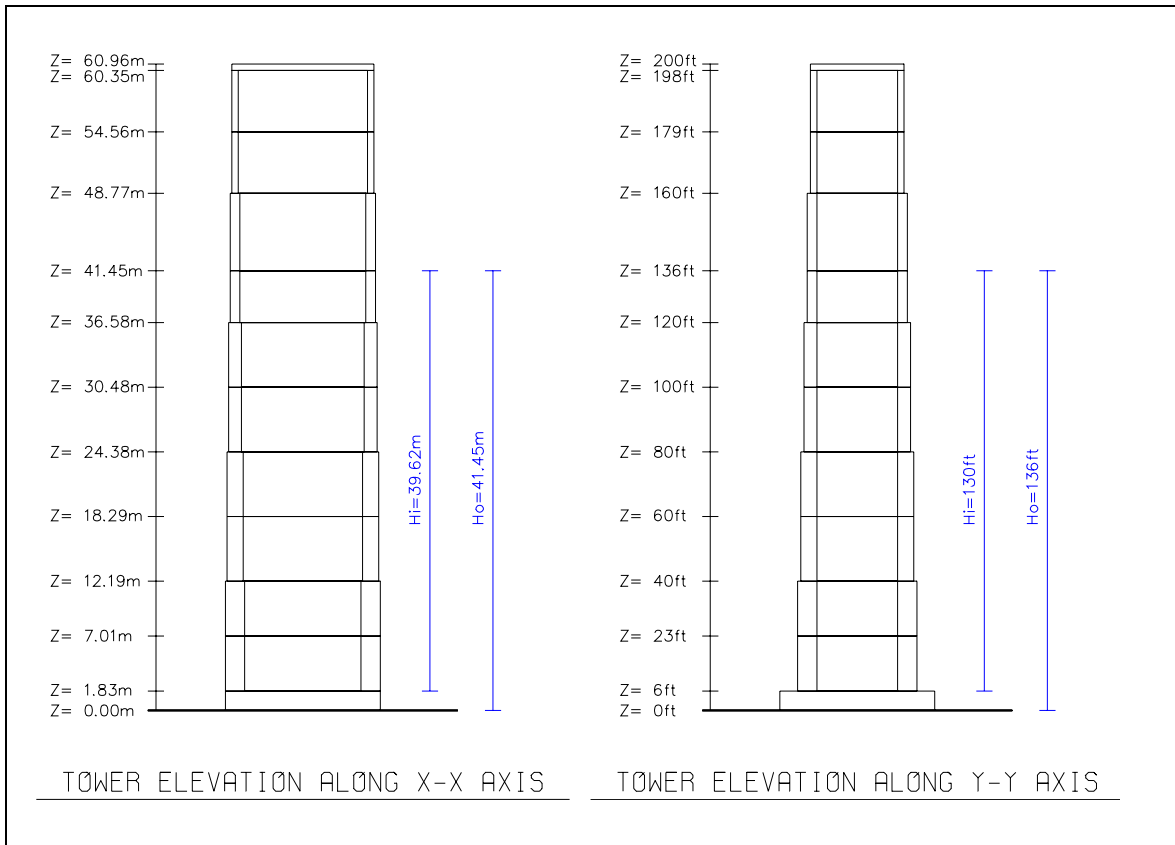


Figure 4-44. Basic geometry of the example tower

Table 4-15 Material Parameters Used in the Study		
Parameter	Value	
Re-bar Material Properties		
Modulus of Elasticity E_s	199,958.46 MPa	29,000.00 ksi
Yield Strength f_y	413.71 MPa	60.00 ksi
Strain Hardening	0.80 %	0.80 %
Steel Ultimate Stress	517.13 MPa	75.00 ksi
Steel Ultimate Strain	5.00 %	5.00 %
Concrete Material Properties		
Modulus of Elasticity E_c	21,526.56 MPa	3,122.00 ksi
Shear Modulus G	8,969.40 MPa	1,300.83 ksi
Poisson's Ratio ν	0.20	0.20
Concrete Strength f'_c	20.69 MPa	3.00 ksi
Modulus of Rupture F_r	2.83 MPa	0.41 ksi
Concrete Ultimate Strain ϵ_c	0.30 %	0.30 %

Table 4-16
Nominal Moment, Cracking Moment, and Shear Capacities for Bottom Three Sections of Tower

Parameter	Section 2	Section 3	Section 4
Height z, m (ft)	1.83-12.19 (6-40)	12.19-24.38 (40-80)	24.38-36.58 (80-120)
Nominal Moment MN_y , kN-m (k-ft)	937,490 (691,421)	881,969 (650,473)	827,955 (610,636.39)
Nominal Moment MN_x , kN-m (k-ft)	719,711 (530,803)	653,529 (481,993)	590,377 (435,417.19)
Cracking Moment Mcr_y , kN-m (k-ft)	814,736 (600,887)	673,358 (496,617)	534,792 (394,421.967)
Cracking Moment Mcr_x , kN-m (k-ft)	675,194 (497,971)	548,840 (404,783)	429,125 (316,489.629)
Shear Capacity Vn_y , kN (kips)	15,537,443 (3,492,773)	12,849,069 (2,888,434)	10,209,724 (2,295,116.85)
Shear Capacity Vn_x , kN (kips)	12,137,049 (2,728,384)	9,756,294 (2,193,187)	7,523,491 (1,691,259.3)

Table 4-17
Calculated Maximum Displacements and Element Forces

Time History No.	Earthquake Record	Maximum Top Displacement, cm (in.)	Maximum Bending Moment, kN-m (k-ft)	Maximum Shear kN (kips)
X-Component of Earthquake Ground Motion (X-Direction)				
1	Cholome #8, 1966 Parkfield	4.96 (1.95)	1,832,986 (1,351,870)	58,492 (13,149)
2	Garvey Reservoir, 1987 Whittier Narrows	5.43 (2.14)	1,970,798 (1,453,510)	68,045 (15,296)
3	Gavilan College, 1989 Loma Prieta	12.18 (4.80)	4,578,458 (3,376,720)	148,169 (33,308)
4	Pacoima Dam, 1971 San Fernando	10.86 (4.28)	3,769,250 (2,779,910)	128,902 (28,977)
Y-Component of Earthquake Ground Motion (Y-Direction)				
1	Cholome #8, 1966 Parkfield	7.76 (3.05)	2,058,380 (1,518,030)	108,066 (24,293)
2	Garvey Reservoir, 1987 Whittier Narrows	6.32 (2.49)	1,375,739 (1,014,640)	64,100 (14,410)
3	Gavilan College, 1989 Loma Prieta	11.59 (4.56)	3,016,094 (2,224,440)	113,106 (25,426)
4	Pacoima Dam, 1971 San Fernando	15.08 (5.94)	3,246,487 (2,394,360)	96,683 (21,734)

d. *Validation of damage criteria.* It is apparent from Figures 4-45 to 4-52 that the bending capacities of the example tower are exhausted and demand-capacity ratios for all the four earthquake records exceed 1. To estimate the expected damage, the performance evaluation curves are developed for all earthquake responses and illustrated in Figure 4-54. In this figure demand-capacity ratio is defined as the ratio of moment demand M_x or M_y to moment capacity M_{xu} or M_{yu} . Based on these results only the recording from the 1966 Parkfield earthquake applied in the longitudinal direction produces damage parameters within the acceptable range. The application of the 1966 Parkfield record in the transverse direction and the other three records in either direction produces significant nonlinear behavior well beyond the acceptable levels set forth for the linear analysis. To validate such findings the example tower was analyzed using nonlinear time-history procedures. The nonlinear analyses were conducted for all four earthquake records using the computer program DRAIN-2DX. The results of nonlinear analyses are summarized in the form of a global displacement ductility factor defined as the ratio of the maximum to yield displacements at the top of the tower (i.e., $m_D = D_m / D_y$). The yield displacement refers to displacement of the top of the tower at the time of the first yield. The global ductility factors listed in Table 4-18 are generally lower than the demand-capacity ratios indicated by linear analysis (Figure 4-54). This is because nonlinear analysis involves both the elastic and hysteretic damping, while linear analysis employs only the elastic damping. Since both the linear and nonlinear analyses show nonlinear deformation in the example tower, it would be prudent to increase the damping for the linear analysis from 5 to 10 percent. On this basis, the linear analyses were repeated with 10 percent modal

damping for all earthquake records. The results of these linear analyses in the form of structural performance curves

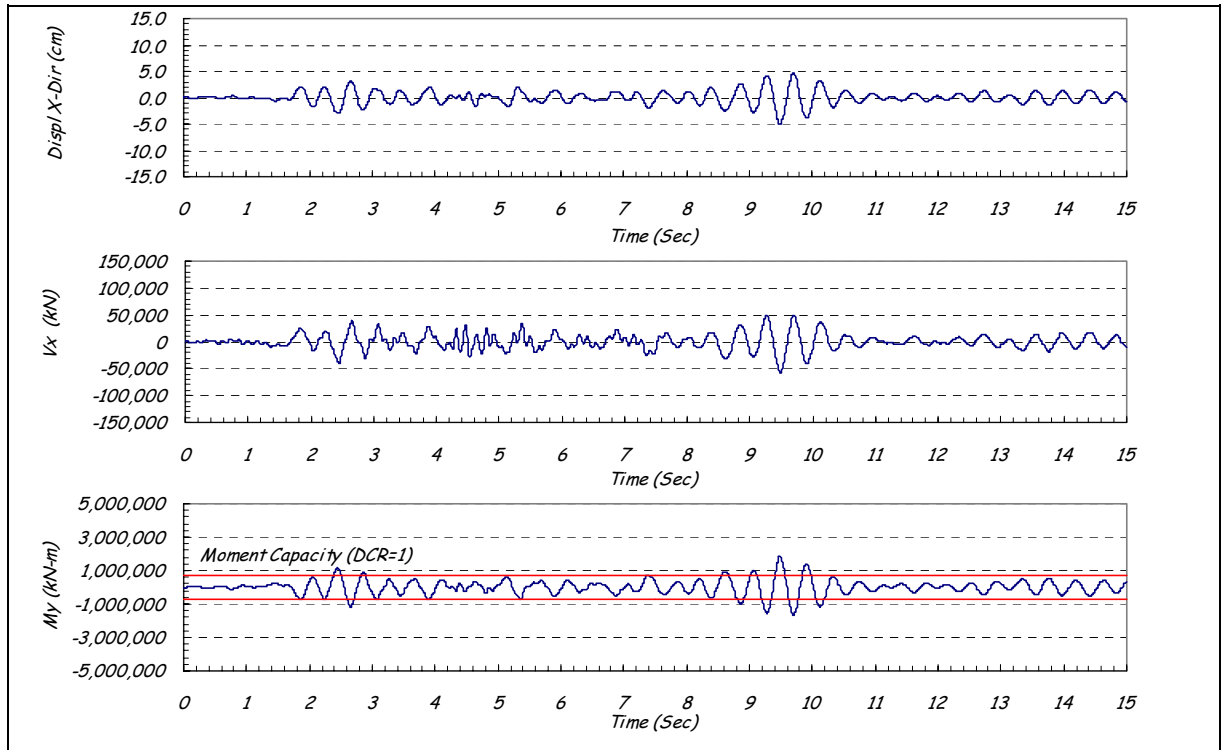


Figure 4-45. Response of the tower in x-direction due to 1966 Parkfield earthquake

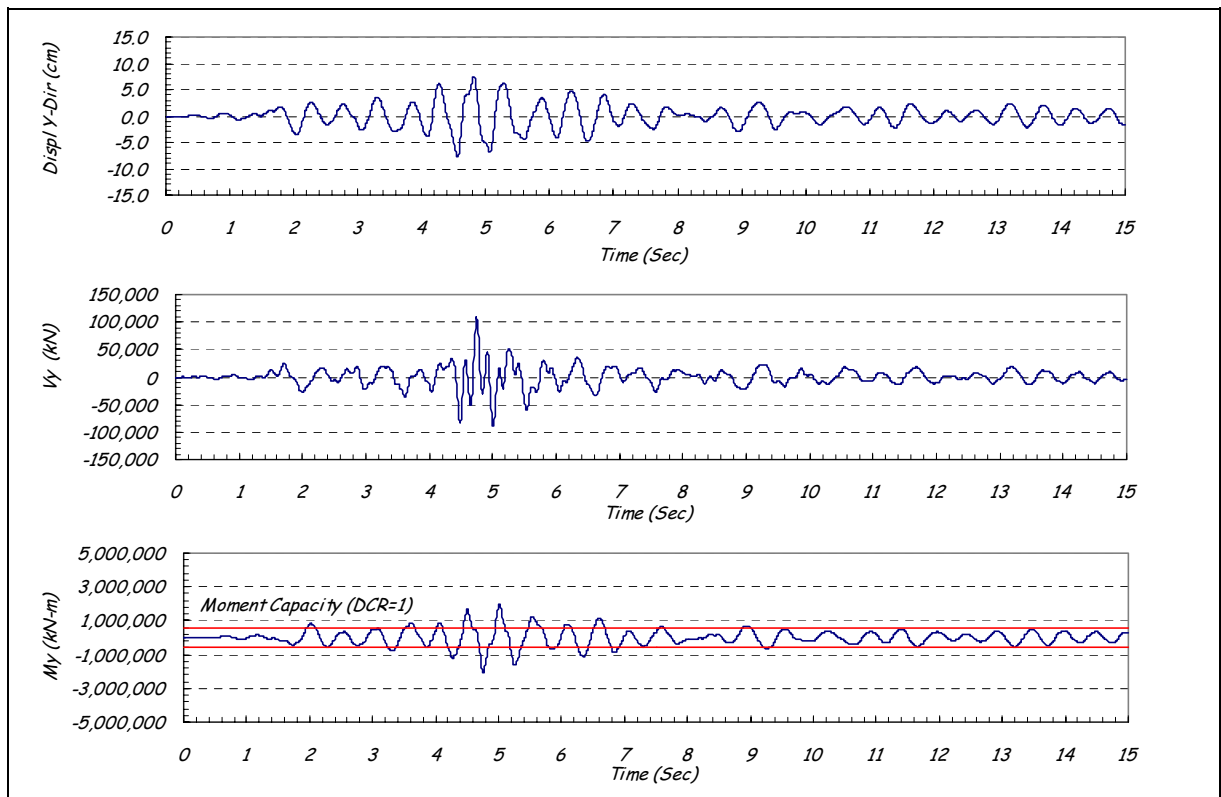


Figure 4-46. Response of the tower in y-direction due to 1966 Parkfield earthquake

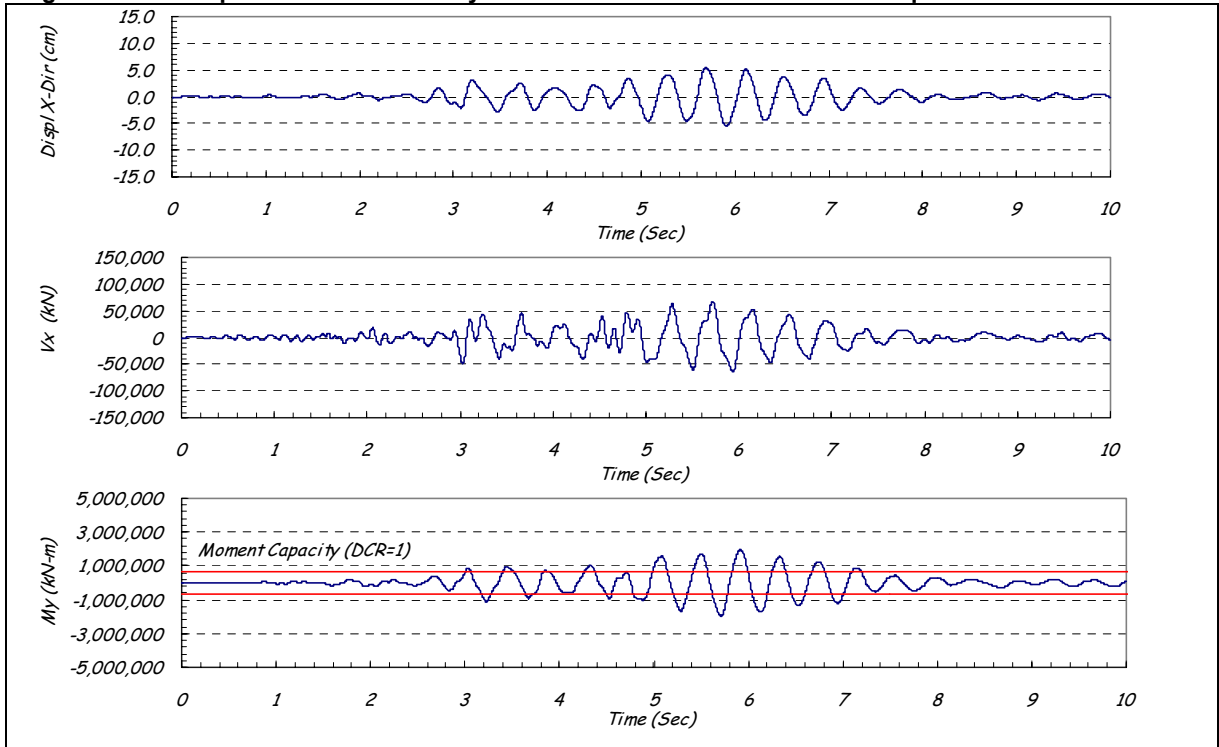


Figure 4-47. Response of the tower in x-direction due to Whittier Narrows earthquake

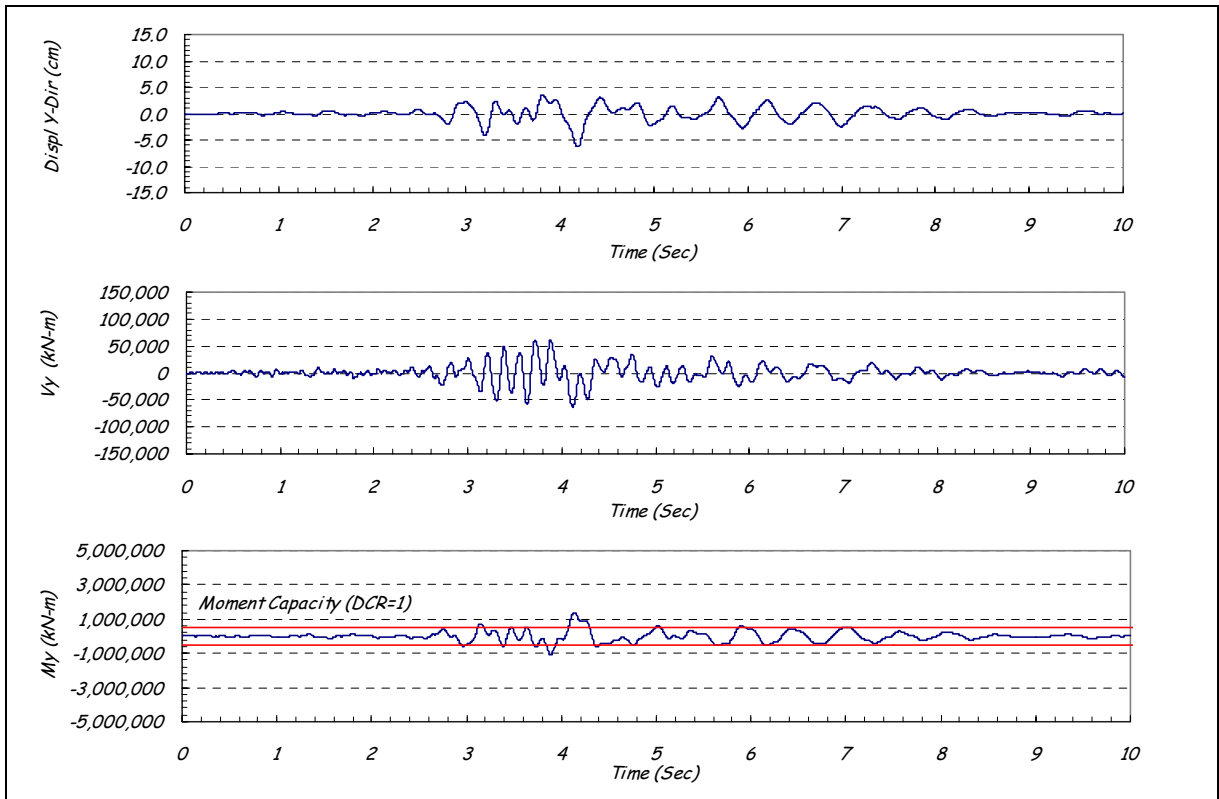


Figure 4-48. Response of the tower in y-direction due to Whittier Narrows earthquake

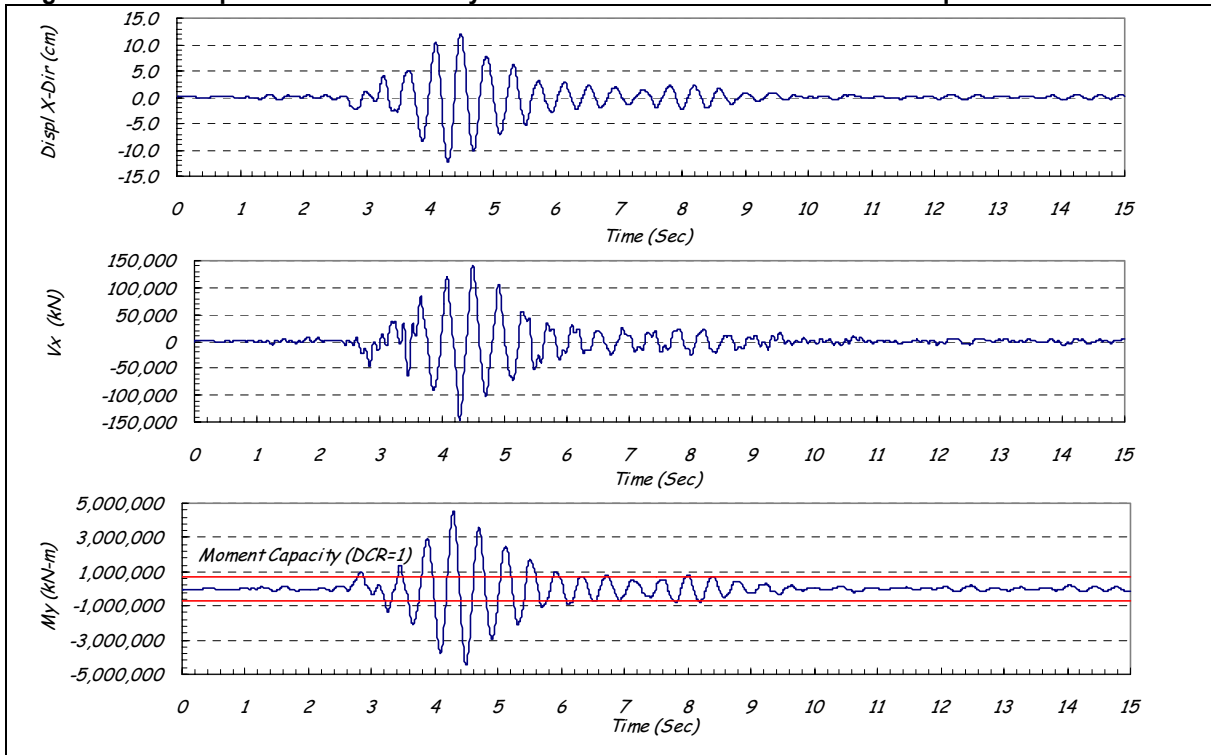


Figure 4-49. Response of the tower in x-direction due to 1989 Loma Prieta earthquake

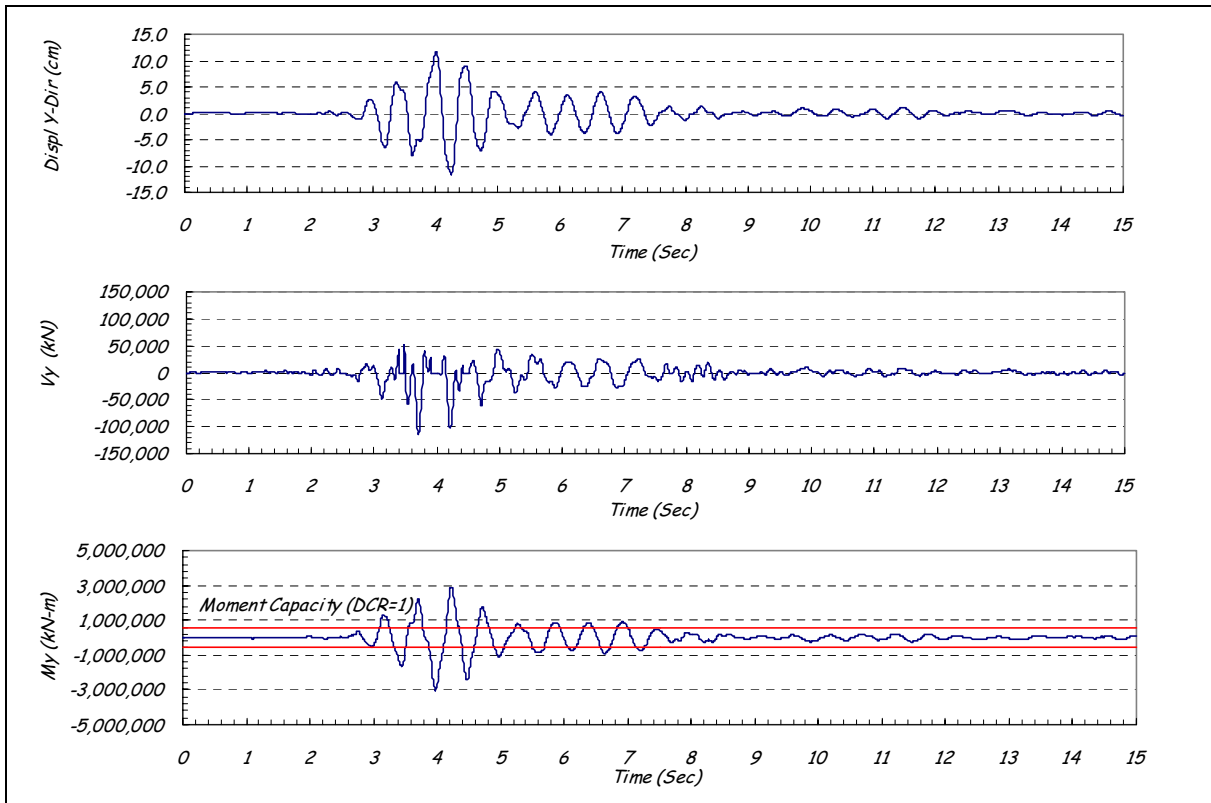


Figure 4-50. Response of the tower in y-direction due to 1989 Loma Prieta earthquake

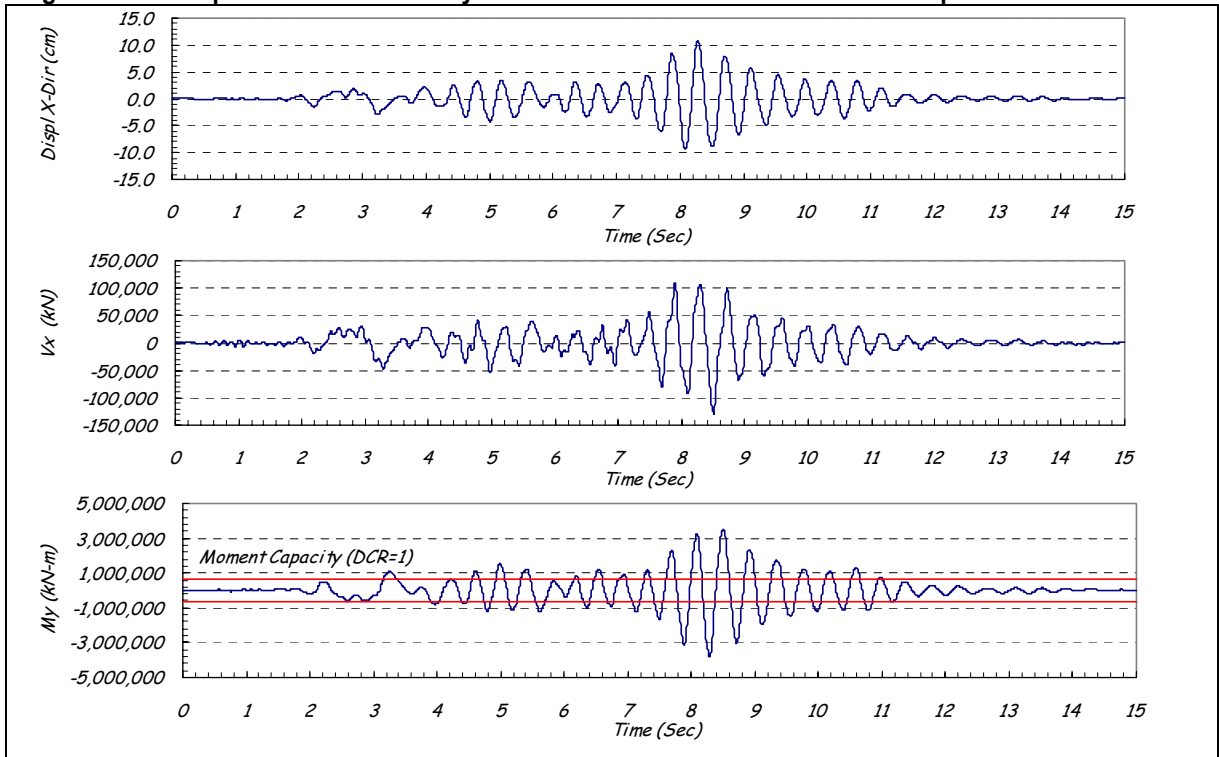


Figure 4-51. Response of the tower in x-direction due to 1971 San Fernando earthquake

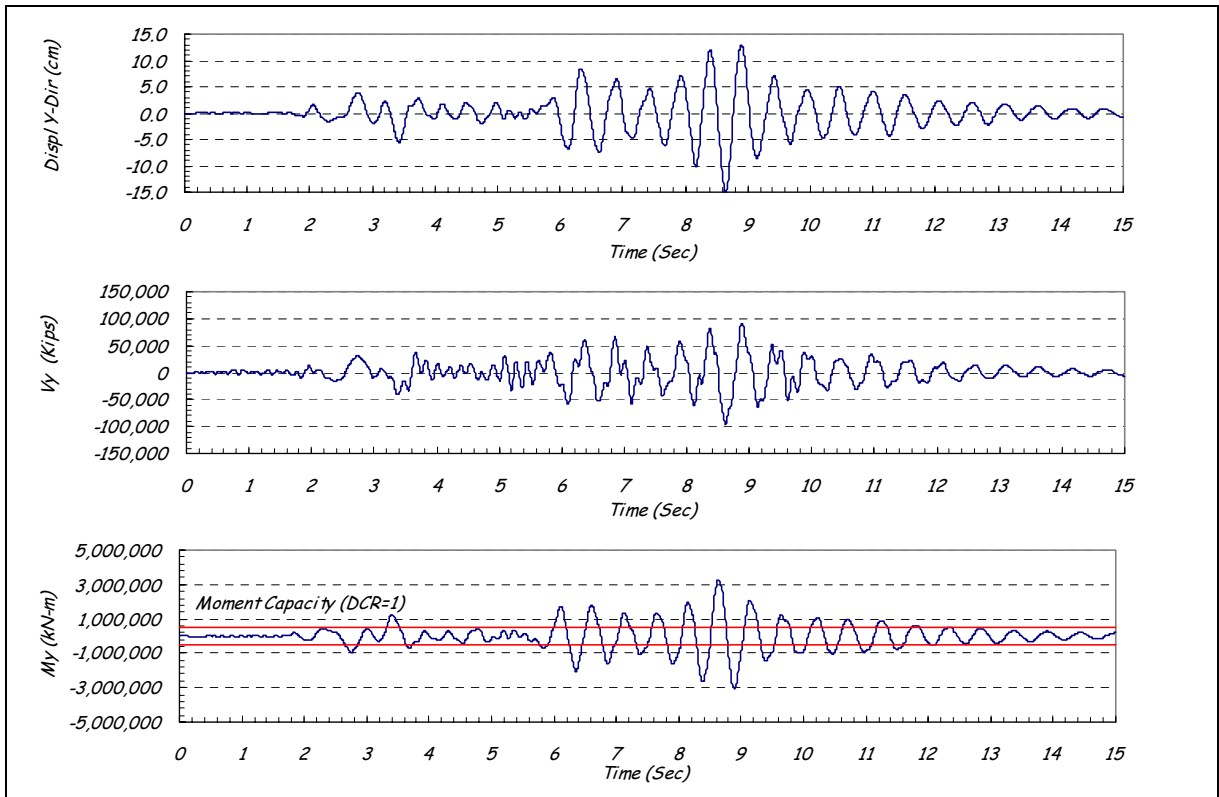


Figure 4-52. Response of the tower in y-direction due to 1971 San Fernando earthquake

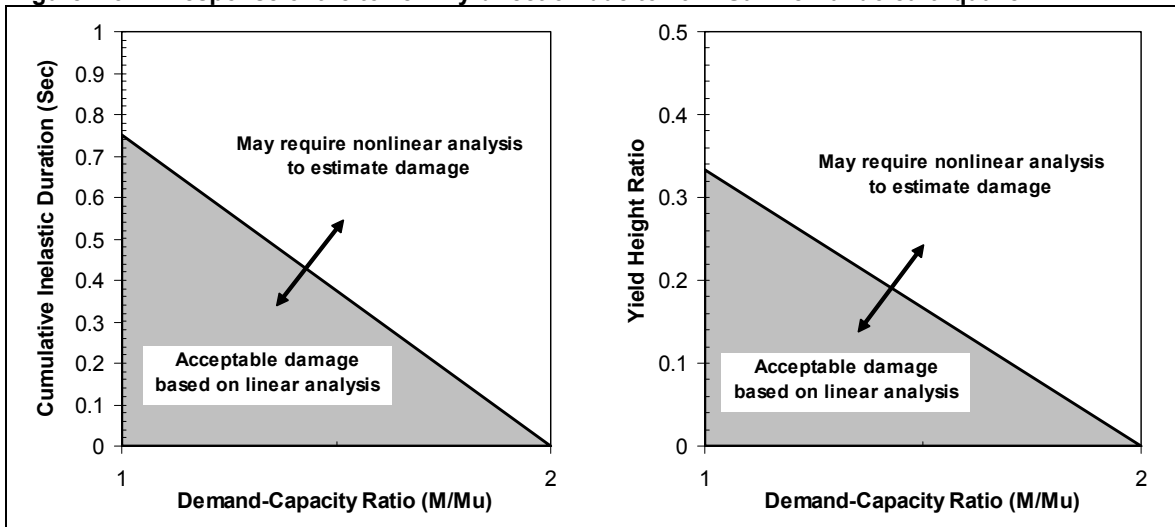


Figure 4-53. Structural performance assessment for free-standing reinforced concrete intake towers based on linear-elastic time-history analysis

(Figure 4-55) show reasonable agreement with the results of nonlinear analyses. The performance curves for the 1966 Parkfield and 1987 Whittier Narrows records fall below the acceptance curves, except for yield height ratios due to the 1966 Parkfield record applied in the transverse direction. The performance curves for the 1989 Loma Prieta and 1971 San Fernando records, even after using a 10 percent damping, rise above the acceptance curves. These results show reasonable agreement with the results of nonlinear analyses, thus validating the accuracy of the damage criteria.

e. Load combination cases. Gravity load in the form of self-weight should be combined with the earthquake ground motion when the analysis includes one or more of the following: axial force-bending moments interaction, vertical component of ground motion, P-delta effect, rocking, or sliding. Furthermore, the rocking or sliding analysis, if required, should include the uplift pressure at the base of the tower as well as the load due to weight of the contained water. Other static loads (i.e., hydrostatic and ice) could be neglected if their effects are negligible.

f. Demand-capacity ratios. The demand-capacity ratio for tower elements is defined as the ratio of calculated maximum force to the corresponding element capacity limit. Demand-capacity ratio should be computed for bending moments as well as axial and shear forces. Under no conditions should the shear or axial forces exceed their capacity limit. When the effects of axial or shear force are critical, the nonlinear analysis should be undertaken to estimate the damage, regardless of the bending moment demand-capacity ratio.

g. Presentation and performance evaluation. An example intake tower was analyzed using four different earthquake records to demonstrate the performance evaluation process discussed in *a*, *b*, and *c* above. The overall process involves presentation and evaluation of the following results:

(1) General description and load combinations. General description of the computer model and all applicable loads and load combinations should be provided. Exclusion of any particular load or load combinations should be discussed and justified.

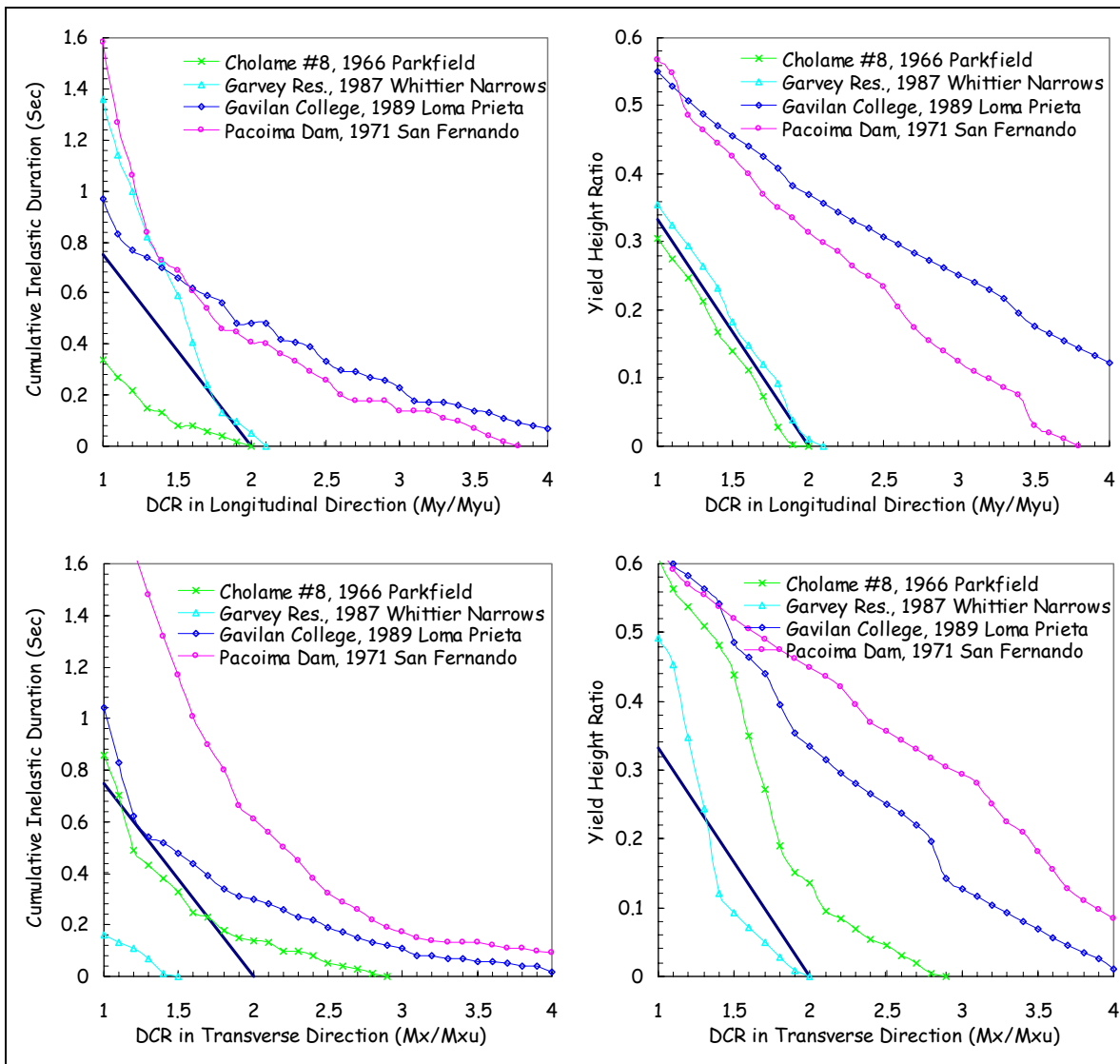


Figure 4-54. Structural performance assessment curves with 5 percent damping

Table 4-18
Global Ductility Factors for Various Ground Excitations

Time-History No.	Earthquake Record	Global Ductility	
		X-Dir.	Y-Dir.
1	Cholame #8, 1966 Parkfield	1.33	1.90
2	Garvey Res. 1987 Whittier Narrows	1.41	1.22
3	Gavilan College, 1989 Loma Prieta	2.96	4.22
4	Pacoima Dam, 1971 San Fernando	2.49	4.45

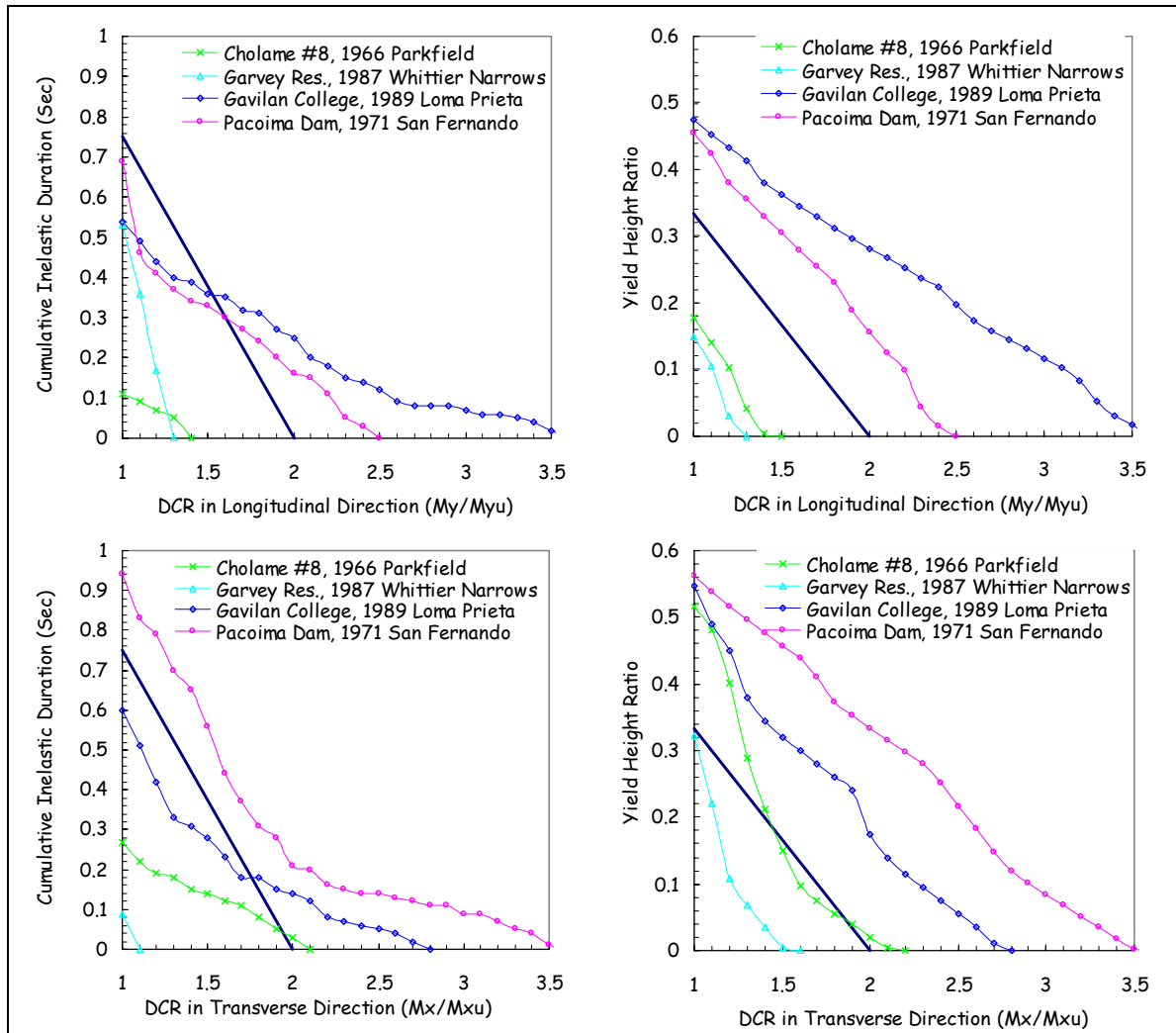


Figure 4-55. Structural performance assessment curves with 10 percent damping

(2) Natural frequencies and mode shapes. Natural frequencies and mode shapes are presented to gain insight into the dynamic characteristics of the tower. The natural frequencies are also used to ensure that the earthquake input is sufficiently energetic in the frequency range of importance to the tower.

(3) Displacement time-history response. The magnitudes and time-histories of displacements at the critical locations, usually at the top of the tower, should be presented.

(4) Time-history of element forces. The magnitudes and time-histories of the section forces exceeding their corresponding capacities should be presented and employed to compute the cumulative inelastic duration.

(5) Demand-capacity ratios. The maximum bending moments and shear and axial forces should be computed and incorporated in plots for comparison with the acceptance performance curves.